

**PALACKÝ UNIVERSITY OLOMOUC**

**Faculty of Science**

**Department of Ecology and Environmental Sciences**



**Investigating crop management factor (C) and potential soil erosion in a large agricultural landscape: spatiotemporal analysis through remote sensing and land use data**

Ph.D. Thesis

**Dawit Ashenafi Ayalew**

Supervisor: Prof. Dr.Ing. Bořivoj Šarapatka, CSc.

Olomouc 2020

I, Dawit Ashenafi Ayalew, thereby declare that I wrote the Ph.D. thesis myself using results of my own work or collaborative work of me and colleagues and with help of other publication resources which are properly cited.

Olomouc, \_\_\_\_ 2020

.....

Dawit Ashenafi Ayalew

© Dawit Ashenafi Ayalew, 2020

## **Abstract**

Soil erosion is a major global land degradation challenge that can result in the loss of soil productivity of agricultural land and in the reduction of the delivery of ecosystem services. It is often aggravated by anthropogenic interferences in land use management and vegetation cover changes. Spatiotemporally monitoring the land cover status and estimating the vulnerability of arable lands to potential soil erosion, especially for large agricultural landscapes, has become a prerequisite to understand other related global phenomena such as such climate change mitigation and hydrological processes on a global scale. Yet, these have been paramount tasks in terms of resource requirements and efficiency. Erosion models play an important role in such cases. The Universal Soil Loss Equation (USLE) is one of the most widely applied models to predict erosion risks by considering the land cover and management factor (C factor) in agricultural land. The C factor is the most dynamic and primary factor which could prevent soil erosion with the appropriate land management planning and execution.

In many cases the C values for large agricultural areas are estimated by traditionally assigning static empirical soil loss ratio (SLR) values from literature to a land use/land cover map. This method is relatively easy but fails to capture the actual spatiotemporal variations of the vegetation covers and hence incurs inaccuracy in the estimation of the C values. When considering the crop management practices such as crop rotation, tillage practice in many of the cases it is rare to find complete C factor values for all arable crops and their associated management practices. In recent decades, using remote sensing data, through the Normalized Difference Vegetation Index (NDVI), has proven to help capture the variabilities in large scale studies. However, the sensitivity of the NDVI-derived C values to several biophysical variations, such as the vitality condition of the vegetation cover, the phenological stages of the crops in question, the soil background differences, and variations in topographical features, could hinder its full applicability. Therefore, this thesis deals with assessing the spatiotemporal dynamics of the cover and management factor in a large agricultural landscape setup by combining multitemporal satellite images with the annually updated Integrated Administrative Control Systems (IACS) land-use data. The overall objectives of the thesis were

- i) to temporally estimate and compare NDVI based ( $C_{ndvi}$ ) and literature-based ( $C_{lit}$ ) values so that the deviation can be quantified,

- ii) to quantify the sensitivity of NDVI based C factor values to biophysical variables in large agricultural landscape set up for future accurate estimations,
- iii) to assess the C factor values for crop management namely crop rotational patterns and predict the ensuing potential soil erosion rate in a large agricultural landscape,
- iv) to analyse the spatiotemporal variations of the impact of various crop rotation patterns on the C factor values in a large landscape scale with the implied application of the results for understanding of ecosystem processes at regional scales.

Combining multitemporal images with the IACS land use/cover datasets enhanced the quantification of the discrepancies between  $C_{ndvi}$  and  $C_{lit}$ . The discrepancy in C values between  $C_{ndvi}$  and  $C_{lit}$  was found to be season dependent with a closer relation observed in early spring to midsummer, with consistently lower RMSE values for data from June. When it comes to the biophysical sensitivity, soil background variation, specifically higher soil erodibility condition, was found to be associated with higher  $C_{ndvi}$  values. Identifying land cover type to specific species level allowed quantifying the sensitivity of  $C_{ndvi}$  to soil background heterogeneity in relation to crops' growth stage. Variation in slope curvature also affected the  $C_{ndvi}$  values. Convex shaped slopes of the study area were found to associate with high  $C_{ndvi}$  values compared with concave or flat shaped topography. Crop phenological stages variations also affected the calculated  $C_{ndvi}$  value. In addition, rotating different crops also showed variability on the  $C_{ndvi}$  and the subsequent soil erosion rate in the study area.

Overall, the results from the research can be useful inputs in improving the capacity of  $C_{ndvi}$  estimation for landscapes as complex as the present study region as well as an input for agricultural land management planning. In addition, utilizing remote sensing data for the purpose of capturing spatiotemporal variation in C factor determination and subsequently serving as input factor for process-based soil erosion modelling can be enhanced by considering the quantified sensitivity of  $C_{ndvi}$  estimations. The rotation impact assessment results of this research could also be an input for further efficient investigation of agronomic practices and their impact on the environment on a large heterogeneous agricultural landscape.

**Keyword:** Soil erodibility; C factor; topography; IACS; crop rotation; remote sensing; landscape.

## Abstrakt

Eroze půdy patří mezi hlavní globální problémy degradace půdy a může vést ke ztrátě produktivity půd a ke snížení poskytovaných ekosystémových služeb. V krajině se tento problém zhoršuje antropogenními zásahy při využívání půdy a změnami vegetačního krytu. Prostorové monitorování stavu půdy a odhad zranitelnosti půdy erozí, zejména v rozsáhlých zemědělských krajinách je i prekvizitou k pochopení řady souvisejících globálních jevů, jako jsou změny klimatu a hydrologické procesy v globálním měřítku. Při řešení všech těchto problémů hrají erozní modely důležitou roli. Jedním z nejpoužívanějších modelů k předpovědi rizik eroze na základě zohlednění krajinného pokryvu a faktoru hospodaření na zemědělské půdě je univerzální rovnice ztráty půdy (USLE) a další modely vycházející z ní. Při využívání těchto modelů je velmi důležitý C factor vegetačního krytu, který má vliv na zmírnění erozních procesů vhodným územním plánováním a realizací protierozních opatření.

V mnoha případech se hodnoty C pro velké zemědělské oblasti odhadují tradičním přiřazením hodnot statického empirického poměru ztrát půdy (SLR) z literatury do map "land use a land cover". Tato metoda není sice složitá, ale na druhé straně nedokáže dostatečně zachytit skutečné časoprostorové změny vegetačních pokryvů, a způsobuje tedy nepřesnosti v odhadu hodnot C faktoru. Při zvažování managementu agrosystémů, jako je střídání plodin, agrotechnika atd. je v mnoha případech složité najít správné hodnoty faktoru C pro všechny plodiny na orné půdě a související způsoby obdělávání. V posledních desetiletích se ukázalo, že použití dat dálkového průzkumu Země prostřednictvím vegetačního indexu normalizovaných rozdílů (NDVI) pomáhá zachytit variabilitu ve studiích velkých územních celků. Citlivost hodnot C odvozených z NDVI na několik variant zahrnujících stav vegetačního krytu, fenologické fáze jednotlivých plodin, rozdíly v půdních podmínkách a variabilitu topografických faktorů by však mohla omezovat použitelnost. Proto se tato práce zabývá hodnocením časoprostorové dynamiky vegetačního krytu a managementových opatření v rozsáhlých celcích zemědělských krajin, a to kombinací multitemporálních satelitních snímků s každoročně aktualizovanými údaji o využívání půdy v rámci Integrated Administrative Control Systems (IACS). Jako cíle práce bylo vytýčeno:

- i) odhadnout a porovnat hodnoty založené na NDVI ( $C_{ndvi}$ ) a údajů z literatury ( $C_{lit}$ ) tak, aby bylo možné odchylku kvantifikovat,

- ii) kvantifikovat citlivost hodnot C faktorů založených na NDVI a na bio-fyzikálních proměnných v rozsáhlé zemědělské krajině a nastavení pro budoucí přesné odhady,
- iii) vyhodnotit hodnoty faktoru C pro konkrétně vzorce střídání a management plodin a předpovědět následnou potenciální míru eroze půdy v zemědělské krajině,
- iv) analyzovat časoprostorové variace dopadu různých osevních postupů na hodnoty faktoru C v rozsáhlých zemědělských krajinách s možnou aplikací výsledků pro pochopení ekosystémových procesů v regionálním měřítku.

Kombinace multitemporálních snímků s datovými soubory “land use a land cover” zlepšila kvantifikaci nesrovnalostí mezi  $C_{ndvi}$  a  $C_{lit}$ . Výzkumem bylo zjištěno, že nesoulad v hodnotách C faktoru mezi  $C_{ndvi}$  a  $C_{lit}$  je závislý na ročním období s užším vztahem pozorovaným na začátku jara, s trvale nižšími hodnotami RMSE pro data z června. Pokud jde o citlivost, bylo zjištěno, že variabilita půdního prostředí, konkrétně podmínky erodovatelnosti, souvisí s vyššími hodnotami  $C_{ndvi}$ . Identifikace typu krajinného pokryvu na úrovni konkrétního druhu umožnila kvantifikaci citlivosti  $C_{ndvi}$  na heterogenitu půdy ve vztahu k plodinám a jejich fázi růstu. Různé typy svahů rovněž ovlivnily hodnoty  $C_{ndvi}$ . Bylo zjištěno, že konvexní svahy studované oblasti mají vyšší hodnoty  $C_{ndvi}$  ve srovnání s konkávními nebo s plochou topografií. Změny fenologických fází plodin rovněž ovlivnily hodnotu  $C_{ndvi}$ . Kromě toho i střídání různých plodin vykazovalo variabilitu  $C_{ndvi}$  a míru eroze půdy ve studované oblasti.

Výsledky předkládaného výzkumu mohou být užitečnými vstupy pro zlepšení odhadu  $C_{ndvi}$  v krajinách tak složitých, jako je studovaný region, stejně jako pro plánování využití zemědělské půdy. Kromě toho lze využít údaje z dálkového průzkumu Země za účelem zachycení časoprostorových variací při stanovení C faktoru a následně jako vstupní faktor sloužící pro modelování eroze půdy. Výsledky tohoto výzkumu by rovněž mohly být vstupem pro další efektivní zkoumání agronomických či agrotechnických postupů a jejich dopadů na životní prostředí v zemědělských krajinách.

**KLÍČOVÁ SLOVA:** Erodovatelnost půdy; Faktor C; topografie; IACS; střídání plodin; dálkový průzkum Země; Krajina.

## **Acknowledgments**

First, I would like to forward my deepest gratitude to my supervisor Prof. Borivoj Sarapatka for his relentless support in my entire Ph.D. study period. I appreciate his guidance both on academic and non-academic issues. My heartfelt gratitude should also be extended to Dr Detlef Deumlich for allowing me to do my research stay in ZALF and providing some of the data used in my study. I have also benefited a lot from his expertise in the field of my research through several discussions. I would also like to thank Dr.Daniel Doktor for allowing me to do an internship at UFZ and for his helpful advice on my research during the internship period and afterwards. It was a great opportunity to get connected with the UFZ staffs to broaden my scientific networks.

Many thanks for the staffs of Ecology and Environmental Sciences department, Palacky University Olomouc. I especially would like to thank Dr Marek Bednar for his unreserved help in setting up analysis software in my computer during my study whenever I request to, thanks for your cooperativeness. I would also like to express my gratitude to Dr Tomáš Václavík for facilitating my research stay in UFZ. I also thank Dr Clémence Chaudron for the conversation we had during my time of handling the rigorous peer-reviewed article writing. Saw and Diana, my colleagues, I thank you very much for the stimulating talks and hanging out in the entire study period.

I also acknowledge the Ministry of Education, Youth and Sports of the Czech Republic for providing scholarship for my PhD study. The faculty of science, Palacky University Olomouc, through its IGA research grant scheme has helped me financially in conducting my research.

I also extend my heartfelt gratitude to my family and friends back home in Ethiopia for their support and encouragement. Last but not least, I would like to immensely thank my dearest wife, Dr Lemlem Teklegiorgis, for her massive encouragement, support, advice, and unreserved love throughout the entire study period. Honestly, I could not achieve this without your support and presence next to me.

## List of Publications

The thesis is based on the following papers:

### Publication I:

**Ayalew, Dawit A.**; Deumlich, Detlef; Šarapatka, Bořivoj; Doktor, Daniel (2020): Quantifying the Sensitivity of NDVI-Based C Factor Estimation and Potential Soil Erosion Prediction using Spaceborne Earth Observation Data. In *Remote Sensing* 12 (7), p. 1136. DOI: 10.3390/rs12071136.

### Publication II:

**Ayalew, Dawit Ashenafi**; Deumlich, Detlef; Šarapatka, Bořivoj (2021): Agricultural landscape -scale C factor determination and erosion prediction for various crop rotations through a remote sensing and GIS approach. In *European Journal of Agronomy*. 123, p. 126203. DOI: 10.1016/j.eja.2020.126203.



## **List of Abbreviations**

**DEM:** Digital Elevation Model

**EVI:** Enhanced Vegetation Index

**GLM:** Generalized Linear Model

**IACS:** Integrated Administrative and Control System

**NDVI:** Normalized Difference Vegetation Index

**NIR:** NearInfraRed

**SAVI:** Soil Adjusted Vegetation Index

**SLR:** Soil Loss Ratio

**USLE:** Universal Soil Loss Equation

# Contents

Abstract.....	iii
Abstrakt .....	v
Acknowledgments .....	vii
List of Publications .....	viii
List of Abbreviations .....	ix
List of Tables .....	xii
List of Figures.....	xiii
<b>1. Introduction.....</b>	<b>1</b>
<b>1.1. Soil erosion and C factor studies in large agricultural landscape .....</b>	<b>1</b>
<b>1.2. Objectives of the research .....</b>	<b>4</b>
<b>1.3. Organisation of the dissertation.....</b>	<b>5</b>
<b>2. State of the art .....</b>	<b>5</b>
<b>2.1. Applications of remote sensing for erosion studies in large spatial scale.....</b>	<b>5</b>
<b>3. Material and Methods .....</b>	<b>9</b>
<b>3.1. Study site description.....</b>	<b>9</b>
<b>3.2. Data and processing.....</b>	<b>9</b>
<b>3.2.1. Remote sensing data.....</b>	<b>9</b>
<b>3.2.2. Land use data .....</b>	<b>11</b>
<b>3.3. C factor determination .....</b>	<b>12</b>
<b>3.3.1. SLR based literature values assigning (<math>C_{lit}</math>).....</b>	<b>12</b>
<b>3.3.2. NDVI based C factor (<math>C_{ndvi}</math>) computation.....</b>	<b>12</b>
<b>3.4. Crop rotation identification .....</b>	<b>12</b>
<b>3.5. Soil erosion modelling.....</b>	<b>13</b>
<b>3.6. Statistical analysis .....</b>	<b>15</b>
<b>3.6.1. Comparison between <math>C_{ndvi}</math> and <math>C_{lit}</math> .....</b>	<b>15</b>
<b>3.6.2. Quantifying the sensitivity of <math>C_{ndvi}</math> to biophysical variables.....</b>	<b>15</b>
<b>3.6.3. Crop rotational impacts on <math>C_{ndvi}</math> and soil erosion rate.....</b>	<b>15</b>
<b>4. Results and discussion .....</b>	<b>17</b>
<b>4.1. Comparison between <math>C_{ndvi}</math> and <math>C_{lit}</math> .....</b>	<b>17</b>
<b>4.2. Quantifying the sensitivity of <math>C_{ndvi}</math> to biophysical variables .....</b>	<b>18</b>
<b>4.3. Crop rotation impacts on C factor values.....</b>	<b>22</b>

<b>4.4. Crop rotation and potential soil erosion rates</b> .....	25
<b>5. Conclusions and outlook</b> .....	27
<b>6. References</b> .....	29
<b>7. Attached publications</b> .....	35
<b>7.1. Publication I</b> .....	35
<b>7.2. Publication II</b> .....	61

## List of Tables

Table 1 Overview of the multitemporal satellite images used for the analysis.....	10
Table 2 regression results showing the influence of biophysical variables on $C_{ndvi}$ across scene dates.....	20
Table 3 Temporal dynamicity of C factor values in relation to crop rotation patterns .....	24

## List of Figures

Figure 1 Overview of the study area: a) location of the study catchment, b) slope steepness in percent, c) land use/cover identified using IACS 2016 data.....	9
Figure 2 Comparison between mean NDVI values derived from two closely sensed Sentinel 2 and Landsat 7 data during May and August. .	11
Figure 3 Area coverage (%) of crop rotations considered in the analysis disaggregated for each cropping calendars (2013/14 to 2015/16). .....	13
Figure 4 Surface reflectance (SR) of NIR and red bands across soil erodibility categories .....	19
Figure 5 Spatial distribution of rotations and associated potential soil loss rate. ....	26

# **1.Introduction**

## **1.1. Soil erosion and C factor studies in large agricultural landscape**

Soil erosion is a major global land degradation threat which can result in the loss of soil productivity of agricultural land and in the reduction of the delivery of ecosystem services (Guerra et al. 2020; Pimentel and Burgess 2013; Yang et al. 2003). Although soil erosion is a natural occurrence, it is often accelerated through various land management practices (Borrelli et al. 2017). Increased soil loss rates are occurring on arable land than natural environment (Lu et al. 2003). This is particularly evident in a temporally differing manner when the vegetation cover is not enough to protect the soil (Borrelli et al. 2018). Yet, monitoring land cover status and assessing the vulnerability of arable land to soil erosion risks, especially for large agricultural landscapes, have been paramount tasks in terms of resource requirements and efficiency (Alexandridis et al. 2015). Erosion models, hence are pertinent tools to predict potential soil erosion risks in such condition (Panagos et al. 2014). The Universal Soil Loss Equation (USLE), an empirically based model, is one of the most widely applied models to predict erosion risks in agricultural land (Wischmeier and Smith 1978). It predicts the long term average annual soil loss rate as a product of six compartmentalized factors namely the rainfall factor (R), the soil erodibility factor (K), topographic factors (L and S), the vegetation cover and management factor (C), and the support practice factor (P).

The cover and management factor (C factor), along with the rainfall erosivity factor (R-factor), is the most dynamic factor controlling the rate of soil loss in the USLE model (Panagos et al. 2014), for which spatiotemporal variations need to be considered in determining the values. The C factor, in association with P factor, is also the primary factor which can prevent soil erosion with the appropriate land management planning and execution (Panagos et al. 2014). In addition to the USLE, several process-based models such as Soil and Water Assessment Tool (SWAT) and

the Agricultural Non-Point Source Pollution model (AGNPS), also employ C factor for erosion prediction (Neitsch et al. 2005; Young et al. 1989).

The C factor is computed based on the soil loss ratios (SLRs) for different crops at different growth stages and management (Morgan 2005; Wischmeier and Smith 1978). The SLR, which itself is a plot scale measured value, represents the ratio of the soil loss measured on a given land covered with specific vegetation type to the corresponding bare soil ploughed along the slope gradient. The summation resultant of the SLR value weighted by the corresponding rainfall erosivity proportion ( $\frac{R_i}{R}$ ) at a given growth stages results in the annual C-factor value (Eq.1).

$$C = \sum_i^n SLR_i \cdot \frac{R_i}{R} , \quad (\text{Eq.1})$$

where C (dimensionless) is the annual cover factor,  $SLR_i$  the soil loss rate at a specified growing stage  $i$ ,  $R_i$  the rainfall erosivity during the growth period  $i$  and  $R$  the annual total rainfall erosivity.

Field measurement of SLR values by considering all crop types and management practices, though it is the appropriate way, requires huge resource and time which rendering it less efficient for large agricultural landscape or regional scale assessment (Alexandridis et al. 2015; Schönbrodt et al. 2010). In many cases the C values for large agricultural areas are estimated by traditionally assigning static empirical SLR derived values from literature to a land use/land cover map. This method is relatively easy but fails to capture the actual spatiotemporal variations of the vegetation covers and hence incurs inaccuracy in the estimation of the C values. When considering the crop management practices such as crop rotation, tillage practice etc., in many of the cases it is rare to find complete C factor values for all arable crops and their associated management practices (Gabriels 2003; Preiti et al. 2017). On the other hand, accounting for the spatiotemporal variability in crop management while determining the C factor has been reported to improve accuracy of soil erosion prediction (Borrelli et al. 2018).

In recent decades, owing to the availability of remotely sensed data, application of satellite born images for the determination of C factor values in particular or identification of erosional areas in general has become a widely applicable tool (Vrieling 2006). The application of remote sensing images for C factor determination through vegetation indices such as the Normalized Difference Vegetation Index (NDVI) has been found to capture the dynamicity of plant cover status and associated management practices in predicting soil erosion (Feng et al. 2018; Schmidt et al. 2018; Alexandridis et al. 2015). However, the sensitivity of the NDVI derived C values to several biophysical variations, such as the vitality conditions of the vegetation cover, the canopy structure of the vegetation, the soil background heterogeneity and variations in topographical features could hinder its full applicability (de Jong 1994; Montandon and Small 2008; Zou and Möttus 2017). This, as a result, entails optimizing the influences of such biophysical variables on NDVI derived C value ( $C_{ndvi}$ ) estimations for various agricultural landscapes. This study therefore investigates the deviation of NDVI based C factor ( $C_{ndvi}$ ) determination from SLR based literature values ( $C_{lit}$ ) and further quantify the sensitivity of the former to various biophysical variables in a large agricultural landscape setup.

In addition, the present study uses remote sensing images to understand the spatiotemporal impact of crop management practices such as crop rotation patterns on C factor determination and soil erosion prediction at a large landscape scale. Remote sensing data provide the platform to study various crop rotation patterns for C factor estimation and subsequent prediction of erosion risks in an efficient way (Preiti et al. 2017). However, so far researches conducted are far too insufficient (Bégué et al. 2018). Bégué et al. (2018) point out that less than 10% of remote sensing studies focused on cropping practices in general. When it comes to crop rotation, the majority of the studies focused on identifying rotational patterns and classifying the pre-crops and succeeding



crops at large (Conrad et al. 2016; Mueller-Warrant et al. 2016; Kipka et al. 2016; Sahajpal et al. 2014; Martínez-Casasnovas et al. 2005; Pimentel and Burgess 2013; Panigrahy and Sharma 1997). However, the influence of cropping practices such as the choice of crops to rotate has been reported to significantly affect soil erosion rates (Simonneaux et al. 2015; Morgan 2005). The present study, therefore, uses multi-temporal satellite images in combination with the Integrated Administration and Control System (IACS) land use data to investigate the influences of various crop rotation patterns on the C factor values and on the subsequent potential soil erosion risks with a broad aim of utilizing the methods and the remote sensing data for large scale studies of agricultural land management impacts on agroecosystem functions.

## **1.2. Objectives of the research**

The specific objectives of the study are:

- To temporally estimate and compare NDVI based ( $C_{ndvi}$ ) and literature-based  $C_{lit}$  values so that the deviation can be quantified.
- To quantify the sensitivity of NDVI based C factor values to biophysical variables in large agricultural landscape set up for future accurate estimations.
- To assess the C factor values for various crop rotational patterns and predict the ensuing potential soil erosion rate in a large agricultural landscape
- To analyse the spatiotemporal variations of the impact of various crop rotation patterns on the C factor values in a large landscape scale with the implied application of the results for understanding ecosystem processes at regional scales.

### **1.3. Organisation of the dissertation**

The dissertation is composed of five chapters; the first including the introduction of the research along with the specific aims of the research and the organisational structure of the dissertation. The second chapter highlights state-of-the-art review of the applications of remote sensing for soil erosion and C factor determination studies and the existing gaps in relation to remote sensing application for erosion studies. The third chapter of the dissertation describes the study area, data processing and methodology employed to achieve the objectives of the present study. In the fourth chapter the major findings of the research are highlighted including discussions of the results. Finally, chapter five draws conclusions and indicates outlook in relation to further line of work.

## **2. State of the art**

### **2.1. Applications of remote sensing for erosion studies in large spatial scale**

The application of satellite observations data for erosion monitoring and assessment at regional or large agricultural landscape scale has been proven to be significantly helpful (Magliulo et al. 2020). The advantages of using remote sensing data for erosion studies lies on its ability of capturing spatiotemporal trends at various scales. Broadly speaking two types of remote sensing tools are used for soil degradation studies namely passive and active sensing tools (Goldshleger et al. 2010). The passive sensing tools involve utilizing reflected solar radiation while the active sensing tools utilize artificial radiation sources such as radar. Freely available satellite images such as the Landsat series are dominantly employed in soil erosion researches in large landscape scale analysis (Sepuru and Dube 2018). However, the application of high spatial and hyperspectral resolution remote sensing data has been gaining momentum in recent years (Bargiel et al. 2013; Goldshleger et al. 2010; Wang et al. 2009; Schmid et al. 2016) though their relatively high acquisition prices constrains their application for large area coverage researches.

More often the images are employed to either indirectly provide inputs, such as C factor values, for various erosion prediction models or to directly identify erosion features such as depositional sites at the fields (Magliulo et al. 2020; Žižala et al. 2019; Vrieling 2006). At national or regional scales, the study of erosion phenomena using remote sensing application requires datasets of ground truthing information or expert's knowledge of the areas being investigated. In the case of the direct assessment of erosional features such as soil removal or depositional site identification, the soil spectral properties of the fields are used to assess erosional phenomenon (Magliulo et al. 2020; Schmid et al. 2016; Chabrillat et al. 2014). It is documented that the spectral properties of eroded soils can be differentiated from noneroded soils due to the associated changes in mineral or textural compositions of the soils (Žižala et al. 2017; Chabrillat et al. 2014). In this particular case, apart from the spatial resolution, the spectral resolution of the remote sensing data plays a major role in finely characterizing the soil surface. Shi et al. (2020) indicate that indirectly predicting the soil aggregate stability, which is an important soil property that determines soil erodibility condition, can be relatively adequately mapped using hyper spectral resolution data. However, Žižala et al. (2017) point out that in highly heterogenous areas the applicability of hyperspectral data needs to be backed up with locally precise topographic and geological data and hence entailing further calibration and validation for various spatial conditions. It can also be noted that soil infiltration rates and surface crust formations, attributes that directly influence soil erosion rates, can be assessed using hyperspectral data (Goldshleger et al. 2010). The application of these high spectral resolution data in large scale studies either through direct assessment of the field conditions or indirectly for spatially explicit model input parameters, however, is still not well exploited.

Synthetic aperture radar (SAR) data has been deployed to detect soil erosion at basin scale (Agnihotri et al. 2019; Amitrano et al. 2013). The mechanism behind detecting the degraded land using SAR data lies on the loss of physical and chemical properties of the eroded soils such as dielectric constant, conductivity and moisture holding capacity as opposed to non-eroded soils. One of the drawbacks of using radar data for large scale application, however, is its inability to penetrate dense vegetation cover and hence the signals unable to reach the ground in addition to the sensitivity of the backscatter to terrain undulations (Baghdadi et al. 2008). SAR images have the advantage of being operable in all weather and temporal conditions.

Remote sensing data have also been widely employed for gully mapping at large landscape scale analysis (Wang et al. 2020; Arabameri et al. 2020). The advancement of machine learning techniques are also improving the accuracy of identifying gully formation at regional scale assessment (Arabameri et al. 2019; Wang et al. 2020). However, the extraction of gully areas at wider scales using remote sensing images requires ancillary input data particularly topographic and land use type data (Wang et al. 2020).

The most common application of remote sensing data for large spatial coverage erosion studies is found to be the indirectly employing of the data to provide model parameter inputs for soil erosion modelling. Empirical models, particularly the (R)USLE, are widely combined with remote sensing images for erosion studies on large scale studies (Phinzi and Ngetar 2019; Sepuru and Dube 2018). In general all the inputs of the USLE model can be parametrized using remote sensing images (Phinzi and Ngetar 2019). There have been successes of computing the R factor from radar detected high temporal resolution rainfall data with relatively adequate accuracy at large landscape (Fischer et al. 2016; Fischer et al. 2018) and regional scale (Alexandridis et al. 2015; Phinzi and Ngetar 2019) studies. The erodibility factor (K) has also been derived from

remote sensing data (Alexakis et al. 2019) with moderately acceptable accuracy, although are very few in number (Phinzi and Ngetar 2019). Deriving C factor value from remote sensing data for regional and global scale studies has already become an established practice, as it has been discussed in section 1.1, for global (Guerra et al. 2020), regional (Alexandridis et al. 2015) and large landscape scale (Feng et al. 2018) investigations worldwide.

In general, despite there is an increasing trend of utilizing remote sensing data for erosion monitoring and assessment at larger spatial scales, it is still not sufficient in addressing several related issues such as spatiotemporal variations in land management practices and the influence on soil erosion at large (Sepuru and Dube 2018). Alewell et al. (2019) stress that without due attention to the assessment and understanding of soil erosion rates beyond plot or field scales, it would be cumbersome to address other related problems such as climate change and carbon sequestration phenomena. One of the major constraints in applying remote sensing data for erosion studies at larger area extent is the relatively low frequency of cloud free available images from the freely available passive remote sensing tools such as the Landsat series. Combining different data sources (Žižala et al. 2019), for instance the recently launched Sentinel 1 and 2 satellites, can enhance the accuracy of capturing spatiotemporal variability of soil erosion at large area extent coverage.

### 3. Material and Methods

#### 3.1. Study site description

The study takes the Quillow catchment (168km<sup>2</sup>) in Uckermark district, Brandenburg state of German, as a case study (Fig.1a). The dominant soil types prevailing in the study area include Luvisols to Calcaric Regosols (at the hilly areas), Luvisol or Haplic Luvisol (in the plateau), and Stagnosols (in the valley areas) (Wulf et al. 2016; Lischeid et al. 2016; Deumlich et al. 2010). The climatic condition of the region is described as temperate and continental type with annual mean air temperature ranging between 7.8 °C and 9.5 °C and mean annual rainfall of 460.3 mm was recorded between the years 1992 to 2016 at Dedelow weather station located in the study area (Vogel et al. 2016). Topographically the area is characterized as gently undulating (Fig.1b) with altitudinal ranges of 14m to 160 m above sea level (Lischeid et al. 2016).

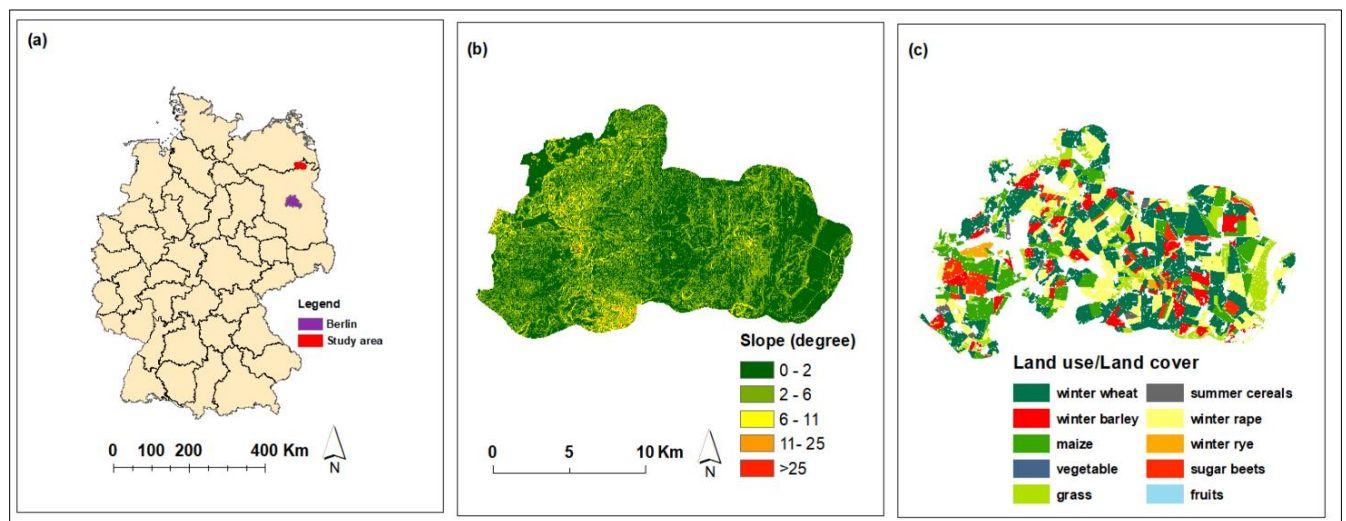


Figure 1 Overview of the study area: a) location of the study catchment, b) slope steepness in percent, c) land use/cover identified using IACS 2016 data.

#### 3.2. Data and processing

##### 3.2.1. Remote sensing data

One of the critical challenges of using satellite images, particularly passive remote sensing sources, for multitemporal investigation of erosion research is acquiring cloud free images. Here combination of Landsat 7 & Landsat 8 (using path 193, row 23) data along with Sentinel 2 (using

tile ID 33UVV) data were downloaded from the USGS (<https://earthexplorer.usgs.gov/>) and from Copernicus Open Access Hub (<https://scihub.copernicus.eu/dhus/#/home>) respectively. In total 29 time series images from 2013 to 2016 were used in the study. The overview of the images used are described in table 1. All the Landsat images are level 2A data that are atmospherically corrected. The Sentinel 2A data are atmospherically corrected using the freely available software Sen2cor (<https://step.esa.int/main/third-party-plugins-2/sen2cor/>). All the scenes used for the analysis are with less than 30% cloud cover.

Table 1 Overview of the multitemporal satellite images used for the analysis

Satellites	Spectral bands used	Spectral description	Spatial resolution	Acquired scene dates
Landsat 7	Band 3	Visible Red	30 m	10 February 2014; 30 March 2014; 01 May 2014; 18 June 2014; 04 July 2014; 06 September 2014; 08 October 2014; 17 March 2015; 05 June 2015; 27 October 2015; 23 June 2016
	Band 4	Near Infrared	30 m	
Landsat 8	Band 4	Visible Red	30 m	29 October 2013; 10 June 2014; 13 August 2014; 25 March 2015; 10 April 2015; 13 June 2015; 03 October 2015;
	Band 5	Near Infrared	30 m	
Sentinel-2A	Band 4	Visible Red	10 m	04 July 2015; 03 August 2015; 15 September 2015; 31 December 2015; 02 April 2016; 22 April 2016; 02 May 2016; 09 May 2016; 12 May 2016; 08 June 2016; 11 June 2016; 21 July 2016
	Band 8a	Vegetation Red edge	20 m	

In order to make sure the radiometric and phenological consistency between two temporally close Landsat and Sentinel images, simple pixel-based correlation analysis was performed. It is indicated that the mean NDVI values computed using the two images resulted in high correlation coefficient (up to  $r^2=0.97$ ) and no statistically significant variation in their mean values detected (Fig. 2). The Sentinel 2A data were re-sampled to 30 m resolution using the nearest neighbourhood method, to align with the Landsat images in further analysis.

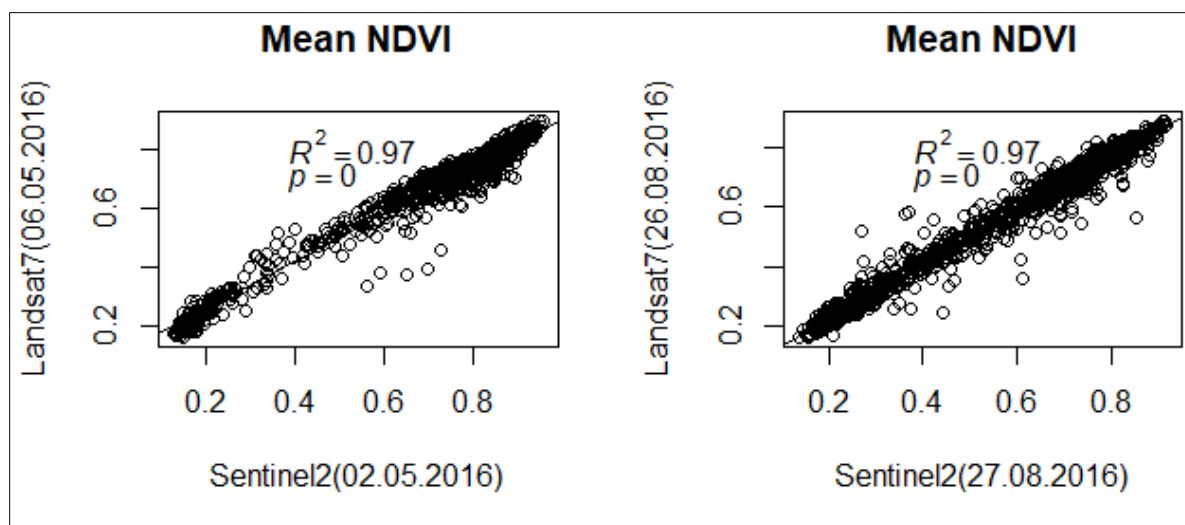


Figure 2 Comparison between mean NDVI values derived from two closely sensed Sentinel 2 and Landsat 7 data during May and August. The Values are the averages of each parcel (n = 1130 parcels) extracted using 2016 IACS data.

### 3.2.2. Land use data

The Integrated Administrative and Control System (IACS) data, provides annually updating information on land use types at field scale as a single vector dataset (Lüker-Jans et al. 2016). The IACS data provides information on agricultural land use types such as arable land or grass land, specific crop type, field block identification, parcel size, etc. for a single parcel of land specified by an official numerical codes (Steinmann and Dobers 2013). Datasets from 2013 to 2016 were used to identify crop types and determine crop sequencing patterns in the study area (see section 3.3. and 3.4). As the focus of this research is on arable lands, other land use types were excluded from the analysis. The proportion of the majorly grown crops in 2016 in the study area can be seen from Fig.1c. Winter Wheat(WW), Winter Barley (WB), Winter Rye (WRy), Winter Rape (WR), Maize (Mz), Sugar beet (SB) and Summer Cereals (SC) are included for the analysis in the present study.



### 3.3. C factor determination

#### 3.3.1. SLR based literature values assigning ( $C_{lit}$ )

In this study, periodic SLR values for each specific crop types, determined by the IACS data, were assigned from long term empirically measured SLR data, as per DIN 19708 (2005). These SLR values were determined according to the corresponding cropping stages of individual crops considered and the annual mean  $C_{lit}$  was assigned to each crop type in the end. For temporally varying  $C_{litM}$  determination erosivity proportion of each month obtained from Deumlich (1999) was used to weight SLR values.

#### 3.3.2. NDVI based C factor ( $C_{ndvi}$ ) computation

First NDVI values from each image scene was calculated using Eq.2:

$$NDVI = \frac{NIR - Red}{NIR + Red}, \quad (Eq.2)$$

the NDVI value ranges between -1 and +1; the higher the NDVI value the greener the vegetation coverage indicating that photosynthetically active vegetation is reflecting much of the near infrared radiation (NIR) while absorbing the visible range (Red) of the spectrum. The NDVI based C factor ( $C_{ndvi}$ ) was then computed from each image scene using the equation (Eq.3) developed by van der Knijff et al. (1999):

$$C_{ndvi} = \exp \left[ -\alpha \cdot \frac{NDVI}{(\beta - NDVI)} \right], \quad (Eq.3)$$

where  $\alpha$  and  $\beta$  are empirical fitting parameters where better goodness of fit was obtained using a value of 2 for  $\alpha$  and 1 for  $\beta$  (van der Knijff et al. 1999).

### 3.4. Crop rotation identification

Crop rotational patterns are determined by intersecting consecutive IACS data (from 2013 to 2016) through the geoprocessing tools of Arc Map (v10.2.2) which in the end provides an intersected polygon map for a cropping calendar. The final intersected polygon then will have its own consecutive years crop history from which the majorly grown crops in the study area were

taken as succeeding crops to determine their pre-crops through the query building tool in the ArcGIS environment. In total 21 year to year crop rotation patterns were used for the analysis based on their proportion of coverage in the study area. The rotations and their coverage proportion in the entire landscape is depicted in Fig.3.

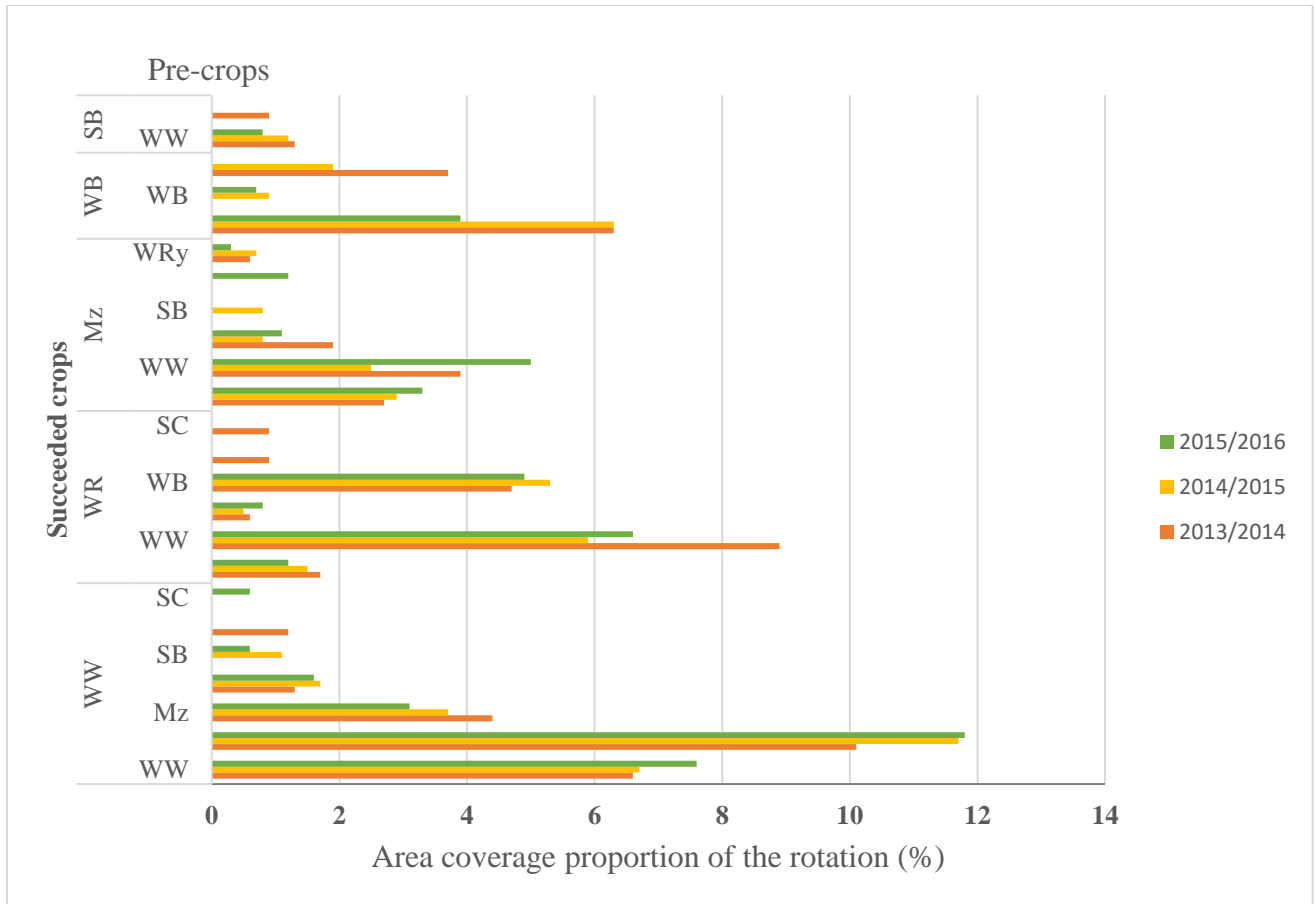


Figure 3 Area coverage (%) of crop rotations considered in the analysis disaggregated for each cropping calendars (2013/14 to 2015/16).

### 3.5. Soil erosion modelling

The Universal soil loss equation (USLE) was employed in the case of potential erosion prediction. The equation compartmentalizes the process of soil erosion into six factors

(Wischmeier and Smith 1978) (Eq.4):

$$A = R \cdot K \cdot L \cdot S \cdot C \cdot P , \tag{Eq.4}$$

where  $A$  is the predicted annual soil loss in  $\text{t ha}^{-1} \text{y}^{-1}$ .  $R$  is the rainfall erosivity factor calculated as the product of the maximum 30-minute rainfall intensity ( $I_{30}$ ) and energy ( $E$ ) of rainfall event. Eight-year average (from 2006 to 2013) of  $EI_{30}$  ( $\text{N h}^{-1}$ ) was calculated using  $1 \times 1$  km spatial and 5-minute temporal resolution radar weather data (RADOLAN) obtained from the German Weather Service (DWD) for the study area. Utilizing radar weather data for rainfall erosivity calculation and erosion prediction has been found to produce adequate results (Fischer et al. 2016).  $K$  represents the soil erodibility factor ( $\text{t h ha}^{-1} \text{N}^{-1}$ ), which was calculated according to Wischmeier and Smith (1978) using data obtained from the German soil appraisal “Bodenschätzung”, a publicly available data of different soil properties in the study area (Vogel et al. 2016). The  $L$  and  $S$  are the topographic factors which represent the slope length ( $L$ ), calculated according to Hickey (2000), and slope steepness ( $S$ ) calculated based on Nearing (1997) using 5 m spatial resolution digital elevation model (DEM). The  $C$  is the unit free cover and management factor, which is the ratio of soil loss under known vegetation cover to that of bare soil. The  $C$  factor is the main manipulation factor in this study hence the potential soil erosion prediction is done for both  $C_{\text{ndvi}}$  and  $C_{\text{lit}}$  values (see section 3.3). The  $P$  factor is the soil protecting practice factor; for this region, a value of 1 is used as no support practice exists.

Finally, the erosion prediction accuracy of using the USLE model was assessed by comparing the model output against long term (1982 to 1996) measured average soil erosion values obtained from field trials at the Holzendorf (Latitude 53.386818, Longitude 13.780225) research station (Deumlich et al. 2018).

### 3.6. Statistical analysis

#### 3.6.1. Comparison between $C_{ndvi}$ and $C_{lit}$

Simple correlation and Root Mean Square Error (RMSE) were employed to quantify the deviation of NDVI based C factor ( $C_{ndvi}$ ) from SLR based C factor values from literature ( $C_{lit}$ ) and the subsequent soil erosion prediction using these two C factor values was compared using RMSE (Eq.5).

$$RMSE_C = \sqrt{\frac{\sum_1^n (C_{lit} - C_{ndvi})^2}{n}} \text{ and } RMSE_{SL} = \sqrt{\frac{\sum_1^n (SL_{C_{lit}} - SL_{C_{ndvi}})^2}{n}} \quad (\text{Eq.5})$$

where,  $RMSE_C$  and  $RMSE_{SL}$  are the root mean square error for C factor and soil loss rate comparison,  $SL_{C_{lit}}$  is the potential soil loss rates predicted using  $C_{lit}$ ,  $SL_{C_{ndvi}}$  is the soil loss rates predicted using  $C_{ndvi}$ , and  $n$  is the number of pixels coinciding in the analysis.

#### 3.6.2. Quantifying the sensitivity of $C_{ndvi}$ to biophysical variables

The sensitivity of NDVI derived C values to various biophysical conditions was assessed through multiple regression analysis. The biophysical variables used in the study are topographic features such as slope steepness (degree), slope shape, slope position, slope aspect, edaphic conditions of the area (proxied through K factor values), and seasonal and crop type variation. Detailed explanation of the variables and procedures are indicated in Ayalew et al. (2020).

#### 3.6.3. Crop rotational impacts on $C_{ndvi}$ and soil erosion rate

The average C factor values and soil loss rates of each parcel (intersected polygon, section 3.4), representing crop rotations, were extracted using the R spatial analysis package (“extract”). Analysis of variance (ANOVA) was used to differentiate the impact of different crop sequencing patterns on C factor values and subsequently on soil erosion rates through the GLM. Means are also separated using Least Significant Difference (LSD) at 5% probability level. However, to control unaccounted variation which could arise from differences in soil type and topography features, six blockings were included. The study area as a result, was divided according to three

blockings of soil erodibility values, (block 1,  $K < 0.15$ ; block 2,  $0.15 < K < 0.3$ ; and block 3,  $K > 0.30$ ) and three blockings of LS factor, representative of topographic variability, (block 4,  $LS < 0.4$ ; block 5,  $0.4 < LS < 0.8$ ; block 6,  $LS > 0.8$ ).

## 4. Results and discussion

### 4.1. Comparison between $C_{ndvi}$ and $C_{lit}$

The results indicated that the  $C_{ndvi}$  and  $C_{lit}$  gave comparably close estimates in a temporally varying manner. Better correlation between monthly  $C_{ndvi}$  and  $C_{lit}$  values was observed in images taken in the months between spring and mid-summer (highest  $r = 0.93$ ), while the lowest correlation was observed in the months of late summer and autumn (lowest  $r = -0.58$ ). This can be explained due to the reduced vitality of many winter-sown crops during the latter part of the year. Incorporating yellow vegetation indices such as normalized difference tillage index (NDTI), and normalized difference senescent vegetation index (NDSVI), in the process of formulating the C factor equation, can improve the C-value estimation across all seasons (Feng et al. 2018). Apart from seasonal variation, variation in land cover types also played role in the discrepancies between the two methods. The average annual C factor values computed using the two methods resulted in higher discrepancies for cereals (up to 85%) than other field crops such as WR (5%) and Mz (5.3%). This variation among different crop types can be explained because of the variation in their canopy orientation of the crops considered. Cereals categorized as erectophile canopy (vertically arranged leaves), reported to trap reflected radiation within the canopy and hence reduce the NDVI (Jackson and Pinter 1986). Therefore, using high resolution and temporally dynamic land use data enables to capture discrepancies to individual crop cover type level.

Spatially speaking, classifying the study area according to C factor values indicated discrepancies between the two C value estimation methods.  $C_{lit}$  resulted in values of less than 0.1 for most of the landscape while using  $C_{ndvi}$  resulted in the same category on 13% of the study area. The average landscape C factor value computed through  $C_{ndvi}$  was 0.204 while  $C_{lit}$  gave average value of 0.128. The discrepancy was much pronounced on the subsequent potential soil loss rate prediction. In aggregate, the soil loss rate obtained by employing  $C_{ndvi}$  as an input ( $SL_{ndvi}$ ) for the

USLE model resulted in two times higher prediction than using  $C_{lit}$  as an input factor ( $SL_{clit}$ ). Spatially, the potential soil loss rates predicted using the two different C factor inputs revealed a RMSE of as high as  $1.17 \text{ t ha}^{-1} \text{ y}^{-1}$ , which was below the maximum tolerable soil erosion limit of the region (Verheijen et al. 2009). In addition, the spatial distribution of the potential soil erosion risk predicted using the two C factor methods varied notably. For example, the proportion of the landscape classified below the maximum tolerable soil loss limit in the case of  $SL_{cndvi}$  was close to 85%, while the same classification in the case of  $SL_{clit}$  accounted for close to 70%. However,  $SL_{cndvi}$  can improve the spatially explicit identification of soil erosion risks as opposed to  $SL_{clit}$  which was indicated from the relatively higher coefficient of variation (CV) 91% compared with the 84% CV in  $SL_{clit}$ . This indicates the potential of utilizing NDVI-based C factor estimation for physically based erosion models such as SWAT, provided that appropriate modifications applied to address the discrepancy or sensitivity of it (see section 4.2 for addressing the sensitivity).

#### **4.2. Quantifying the sensitivity of $C_{ndvi}$ to biophysical variables**

The regression analysis indicated that  $C_{ndvi}$  was found to respond to variations in edaphic and topographic conditions of the landscape (Table 2). The sensitivity of  $C_{ndvi}$  values to heterogenous soil condition of the landscape was consistently captured through the soil erodibility factor. In the present study, an increase in the value of soil erodibility resulted in incremental change in the values of  $C_{ndvi}$ , though the magnitude varied in different months of a year. Sizeable influence, in terms of magnitude, was observed during spring and the beginning of the summer months, when the ground cover contrast was expected to be high. It is well documented that the soil characteristics such as organic matter content, soil colour, soil texture, surface roughness influence the spectral properties of a surface (Ding et al. 2014). In the present study, consistent variations in the reflectance values of both Red and NIR spectrum were observed on soils with an

erodibility class of greater than  $0.3 \text{ t h ha}^{-1}\text{N}^{-1}$ (Fig.4). The higher the erodibility values the higher the estimated  $C_{\text{ndvi}}$  values which could be due to the change in soil condition such as organic matter content or soil colour.

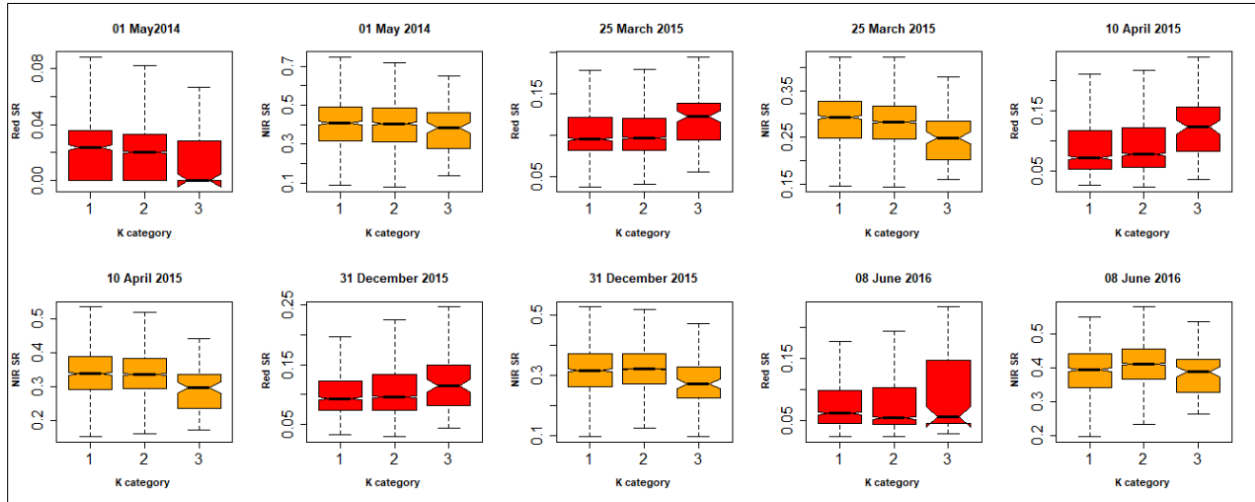


Figure 4 Surface reflectance (SR) of NIR and red bands across soil erodibility categories (K categories: 1,  $\leq 0.15$ ; 2= 0.15 to 0.3; 3  $\geq 0.3$ ) and different seasons (adopted from Ayalew et al. (2020))

The influence of soil heterogeneity on  $C_{\text{ndvi}}$  values also varied across different cover types in the study area. Even at the same growth stages, parcels covered with WR showed less sensitivity to soil erodibility variation as compared to parcels covered with WRy. WR, belonging to the plagiophile canopy, is reported to have a higher plant area index compared with WRy or WW (belonging to the erectophile canopy) at the same phenological stage (Truckenbrodt and Schnullius 2018). Identifying land cover type to specific species level, by coupling remote sensing data with the IACS data, enabled quantifying the sensitivity of  $C_{\text{ndvi}}$  estimation to soil background heterogeneity in relation to various crops' growth stage.



Table 2 Regression results showing the influence of biophysical variables on  $C_{ndvi}$  across scene dates.

Scene Dates		Biophysical variables									
		Slope shapes			Crop types (with reference to WW)						
		K factor	convex	concave	WB	Mz	SC	WR	WRy	SB	Constant
R <sup>2</sup>	Coef.	Coef.	Coef.	Coef.	Coef.	Coef.	Coef.	Coef.	Coef.	Coef.	
29 Oct. 2013	0.4	0.06	0.00	-0.12	-0.11*	0.03*	0.14*	-0.24*	-0.02	0.21*	0.25*
10 Feb. 2014	0.6	0.08	0.01*	0.01	-0.10*	0.23*	0.25*	-0.17*	-0.13*	0.29*	0.22*
30 Mar. 2014	0.8	0.05	0.01*	0.01	-0.03*	0.40*	0.35*	-0.05*	-0.03*	0.47*	0.04*
01 May 2014	0.8	0.16*	0.00	0.00	-0.02*	0.49*	0.02	0.06*	-0.01	0.55*	-0.01
10 June 2014	0.7	0.11*	0.01*	0.00	0.02*	0.19*	0.01	-0.00	0.02*	0.02*	-0.02*
04 July 2014	0.5	0.09*	0.01	-0.02*	0.31*	0.01	-0.01	0.08*	0.26*	-0.06*	0.05*
13 Aug. 2014	0.6	0.07	0.02	-0.01	-0.03*	-0.45*	-0.30*	-0.25*	-0.11*	-0.45*	0.42*
06 Sept. 2014	0.7	0.08	0.04*	0.00	0.04*	-0.43*	-0.21*	0.12*	0.13*	-0.41*	0.40*
08 Oct. 2014	0.4	0.02	0.01	-0.01	0.00	-0.17*	-0.27*	-0.32*	-0.17*	-0.19*	0.38*
25 Mar. 2015	0.7	0.17*	0.02*	0.01	-0.06*	0.33*	0.36*	-0.06*	0.17*	0.39*	0.10*
10 Apr. 2015	0.8	0.16*	0.01*	0.00	-0.05*	0.44*	0.47*	-0.05*	0.15*	0.51*	0.03*
13 June 2015	0.8	0.14*	0.01	-0.00	0.03*	0.39*	0.01	-0.00	0.03*	0.20*	-0.02*
04 July 2015	0.5	0.09*	0.01*	-0.01*	0.27*	0.15*	-0.02	-0.04*	0.09*	0.00	0.05*
03 Aug. 2015	0.8	0.09*	-0.01	-0.02*	0.02*	-0.50*	-0.14*	-0.06*	-0.02	-0.52*	0.53*
03 Oct. 2015	0.4	0.13	0.01	0.00	0.02	-0.30*	-0.24*	-0.31*	-0.09*	-0.06*	0.46*
31 Dec. 2015	0.4	0.28*	0.03*	-0.01	-0.14*	0.16*	0.41*	-0.16*	0.06*	0.33*	0.14*
02 Apr. 2016	0.6	0.16*	0.05*	0.01	-0.06*	0.31*	0.42*	-0.14*	-0.14*	0.42*	0.19*
22 Apr. 2016	0.7	0.15*	0.03*	0.00	0.00	0.49*	0.42*	-0.05*	-0.09*	0.54*	0.06*
12 May 2016	0.9	0.15*	0.01*	0.00	0.00	0.60*	0.06*	0.04*	-0.03	0.66*	-0.01
08 June 2016	0.8	0.21*	0.02*	-0.01	0.01*	0.38*	0.00	0.00	-0.01	0.14*	-0.04*
23 June 2016	0.5	0.02	0.01	-0.01	0.26*	0.04*	-0.02	0.00	0.04*	-0.02	0.01

\* indicates coefficients statistically significant at  $P < 0.01$ ; coef., regression coefficients. Adopted from Ayalew et al. (2020)

Spectral indices other than NDVI, such as enhanced vegetation index (EVI) and soil adjusted vegetation index (SAVI), have been proposed to enhance the sensitivity to biomass variation while reducing soil background noise on vegetation spectral property of a landscape (Huete et al. 2002). However, these indices may present a higher sensitivity to topographic variability which might take effect in rugged landscapes. Therefore, consideration of all biophysical variables in calibrating spectral indices for the purpose of environmental monitoring such as erosion risk assessment remains essential.

In the present study topographic features in the form of slope shape showed consistent influence on  $C_{ndvi}$  values. Convex shaped slope, as compared to flat slope, demonstrated consistently significant incremental implications on  $C_{ndvi}$  values, with the highest coefficient of 0.05 ( $P < 0.01$ ;  $R^2 = 0.57$ ) predicted on the image taken on 02 April 2016 (Table2). Concave slope, on the other hand, had a negative relation with the estimated  $C_{ndvi}$  values in a temporally dependant manner. In general, the influence of topographic variation is explained to be in two direct and indirect ways. Directly, the landform change (e.g., from flat to hilly topography) on the spectrum reflectance property of the surface or indirectly through the influence of topographic features on the greenness of the vegetation cover (Ding et al. 2014; Matsushita et al. 2007). The influence of concaved slope on  $C_{ndvi}$  values was predominantly observed on images taken from the end of June to August. This can be attributed to the indirect influence of topographic features on vegetation status. Concave slopes, located towards the depression parts of the study area (Deumlich et al. 2010), are most likely to be cooler in summer as compared to flat land, in addition to their being depositional sites where by their water drainage pattern and soil properties differ as compared to erosional sites of the convex shaped slopes. These attributes of the landscape could also play a role in the status of crop growth and subsequently in  $C_{ndvi}$  estimates. In general, while using NDVI for

C factor estimations, considerations must be taken into account to accommodate land formation influences on the status of the vegetation.

#### **4.3. Crop rotation impacts on C factor values**

From the intersects of the consecutive IACS data, it was possible to identify that the most prevalent year to year crop rotations, in terms of their share in the study area, involves WW, WR, and Mz crops in all the three years considered. The ANOVA result revealed that different crop rotation patterns had significant implications on both average annual C values and predicted average annual potential soil erosion rates in all the years considered. Mz and SB, used both as pre crop and succeeding crops, found to be associated with high average annual C factor values, particularly self-sequencing of maize year after year. It was also possible to identify the importance of pre-crops in reducing the C factor values by incorporating WR as a pre crop for Mz cultivation than using other crops such as SB. The highest average annual C factor value of 0.39 was computed on SB/Mz rotation parcels.

Crop sequences involving WR inclined to reduce the average annual C values consistently. The lowest average annual C value, amounting to 0.07, was computed on parcels covered with WR preceded by pre-crops of winter cereals. Among the pre-crops of WR, however, Mz was found to result in higher C values when it preceded WR hence rotations composing of Mz and WR requires a due attention.

Considering the widely grown crop, i.e. WW, when succeeded from WR it was indicated to have the potential to reduce the annual average C value as compared to succeeded from the alternative pre-crop of SB or self-sequencing of WW. Peltonen-Sainio et al. (2019), through regional scale NDVI analysis, also indicate the positive influence of rapeseed as a pre-crop for various succeeding crops. Therefore, with respect to C factor management and soil erosion

considerations, sequencing of WW after WR could perform better in the study area as compared to succeeding from Mz or SB.

The study also indicated the temporal variability of C factor determination in relation to crop rotation patterns. The temporal variation can be associated with operational timing of different crops on consecutive cropping years. For example, Table 3 depicts that WW parcels which were pre-cropped with SB had significantly lower monthly C values than WW parcels preceded by any other pre-crops during early autumn season (September or October). This could be due mainly to the fact that parcels covered with SB had not yet been harvested in these months and hence the vitality of the vegetation cover status of SB remained vital to lower the values. However, during early spring (March and April), WW succeeded from SB indicated significantly higher monthly C values (0.29 in March and 0.162 in April) as compared to, for example WR/WW (0.118 in March and 0.054 in April). This can be attributed to the late sowing dates inflicted on WW as a consequence of late harvesting operation by the SB pre-crop cultivation (Castellazzi et al. 2008). Overall, the results indicate the possibility of using remote sensing data for large scale agricultural operation management in relation to environmental protection objectives in a temporally explicit manner.

Spatially it was also possible to indicate the association between crop rotation distributions and their annual C factor values at the parcel level. Again, rotations involving Mz and SB, in 2015/16 cropping calendar, covered around 17% (2,931 ha) of the entire agricultural landscape which corresponded well with the 21% classification of the landscape into annual C values of greater than 0.3. the lowest C factor values of less 0.1 corresponded with the spatial distribution of WR and Gr rotated parcels.

Table 3 Temporal dynamicity of C factor values in relation to crop rotation patterns

Succeeded crops	Pre-crops	Months*									
		February	March	April	May	June	July	August	September	October	December
WW	WW	0.223 <sup>abcd</sup>	0.168 <sup>fg</sup>	0.079 <sup>de</sup>	0.060 <sup>d</sup>	0.013 <sup>f</sup>	0.098 <sup>de</sup>	0.498 <sup>a</sup>	0.471 <sup>a</sup>	0.363 <sup>a</sup>	0.170 <sup>bc</sup>
	WR	0.199 <sup>abcd</sup>	0.118 <sup>g</sup>	0.054 <sup>de</sup>	0.018 <sup>d</sup>	0.007 <sup>f</sup>	0.068 <sup>e</sup>	0.490 <sup>a</sup>	0.473 <sup>a</sup>	0.420 <sup>a</sup>	0.132 <sup>bc</sup>
	Mz	0.314 <sup>a</sup>	0.228 <sup>ef</sup>	0.128 <sup>cd</sup>	0.052 <sup>d</sup>	0.034 <sup>ef</sup>	0.094 <sup>de</sup>	0.430 <sup>ab</sup>	0.233 <sup>bc</sup>	0.321 <sup>ab</sup>	0.296 <sup>ab</sup>
	WB	0.138 <sup>cd</sup>	0.132 <sup>g</sup>	0.054 <sup>de</sup>	0.038 <sup>d</sup>	0.008 <sup>f</sup>	0.068 <sup>e</sup>	0.489 <sup>a</sup>	0.485 <sup>ab</sup>	0.351 <sup>ab</sup>	0.121 <sup>bc</sup>
	SB	-	0.290 <sup>de</sup>	0.162 <sup>cd</sup>	0.009 <sup>d</sup>	0.034 <sup>ef</sup>	0.099 <sup>cde</sup>	0.469 <sup>a</sup>	0.021 <sup>c</sup>	0.125 <sup>b</sup>	0.361 <sup>a</sup>
	SC	0.233 <sup>abcd</sup>	0.141 <sup>efg</sup>	0.054 <sup>de</sup>	0.026 <sup>d</sup>	0.001 <sup>if</sup>	0.078 <sup>de</sup>	0.354 <sup>ab</sup>	0.385 <sup>a</sup>	0.334 <sup>ab</sup>	0.174 <sup>bc</sup>
	WRy	0.298 <sup>a</sup>	0.147 <sup>fg</sup>	0.084 <sup>cde</sup>	0.031 <sup>d</sup>	0.024 <sup>f</sup>	0.222 <sup>ab</sup>	0.470 <sup>a</sup>	0.564 <sup>a</sup>	0.515 <sup>a</sup>	-
WR	WW	0.121 <sup>d</sup>	0.116 <sup>g</sup>	0.037 <sup>e</sup>	0.084 <sup>d</sup>	0.005 <sup>f</sup>	0.043 <sup>e</sup>	0.486 <sup>a</sup>	0.411 <sup>a</sup>	0.179 <sup>b</sup>	0.077 <sup>c</sup>
	WR	0.147 <sup>cd</sup>	0.130 <sup>g</sup>	0.060 <sup>de</sup>	0.035 <sup>d</sup>	0.013 <sup>f</sup>	0.041 <sup>e</sup>	0.462 <sup>a</sup>	0.444 <sup>a</sup>	0.296 <sup>ab</sup>	0.116 <sup>bc</sup>
	Mz	0.282 <sup>ab</sup>	0.200 <sup>fg</sup>	0.078 <sup>de</sup>	0.196 <sup>c</sup>	0.019 <sup>f</sup>	0.042 <sup>e</sup>	0.305 <sup>ab</sup>	0.337 <sup>ab</sup>	0.293 <sup>ab</sup>	0.188 <sup>bc</sup>
	WB	0.124 <sup>d</sup>	0.133 <sup>g</sup>	0.043 <sup>e</sup>	0.057 <sup>d</sup>	0.008 <sup>f</sup>	0.033 <sup>e</sup>	0.407 <sup>ab</sup>	0.435 <sup>a</sup>	0.190 <sup>b</sup>	0.075 <sup>c</sup>
	WRy	0.120 <sup>d</sup>	0.095 <sup>g</sup>	0.009 <sup>e</sup>	0.097 <sup>d</sup>	0.001 <sup>f</sup>	0.077 <sup>de</sup>	0.442 <sup>ab</sup>	0.499 <sup>a</sup>	0.391 <sup>a</sup>	0.172 <sup>bc</sup>
Mz	WW	0.275 <sup>ab</sup>	0.342 <sup>cd</sup>	0.341 <sup>b</sup>	0.422 <sup>a</sup>	0.383 <sup>bc</sup>	0.204 <sup>b</sup>	0.102 <sup>cd</sup>	0.303 <sup>abc</sup>	0.171 <sup>b</sup>	0.158 <sup>bc</sup>
	WR	0.295 <sup>a</sup>	0.260 <sup>def</sup>	0.201 <sup>c</sup>	0.249 <sup>bc</sup>	0.169 <sup>d</sup>	0.171 <sup>bc</sup>	0.162 <sup>bcd</sup>	0.445 <sup>a</sup>	0.228 <sup>ab</sup>	0.130 <sup>bc</sup>
	Mz	0.437 <sup>a</sup>	0.435 <sup>b</sup>	0.426 <sup>c</sup>	0.441 <sup>a</sup>	0.354 <sup>c</sup>	0.171 <sup>b</sup>	0.125 <sup>bcd</sup>	0.106 <sup>c</sup>	0.219 <sup>ab</sup>	0.443 <sup>a</sup>
	WB	0.272 <sup>abc</sup>	0.229 <sup>efg</sup>	0.168 <sup>cd</sup>	0.369 <sup>ab</sup>	0.153 <sup>de</sup>	0.140 <sup>bcde</sup>	0.233 <sup>bc</sup>	0.181 <sup>bc</sup>	0.094 <sup>b</sup>	0.153 <sup>bc</sup>
	SB	-	0.544 <sup>a</sup>	0.537 <sup>a</sup>	0.481 <sup>a</sup>	0.491 <sup>a</sup>	0.265 <sup>a</sup>	0.066 <sup>cd</sup>	0.028 <sup>c</sup>	0.082 <sup>b</sup>	0.429 <sup>a</sup>
	SC	0.544 <sup>a</sup>	0.570 <sup>ab</sup>	0.565 <sup>ab</sup>	0.369 <sup>a</sup>	0.371 <sup>cd</sup>	0.148 <sup>bcde</sup>	0.009 <sup>cd</sup>	0.325 <sup>abc</sup>	0.031 <sup>b</sup>	0.232 <sup>abc</sup>
R <sup>2</sup>		0.44	0.62	0.70	0.62	0.73	0.44	0.61	0.60	0.55	0.35

Means followed by the same letters in a column are not significantly different from each other per LSD (P<0.05). (-) indicates not considered in the analysis. Adopted from Ayalew et al. (2021)

#### **4.4. Crop rotation and potential soil erosion rates**

The rotational patterns also indicated significant differences among themselves with respect to average annual soil erosion rates. Crop rotations involving SB and Mz as succeeding crops consistently and significantly resulted in higher average annual soil loss rates. These crops are row planted and widely spaced crops. Particularly, self-sequencing of maize (Mz/Mz) resulted in soil erosion rate as high as 72% compared to self-sequencing of WR and as high as 51% compared to self-sequencing of WW. This can be explained from the fact that Mz could not be able to provide year-round soil cover protection unlike WR or winter cereals self-sequencing patterns which more or less could provide better soil coverage. It is documented that rotations involving wide spaced row crops like potato, generate highest runoff amount in a plot experiment (Preiti et al. 2017).

Spatial distribution of the considered rotation patterns and their association with the potential soil erosion rate also indicated that rotation of root crops (SB) and row cultivated plants (Mz), need to be considered for rotation scheme on less sloping or flat areas. Overall, the result from the present study could help in identifying trends of potential soil erosion risks in relation to crop management patterns, as depicted in Figure 5, in a large agricultural landscape setup efficiently without requiring to conducting plot scale multi location trials.

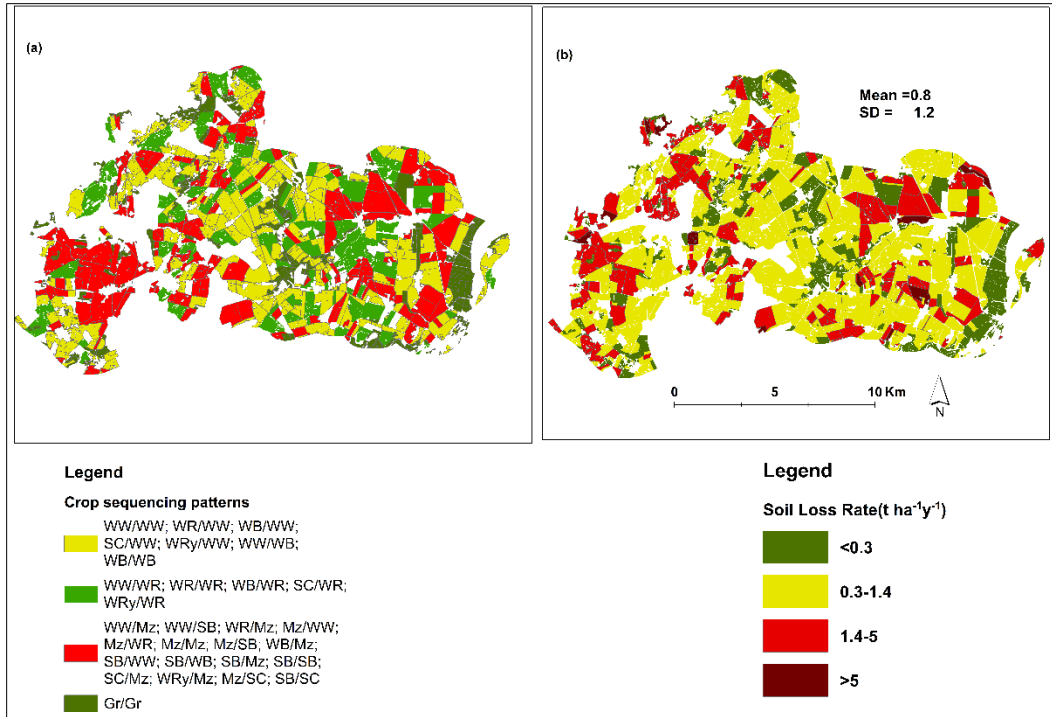


Figure 5 Spatial distribution of rotations and predicted potential soil loss rate. Modified from Ayalew et al. (2021)

Finally, to validate the accuracy of the USLE model prediction, the output from the current soil loss prediction of Mz/Mz parcel was compared with a long-term soil erosion rate measured from maize monocropping experimental plot. The potential soil erosion modelling of the Mz/Mz sequence in the 2013/14 cropping calendar resulted in an average soil loss rate of 1.87 t ha<sup>-1</sup>y<sup>-1</sup> a comparatively close prediction and within the range of the actual measured soil loss rate for Mz monoculture (1 t ha<sup>-1</sup> y<sup>-1</sup>).

## 5. Conclusions and outlook

The present research indicated the discrepancy between NDVI based and empirical based C factor estimation methods and subsequently the importance of quantifying the sensitivity of NDVI based C factor estimations while dealing with large heterogeneous landscapes by utilizing annually updating land use data and time series optical satellite data. It was presented that biophysical variables such as soil conditions and topographic features need to be considered in the process of deriving NDVI based C factor values. In quantifying the sensitivity of  $C_{ndvi}$ , the soil erodibility condition (K factor) was reliable and consistent to explain the response of  $C_{ndvi}$  values to soil background heterogeneity. It was also indicated that the relationship between  $C_{ndvi}$  estimates and heterogeneous soil conditions can be further dissected according to canopy structure of different crop cover types. Further research on this regard, with ground measurements, however, is needed to further understand the relationship of crop canopy structure and NDVI based C factor value estimation for future. It was also possible to quantify the sensitivity of NDVI based C factor derivation to topographical variations across different temporal periods.

Combining multitemporal satellite data with land use data enabled to compute C factor values for various crop rotational patterns and subsequently determine the potential soil erosion rates at large agricultural landscape level. Interannual variability of the influence of various crop rotations on C values was captured by the method employed.

For the future, research needs to be directed towards formulating C factor value estimation by considering all relevant biophysical variables such as spatially explicit temperature and rainfall data, as the NDVI is directly influenced by temperature in the middle latitude and rainfall in the tropical areas, along with yellow vegetation indices in order to improve the accuracy of using remote sensing images for the purpose. In determining the influence of cropping practices on C factor values and subsequent soil erosion prediction, data including agricultural management



decisions such as, tillage and residue management practice and fertilization schemes could further improve. As the study also indicated the spatial and temporal aspect of the crop rotation impacts it could be feasible to employ process-based models for future endeavours.

## 6. References

- Agnihotri, Ashwani Kumar; Ohri, Anurag; Gaur, Shishir; Shivam; Das, Nilendu; Mishra, Sachin (2019): Flood inundation mapping and monitoring using SAR data and its impact on Ramganga River in Ganga basin. In *Environmental monitoring and assessment* 191 (12), p. 760. DOI: 10.1007/s10661-019-7903-4.
- Alewell, Christine; Borrelli, Pasquale; Meusburger, Katrin; Panagos, Panos (2019): Using the USLE: Chances, challenges and limitations of soil erosion modelling. In *International Soil and Water Conservation Research* 7 (3), pp. 203–225. DOI: 10.1016/j.iswcr.2019.05.004.
- Alexakis, Dimitrios D.; Tapoglou, Evdokia; Vozinaki, Anthi-Eirini K.; Tsanis, Ioannis K. (2019): Integrated Use of Satellite Remote Sensing, Artificial Neural Networks, Field Spectroscopy, and GIS in Estimating Crucial Soil Parameters in Terms of Soil Erosion. In *Remote Sensing* 11 (9), p. 1106. DOI: 10.3390/rs11091106.
- Alexandridis, Thomas K.; Sotiropoulou, Anastasia M.; Bilas, George; Karapetsas, Nikolaos; Silleos, Nikolaos G. (2015): The Effects of Seasonality in Estimating the C-Factor of Soil Erosion Studies. In *Land Degrad. Develop.* 26 (6), pp. 596–603. DOI: 10.1002/ldr.2223.
- Amitrano, Donato; Di Martino, Gerardo; Iodice, Antonio; Riccio, Daniele; Ruello, Giuseppe; Papa, Maria Nicolina et al. (2013): High Resolution SAR for Monitoring of Reservoirs Sedimentation and Soil Erosion in Semi-Arid Regions. In : 2013 IEEE International Geoscience and Remote Sensing Symposium (IGARSS). IEEE Inst Elect & Elect Engineers, Geoscience & Remote Sensing Soc. 345 E 47TH ST, NEW YORK, NY 10017 USA: IEEE, pp. 911–914.
- Arabameri, Cerda; Rodrigo-Comino; Pradhan; Sohrabi; Blaschke; Bui, Tien (2019): Proposing a Novel Predictive Technique for Gully Erosion Susceptibility Mapping in Arid and Semi-arid Regions (Iran). In *Remote Sensing* 11 (21), p. 2577. DOI: 10.3390/rs11212577.
- Arabameri, Alireza; Pradhan, Biswajeet; Bui, Dieu Tien (2020): Spatial modelling of gully erosion in the Ardib River Watershed using three statistical-based techniques. In *CATENA* 190, p. 104545. DOI: 10.1016/j.catena.2020.104545.
- Ayalew, Dawit A.; Deumlich, Detlef; Šarapatka, Bořivoj; Doktor, Daniel (2020): Quantifying the Sensitivity of NDVI-Based C Factor Estimation and Potential Soil Erosion Prediction using Spaceborne Earth Observation Data. In *Remote Sensing* 12 (7), p. 1136. DOI: 10.3390/rs12071136.
- Ayalew, Dawit Ashenafi; Deumlich, Detlef; Šarapatka, Bořivoj (2021): Agricultural landscape-scale C factor determination and erosion prediction for various crop rotations through a remote sensing and GIS approach. In *Eur. J. Agron.* 123, p. 126203. DOI: 10.1016/j.eja.2020.126203.
- Baghdadi, Nicolas; Cerdan, Olivier; Zribi, Mehrez; Auzet, Véronique; Darboux, Frédéric; El Hajj, Mahmoud; Kheir, Rania Bou (2008): Operational performance of current synthetic aperture radar sensors in mapping soil surface characteristics in agricultural environments: application to hydrological and erosion modelling. In *Hydrol. Process.* 22 (1), pp. 9–20. DOI: 10.1002/hyp.6609.
- Bargiel, D.; Herrmann, S.; Jadczyzyn, J. (2013): Using high-resolution radar images to determine vegetation cover for soil erosion assessments. In *Journal of environmental management* 124, pp. 82–90. DOI: 10.1016/j.jenvman.2013.03.049.
- Bégué, Agnès; Arvor, Damien; Bellon, Beatriz; Betbeder, Julie; Abelleira, Diego de; P. D. Ferraz, Rodrigo et al. (2018): Remote Sensing and Cropping Practices: A Review. In *Remote Sensing* 10 (2), p. 99. DOI: 10.3390/rs10010099.

- Borrelli, Pasquale; Meusburger, Katrin; Ballabio, Cristiano; Panagos, Panos; Alewell, Christine (2018): Object-oriented soil erosion modelling: A possible paradigm shift from potential to actual risk assessments in agricultural environments. In *Land Degrad Dev* 29 (4), pp. 1270–1281. DOI: 10.1002/ldr.2898.
- Borrelli, Pasquale; Robinson, David A.; Fleischer, Larissa R.; Lugato, Emanuele; Ballabio, Cristiano; Alewell, Christine et al. (2017): An assessment of the global impact of 21st century land use change on soil erosion. In *Nat. Commun.* 8 (1), p. 2013. DOI: 10.1038/s41467-017-02142-7.
- Castellazzi, M. S.; Wood, G. A.; Burgess, P. J.; Morris, J.; Conrad, K. F.; Perry, J. N. (2008): A systematic representation of crop rotations. In *Agr. Syst.* 97 (1-2), pp. 26–33. DOI: 10.1016/j.agsy.2007.10.006.
- Chabrillat, S.; Milewski, R.; Schmid, T.; Rodriguez, M.; Escibano, P.; Pelayo, M.; Palacios-Orueta, A. (2014): Potential of hyperspectral imagery for the spatial assessment of soil erosion stages in agricultural semi-arid Spain at different scales. In : 2014 IEEE Geoscience and Remote Sensing Symposium. 2014 IEEE Geoscience and Remote Sensing Symposium, pp. 2918–2921.
- Conrad, C.; Lamers, J.P.A.; Ibragimov, N.; Löw, F.; Martius, C. (2016): Analysing irrigated crop rotation patterns in arid Uzbekistan by the means of remote sensing: A case study on post-Soviet agricultural land use. In *Journal of Arid Environments* 124, pp. 150–159. DOI: 10.1016/j.jaridenv.2015.08.008.
- de Jong, Steven M. (1994): Derivation of vegetative variables from a Landsat TM image for modelling soil erosion. In *Earth Surf. Process. Landforms* 19 (2), pp. 165–178. DOI: 10.1002/esp.3290190207.
- Deumlich, D.; Ellerbrock, R. H.; Frielinghaus, Mo. (2018): Estimating carbon stocks in young moraine soils affected by erosion. In *Catena* 162, pp. 51–60. DOI: 10.1016/j.catena.2017.11.016.
- Deumlich, Detlef (1999): Erosive Niederschläge und ihre Eintrittswahrscheinlichkeit im Nordosten Deutschlands. In *Meteorol. Z.* 8 (5), pp. 155–161. DOI: 10.1127/metz/8/1999/155.
- Deumlich, Detlef; Schmidt, Rolf; Sommer, Michael (2010): A multiscale soil-landform relationship in the glacial-drift area based on digital terrain analysis and soil attributes. In *Z. Pflanzenernähr. Bodenk.* 173 (6), pp. 843–851. DOI: 10.1002/jpln.200900094.
- DIN 19708 (2005): Bodenbeschaffenheit - Ermittlung der Erosionsgefährdung von Böden durch Wasser mit Hilfe der ABAG. Soil quality - Determination of soil erosion risk of soils by water using ABAG (In German). Beuth Verlag, Berlin.
- Ding, Yanling; Zhao, Kai; Zheng, Xingming; Jiang, Tao (2014): Temporal dynamics of spatial heterogeneity over cropland quantified by time-series NDVI, near infrared and red reflectance of Landsat 8 OLI imagery. In *Int. J. Appl. Earth Obs.* 30, pp. 139–145. DOI: 10.1016/j.jag.2014.01.009.
- Feng, Qiang; Zhao, Wenwu; Ding, Jingyi; Fang, Xuening; Zhang, Xiao (2018): Estimation of the cover and management factor based on stratified coverage and remote sensing indices. A case study in the Loess Plateau of China. In *J. Soils Sediments* 18 (3), pp. 775–790. DOI: 10.1007/s11368-017-1783-4.
- Fischer, Franziska; Hauck, Julia; Brandhuber, Robert; Weigl, Elmar; Maier, Harald; Auerswald, Karl (2016): Spatio-temporal variability of erosivity estimated from highly resolved and

- adjusted radar rain data (RADOLAN). In *Agricultural and Forest Meteorology* 223, pp. 72–80. DOI: 10.1016/j.agrformet.2016.03.024.
- Fischer, Franziska Katharina; Kistler, Michael; Brandhuber, Robert; Maier, Harald; Treisch, Melanie; Auerswald, Karl (2018): Validation of official erosion modelling based on high-resolution radar rain data by aerial photo erosion classification. In *Earth Surf. Process. Landforms* 43 (1), pp. 187–194. DOI: 10.1002/esp.4216.
- Gabriels, D. (2003): Assessment of USLE cover-management C-factors for 40 crop rotation systems on arable farms in the Kemmelbeek watershed, Belgium. In *Soil and Tillage Research* 74 (1), pp. 47–53. DOI: 10.1016/S0167-1987(03)00092-8.
- Goldshleger, Naftali; Ben-Dor, E.; Lugassi, R.; Eshel, G. (2010): Soil Degradation Monitoring by Remote Sensing: Examples with Three Degradation Processes. In *Soil Sci. Soc. Am. J.* 74 (5), pp. 1433–1445. DOI: 10.2136/sssaj2009.0351.
- Guerra, Carlos A.; Rosa, Isabel M. D.; Valentini, Emiliana; Wolf, Florian; Filippini, Federico; Karger, Dirk N. et al. (2020): Global vulnerability of soil ecosystems to erosion. In *Landscape ecology* 35, pp. 823–842. DOI: 10.1007/s10980-020-00984-z.
- Hickey, Robert (2000): Slope Angle and Slope Length Solutions for GIS. In *Cartography* 29 (1), pp. 1–8. DOI: 10.1080/00690805.2000.9714334.
- Huete, A.; Didan, K.; Miura, T.; Rodriguez, E.P; Gao, X.; Ferreira, L.G (2002): Overview of the radiometric and biophysical performance of the MODIS vegetation indices. In *Remote Sens. Environ* 83 (1), pp. 195–213. DOI: 10.1016/S0034-4257(02)00096-2.
- Jackson, Ray D.; Pinter, Paul J. (1986): Spectral response of architecturally different wheat canopies. In *Remote Sens. Environ* 20 (1), pp. 43–56. DOI: 10.1016/0034-4257(86)90013-1.
- Kipka, Holm; Green, Timothy R.; David, Olaf; Garcia, Luis A.; Ascough, James C.; Arabi, Mazdak (2016): Development of the Land-use and Agricultural Management Practice web-Service (LAMPS) for generating crop rotations in space and time. In *Soil Till. Res.* 155, pp. 233–249. DOI: 10.1016/j.still.2015.08.005.
- Lischeid, Gunnar; Kalettka, Thomas; Merz, Christoph; Steidl, Jörg (2016): Monitoring the phase space of ecosystems: Concept and examples from the Quillow catchment, Uckermark. In *Ecological Indicators* 65, pp. 55–65. DOI: 10.1016/j.ecolind.2015.10.067.
- Lu, Hua; Prosser, Ian P.; Moran, Chris J.; Gallant, John C.; Priestley, Graeme; Stevenson, Janelle G. (2003): Predicting sheetwash and rill erosion over the Australian continent. In *Soil Res.* 41 (6), p. 1037. DOI: 10.1071/SR02157.
- Lüker-Jans, Nicola; Simmering, Dietmar; Otte, Annette (2016): Analysing Data of the Integrated Administration and Control System (IACS) to Detect Patterns of Agricultural Land-Use Change at Municipality Level. In *LO* 48, pp. 1–24. DOI: 10.3097/LO.201648.
- Magliulo, Paolo; Russo, Filippo; Lo Curzio, Sergio (2020): Detection of permanently eroded landsurfaces through multitemporal analysis of Landsat data: a case study from an agricultural area in southern Italy. In *Environ Earth Sci* 79 (3), p. 174. DOI: 10.1007/s12665-020-8814-y.
- Martínez-Casasnovas, José A.; Martín-Montero, Almudena; Auxiliadora Casterad, M. (2005): Mapping multi-year cropping patterns in small irrigation districts from time-series analysis of Landsat TM images. In *Eur. J. Agron.* 23 (2), pp. 159–169. DOI: 10.1016/j.eja.2004.11.004.
- Matsushita, Bunkei; Yang, Wei; Chen, Jin; Onda, Yuyichi; Qiu, Guoyu (2007): Sensitivity of the Enhanced Vegetation Index (EVI) and Normalized Difference Vegetation Index (NDVI) to

- Topographic Effects: A Case Study in High-density Cypress Forest. In *Sensors* 7 (11), pp. 2636–2651. DOI: 10.3390/s7112636.
- Montandon, L. M.; Small, E. E. (2008): The impact of soil reflectance on the quantification of the green vegetation fraction from NDVI. In *Remote Sens. Environ.* 112 (4), pp. 1835–1845. DOI: 10.1016/j.rse.2007.09.007.
- Morgan, R.P.C (2005): *Soil Erosion and Conservation*. Third. UK: Blackwell Publishing, checked on 11/13/2016.
- Mueller-Warrant, George W.; Sullivan, Clare; Anderson, Nicole; Whittaker, Gerald W. (2016): Detecting and correcting logically inconsistent crop rotations and other land-use sequences. In *Int. J. Remote Sens.* 37 (sup1), pp. 29–59. DOI: 10.1080/01431161.2016.1184354.
- Nearing, M. A. (1997): A Single, Continuous Function for Slope Steepness Influence on Soil Loss. In *Soil Sci. Soc. Am. J.* 61 (3), pp. 917–919. DOI: 10.2136/sssaj1997.03615995006100030029x.
- Neitsch, S. L.; Arnold, J. G.; Kiniry, J. R.; Williams, J. R. (2005): *Soil and Water Assessment Tool Theoretical Documentation*. Version 2005. Temple, Tex.: USDA-ARS Grassland Soil and Water Research Laboratory, and Texas A&M University, Blackland Research and Extension Center (Version 2005). Available online at <https://swat.tamu.edu/media/1292/SWAT2005theory.pdf>, checked on 11/27/2019.
- Panagos, Panos; Karydas, Christos; Borrelli, Pasquale; Ballabio, Cristiano; Meusbürger, Katrin (2014): Advances in soil erosion modelling through remote sensing data availability at European scale. In Diofantos G. Hadjimitsis, Kyriacos Themistocleous, Silas Michaelides, Giorgos Papadavid (Eds.): *Second International Conference on Remote Sensing and Geoinformation of the Environment (RSCy2014)*. Paphos, Cyprus, Monday 7 April 2014: SPIE (SPIE Proceedings), 92290I.
- Panigrahy, S.; Sharma, S. A. (1997): Mapping of crop rotation using multirate Indian Remote Sensing Satellite digital data. In *ISPRS J. Photogramm.* 52 (2), pp. 85–91. DOI: 10.1016/S0924-2716(97)83003-1.
- Peltonen-Sainio, Pirjo; Jauhiainen, Lauri; Honkavaara, Eija; Wittke, Samantha; Karjalainen, Mika; Puttonen, Eetu (2019): Pre-crop Values From Satellite Images for Various Previous and Subsequent Crop Combinations. In *Front. Plant Sci.* 10, p. 462. DOI: 10.3389/fpls.2019.00462.
- Phinzi, Kwanele; Ngetar, Njoya Silas (2019): The assessment of water-borne erosion at catchment level using GIS-based RUSLE and remote sensing: A review. In *International Soil and Water Conservation Research* 7 (1), pp. 27–46. DOI: 10.1016/j.iswcr.2018.12.002.
- Pimentel, David; Burgess, Michael (2013): Soil Erosion Threatens Food Production. In *Agriculture* 3 (3), pp. 443–463. DOI: 10.3390/agriculture3030443.
- Preiti, G.; Romeo, M.; Bacchi, M.; Monti, M. (2017): Soil loss measure from Mediterranean arable cropping systems: Effects of rotation and tillage system on C-factor. In *Soil and Tillage Research* 170, pp. 85–93. DOI: 10.1016/j.still.2017.03.006.
- Sahajpal, Ritvik; Zhang, Xuesong; Izaurralde, Roberto C.; Gelfand, Ilya; Hurtt, George C. (2014): Identifying representative crop rotation patterns and grassland loss in the US Western Corn Belt. In *Comput. Electron. Agr.* 108, pp. 173–182. DOI: 10.1016/j.compag.2014.08.005.
- Schmid, Thomas; Rodriguez-Rastrero, Manuel; Escribano, Paula; Palacios-Orueta, Alicia; Bendor, Eyal; Plaza, Antonio et al. (2016): Characterization of Soil Erosion Indicators Using Hyperspectral Data From a Mediterranean Rainfed Cultivated Region. In *IEEE J. Sel. Top.*

- Appl. Earth Observations Remote Sensing* 9 (2), pp. 845–860. DOI: 10.1109/JSTARS.2015.2462125.
- Schmidt, Simon; Alewell, Christine; Meusburger, Katrin (2018): Mapping spatio-temporal dynamics of the cover and management factor (C-factor) for grasslands in Switzerland. In *Remote Sensing of Environment* 211, pp. 89–104. DOI: 10.1016/j.rse.2018.04.008.
- Schönbrodt, Sarah; Saumer, Patrick; Behrens, Thorsten; Seeber, Christoph; Scholten, Thomas (2010): Assessing the USLE crop and management factor C for soil erosion modeling in a large mountainous watershed in Central China. In *J. Earth Sci.* 21 (6), pp. 835–845. DOI: 10.1007/s12583-010-0135-8.
- Sepuru, Terrence Koena; Dube, Timothy (2018): An appraisal on the progress of remote sensing applications in soil erosion mapping and monitoring. In *Remote Sensing Applications: Society and Environment* 9, pp. 1–9. DOI: 10.1016/j.rsase.2017.10.005.
- Shi, Pu; Castaldi, Fabio; van Wesemael, Bas; van Oost, Kristof (2020): Large-Scale, High-Resolution Mapping of Soil Aggregate Stability in Croplands Using APEX Hyperspectral Imagery. In *Remote Sensing* 12 (4), p. 666. DOI: 10.3390/rs12040666.
- Simonneaux, Vincent; Cheggour, Aouatif; Deschamps, Charles; Mouillot, Florent; Cerdan, Olivier; Le Bissonnais, Yves (2015): Land use and climate change effects on soil erosion in a semi-arid mountainous watershed (High Atlas, Morocco). In *J. Arid Environ.* 122, pp. 64–75. DOI: 10.1016/j.jaridenv.2015.06.002.
- Steinmann, Horst-Henning; Dobers, Eike Stefan (2013): Spatio-temporal analysis of crop rotations and crop sequence patterns in Northern Germany: potential implications on plant health and crop protection. In *Journal of Plant Diseases and Protection* 120 (2), pp. 85–94. DOI: 10.1007/BF03356458.
- Truckenbrodt, Sina C.; Schmullius, Christiane C. (2018): Seasonal evolution of soil and plant parameters on the agricultural Gebesee test site. A database for the set-up and validation of EO-LDAS and satellite-aided retrieval models. In *Earth Syst. Sci. Data* 10 (1), pp. 525–548. DOI: 10.5194/essd-10-525-2018.
- van der Knijff, J. M.; Jones, R.J.A; Montanarella L. (1999): Soil Erosion Risk Assessment in Italy. EUR 19022 EN., European Soil Bureau. JointResearch Center of the European Commission. EUR 19022 EN.
- Verheijen, F.G.A.; Jones, R.J.A.; Rickson, R. J.; Smith, C. J. (2009): Tolerable versus actual soil erosion rates in Europe. In *Earth-Sci. Rev.* 94 (1-4), pp. 23–38. DOI: 10.1016/j.earscirev.2009.02.003.
- Vogel, Elisabeth; Deumlich, Detlef; Kaupenjohann, Martin (2016): Bioenergy maize and soil erosion — Risk assessment and erosion control concepts. In *Geoderma* 261, pp. 80–92. DOI: 10.1016/j.geoderma.2015.06.020.
- Vrieling, Anton (2006): Satellite remote sensing for water erosion assessment: A review. In *CATENA* 65 (1), pp. 2–18. DOI: 10.1016/j.catena.2005.10.005.
- Wang, Biwei; Zhang, Zengxiang; Wang, Xiao; Zhao, Xiaoli; Yi, Ling; Hu, Shunguang (2020): Object-Based Mapping of Gullies Using Optical Images: A Case Study in the Black Soil Region, Northeast of China. In *Remote Sensing* 12 (3), p. 487. DOI: 10.3390/rs12030487.
- Wang, Jing; He, Ting; Li, Yuhuan; Chen, Yongqi; Lv, Chunyan (2009): Hyperspectral remote sensing for land degradation mapping in China. In Xianfeng Zhang, Jonathan Li, Guoxiang Liu, Xiaojun Yang (Eds.): Second International Conference on Earth Observation for Global Changes. Second International Conference on Earth Observation for Global Changes. Chengdu, China, Monday 25 May 2009: SPIE (SPIE Proceedings), 74710M.

- Wischmeier, W. H.; Smith, D. D. (1978): Predicting rainfall erosion losses—a guide to conservation planning. Handbook. Edited by U.S. Department of Agriculture. U.S. Department of Agriculture. U.S. Department of Agriculture, Agriculture Handbook No. 537.
- Wulf, Monika; Jahn, Ute; Meier, Kristin (2016): Land cover composition determinants in the Uckermark (NE Germany) over a 220-year period. In *Reg Environ Change* 16 (6), pp. 1793–1805. DOI: 10.1007/s10113-016-0930-6.
- Yang, Dawen; Kanae, Shinjiro; Oki, Taikan; Koike, Toshio; Musiake, Katumi (2003): Global potential soil erosion with reference to land use and climate changes. In *Hydrol. Process.* 17 (14), pp. 2913–2928. DOI: 10.1002/hyp.1441.
- Young, R. A.; Onstad, C. A.; Bosch, D. D.; Anderson, W. P. (1989): AGNPS - A Nonpoint-Source Pollution Model for Evaluating Agricultural Watersheds. In *J. Soil Water Conserv.* 44 (2), pp. 168–173.
- Žížala, D.; Juřicová, A.; Zádorová, T.; Zelenková, K.; Minařík, R. (2019): Mapping soil degradation using remote sensing data and ancillary data: South-East Moravia, Czech Republic. In *European Journal of Remote Sensing* 52 (sup1), pp. 108–122. DOI: 10.1080/22797254.2018.1482524.
- Žížala, D.; Zádorová, T.; Kapička, J. (2017): Assessment of Soil Degradation by Erosion Based on Analysis of Soil Properties Using Aerial Hyperspectral Images and Ancillary Data, Czech Republic. In *Remote Sensing* 9 (1), p. 28. DOI: 10.3390/rs9010028.
- Zou, Xiaochen; Möttus, Matti (2017): Sensitivity of Common Vegetation Indices to the Canopy Structure of Field Crops. In *Remote Sensing* 9 (10), p. 994. DOI: 10.3390/rs9100994.

## **7. Attached publications**

### **7.1. Publication I**

**Ayalew, Dawit A.**; Deumlich, Detlef; Šarapatka, Bořivoj; Doktor, Daniel (2020): Quantifying the Sensitivity of NDVI-Based C Factor Estimation and Potential Soil Erosion Prediction using Spaceborne Earth Observation Data. In *Remote Sensing* 12 (7), p. 1136. DOI: 10.3390/rs12071136.

**[IF<sub>2019</sub>, 4.509]**



Article

# Quantifying the Sensitivity of NDVI-Based C Factor Estimation and Potential Soil Erosion Prediction using Spaceborne Earth Observation Data

Dawit A. Ayalew <sup>1,\*</sup>, Detlef Deumlich <sup>2</sup> , Bořivoj Šarapatka <sup>1</sup> and Daniel Doktor <sup>3</sup>

<sup>1</sup> Department of Ecology and Environmental Sciences, Palacký University Olomouc, Šlechtitelů 27, 783 71 Olomouc, Czech Republic; borivoj.sarapatka@upol.cz

<sup>2</sup> Working Group “Hydropedology”, Leibniz-Centre for Agricultural Landscape Research (ZALF), RA1, Eberswalder Straße 84, 15374 Müncheberg, Germany; ddeumlich@zalf.de

<sup>3</sup> Working Group Remote Sensing of Ecosystems, Department of Computational Landscape Ecology, Helmholtz Centre for Environmental Research-UFZ, Permoser Straße 15, 04318 Leipzig, Germany; daniel.doktor@ufz.de

\* Correspondence: dawitashenafi.ayalew01@upol.cz

Received: 10 March 2020; Accepted: 30 March 2020; Published: 2 April 2020



**Abstract:** The Normalized Difference Vegetation Index (NDVI), has been increasingly used to capture spatiotemporal variations in cover factor (C) determination for erosion prediction on a larger landscape scale. However, NDVI-based C factor ( $C_{ndvi}$ ) estimation per se is sensitive to various biophysical variables, such as soil condition, topographic features, and vegetation phenology. As a result,  $C_{ndvi}$  often results in incorrect values that affect the quality of soil erosion prediction. The aim of this study is to multi-temporally estimate  $C_{ndvi}$  values and compare the values with those of literature values ( $C_{lit}$ ) in order to quantify discrepancies between C values obtained via NDVI and empirical-based methods. A further aim is to quantify the effect of biophysical variables such as slope shape, erodibility, and crop growth stage variation on  $C_{ndvi}$  and soil erosion prediction on an agricultural landscape scale. Multi-temporal Landsat 7, Landsat 8, and Sentinel 2 data, from 2013 to 2016, were used in combination with high resolution agricultural land use data of the Integrated Administrative and Control System, from the Uckermark district of north-eastern Germany. Correlations between  $C_{ndvi}$  and  $C_{lit}$  improved in data from spring and summer seasons (up to  $r = 0.93$ ); nonetheless, the  $C_{ndvi}$  values were generally higher compared with  $C_{lit}$  values. Consequently, modelling erosion using  $C_{ndvi}$  resulted in two times higher rates than modelling with  $C_{lit}$ . The  $C_{ndvi}$  values were found to be sensitive to soil erodibility condition and slope shape of the landscape. Higher erodibility condition was associated with higher  $C_{ndvi}$  values. Spring and summer taken images showed significant sensitivity to heterogeneous soil condition. The  $C_{ndvi}$  estimation also showed varying sensitivity to slope shape variation; values on convex-shaped slopes were higher compared with flat slopes. Quantifying the sensitivity of  $C_{ndvi}$  values to biophysical variables may help improve capturing spatiotemporal variability of C factor values in similar landscapes and conditions.

**Keywords:** C factor; Landsat 7; Landsat 8; Sentinel 2; soil erodibility; slope shape; soil erosion; IACS; Germany

## 1. Introduction

Soil erosion is a major global land degradation threat that can result in the loss of soil productivity of agricultural land and in the reduction of the delivery of ecosystem services [1]. Although it is an inevitable natural phenomenon, soil erosion is often aggravated by anthropogenic interference in land use and changes in vegetation land cover [2,3]. Spatiotemporal monitoring of land cover status and

estimation of the vulnerability of arable lands to soil erosion risk, especially for large agricultural landscapes, have become paramount tasks in terms of resource requirements and efficiency [4,5].

Soil erosion risk is usually assessed through erosion prediction modelling. The Universal Soil Loss Equation (USLE) and its revised form, the Revised Universal Soil Loss Equation, are the most widely applied models. The USLE, an empirical model, was designed to estimate long-term average annual soil erosion rates of agricultural land [4,6]. It predicts annual soil loss as a product of six factors: rainfall erosivity, soil erodibility (K), topography (slope length (L) and slope steepness (S)), cover and management (C), and support practice (P). Among these factors, the vegetation cover management (C) factor is comparatively the most readily influenced by anthropogenic intervention and exhibits a negative exponential relationship to soil loss rates [7,8]. Apart from the USLE, several process-based models such as the Soil and Water Assessment Tool (SWAT) through the Modified Universal Soil Loss Equation [9,10], and the Agricultural Non-Point Source Pollution model (Young et al. [11]) also employ C factor for erosion prediction.

The C factor is expressed as a soil loss ratio (SLR) of a given plot of land covered with specified vegetation to a bare seedbed-prepared plot ploughed up and down along the slope gradient [6,12]. For arable farming, the SLR is measured several times (periods) a year corresponding to the different phenological stages of a given crop starting from seedbed preparation up to harvesting; these periodic SLR values are weighted by their corresponding proportional R values and the final summation (Equation (1)) yields the annual C value [13]:

$$C = \sum_i^n SLR_i \cdot \frac{R_i}{R} \quad (1)$$

where  $C$  is the dimensionless cover management factor,  $SLR_i$  the soil loss ratio for the month  $i$ ,  $R_i$  the rainfall erosivity of the month  $i$ ,  $R$  is the annual rainfall erosivity, and  $n$  is the number of months (periods) used in the summation.

The C factor intrinsically does not assume static values, but rather reflects various spatial, temporal, and cover-type conditions if constructed for multiple locations. For a large agricultural landscape scales or regional scale, however, it is costly and less efficient to perform periodic SLR measurements [14]. Hence, in many cases the C values for large agricultural areas are estimated by traditionally assigning uniform empirical values from literature to land use/land cover data [15,16]. This method is relatively easy but fails to capture the actual spatiotemporal variations of the vegetation cover and hence induces inaccuracy in the estimation of the C values [12]. Utilizing remotely sensed images for generating C factor maps based on vegetation indices such as the Normalized Difference Vegetation Index (NDVI) has become a common practice [4,7,14,17,18]. Comparatively, this method allows us to capture vegetation cover status and spatiotemporal variation in estimating values [4]. However, the sensitivity of the NDVI-derived C values to several biophysical variations, such as the vitality condition of the vegetation cover, soil background differences, and variations in topographical features, could hinder its full applicability [19–22]. This, as a result, entails optimizing the influence of such biophysical variables on NDVI derived C value estimations for various agricultural landscapes.

In general, efforts to quantify the sensitivity of NDVI-derived C values to biophysical variables are scant. Few studies have been conducted to quantify the influence of biophysical variables on NDVI or on NDVI-derived C values. However, some studies employed single-time image analysis [19,23,24], with less emphasis on the temporal variation of NDVI sensitivity. Despite using multi temporal images, other studies lack finer scale and dynamic land use/land cover input data and/or appropriate resolution satellite image data to indicate various cover types and their associated phenological stage variations and to incorporate spatial heterogeneity [4,25]. Both spatial and temporal scales are reported to have an influence on capturing the sensitivities in NDVI. Particular for spatial resolution, Ding et al. [26] reported that spatial resolution beyond 120 m would smother spatial heterogeneity in NDVI calculations. There is also limited information regarding the influence of the interactions

of intra-annual variation of different crop cover types in relation to spatial heterogeneity on C value calculations [27].

It is well documented that, even within similar land use types, species variation influences the reflectance of different spectra due to the variation in canopy architecture, leaf orientation, etc. [28,29]. In the process of quantifying the sensitivity of NDVI-derived C values, finely resolved and temporally dynamic land use information is imperative in order to identify plant cover to specific crop type level and accurately estimate C values for large agricultural landscapes [27]. In addition, topographical variations within a uniform land use type also affect the NDVI-derived C values. The effect of topography on vegetation indices is explained by (i) the direct effect of the change landform (e.g., from flat to hilly) on the spectrum reflectance property of the surface and (ii) by the indirect influence of topographic features on vegetation cover status and subsequent greenness of the vegetation [19,26].

In the present research, we endeavored to combine multi-temporal high resolution remote sensing data along with annually-updated land use data, the Integrated Administration and Control System (IACS), and topographic and soil attributes data to quantify the sensitivity of NDVI-derived C values in a large agricultural landscape. The first objective of this study is to temporally estimate NDVI-based C factor values and compare the values with corresponding empirical values in order to quantify the deviation between the values obtained via the NDVI and empirical based methods. The second objective is to quantify the sensitivity of effect of biophysical variables such as soil condition, topographic features, and crop phenological stage variation on  $C_{ndvi}$  values and on soil erosion prediction on an agricultural landscape scale.

## 2. Materials and Methods

### 2.1. Study Area

The Uckermark district of the Brandenburg region (53°21′50′ N; 13°48′10′ E), in north eastern Germany, was the study area (Figure 1a). The land formation of the study region was shaped as a result of the advancement and cessation of glaciers during the last glaciations [30] resulting in moderately undulating topography with elevation ranging from 14 m to 132 m above sea level. The land formation process influenced the pedogenesis in the region, which caused the heterogeneity in soil types across different topographical forms [31,32]. The main soil type on hill tops and upper slopes ranges from slightly eroded Luvisols to Calcaric Regosols. The soils at mid slopes and on plateau primarily consist of Luvisol, Haplic Luvisol, while the depressions consist of Pseudogley (classified as Stagnosols, according to WRB-IUSS [33] soil types [31,32]. The climate of the region can be characterized as temperate and continental with an annual average air temperature ranging between 7.8 °C and 9.5 °C [34]. A mean annual precipitation of 460.2 mm was recorded between the years 1992 to 2016 at Grünow weather station [35]. Regarding the land use in the region, 75% is used for arable farming [30], predominantly covered by winter cereals, winter rape, maize, and sugar beet (Figure 1b,c).

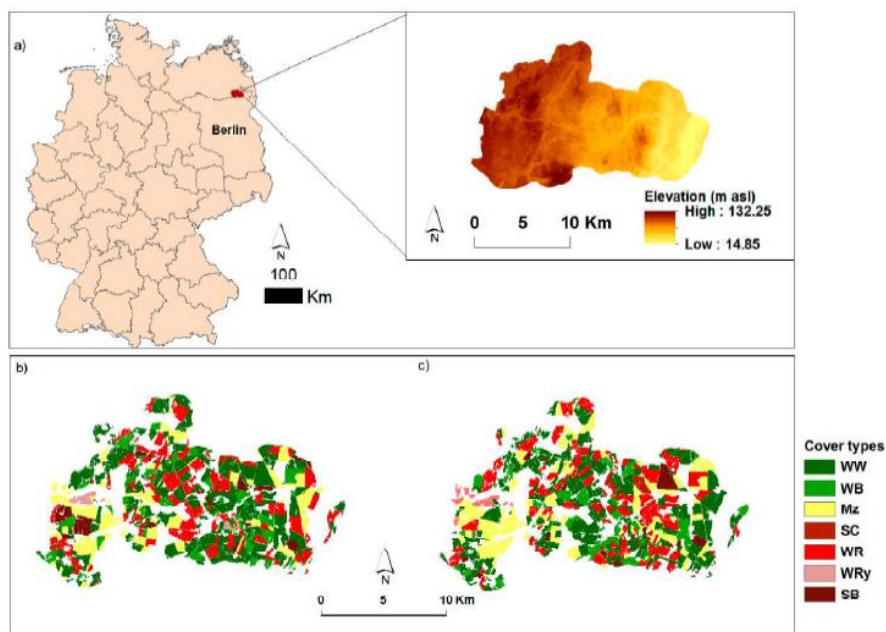


**Figure 1.** (a) Overview and elevation of the study area (Source country border: <http://www.diva-gis.org/gdata>); (b) and (c) IACS data representing the agricultural land use of the study area in the year 2015 and 2016 (masked out are forests, grasslands, and built up areas). WW, winter wheat; WB, winter barley; Mz, maize; SC, Summer cereals; WR, winter rape; WRy, winter rye; SB, sugar beets.

## 2.2. Dataset and Processing

### 2.2.1. Satellite Imagery

Here, we combined Landsat 7 and 8 data with Sentinel 2 data in order to obtain temporally representative cloud free images. Time series of satellite observations (in total 30 images) Landsat 7 and 8 (using path 193, row 23) and Sentinel 2 (using tile ID 33UVV) data acquisitions from 2013 to 2016 were downloaded from United States Geological Survey (<https://earthexplorer.usgs.gov/>) and from the Copernicus Open Access Hub (<https://scihub.copernicus.eu/dhus/#/home>), respectively. In order to represent the different cropping stages (as depicted in Table 1), we included at least one image from each season of the given considered year. For analysis, scenes were selected with cloud cover of less than 30%. Most of the images covering the study area were cloud free and all images were atmospherically corrected. Cloud and snow cover masks (obtained along with the images) were used to exclude any cloud and snow-covered pixels from further analysis. With respect to the Landsat 7 data, the Scan Line Corrector failure affected less than 3% of the study area and this did not influence the result significantly, as indicated by a comparison of the NDVI values from two closely taken Landsat 7 and Landsat 8 images (see Appendix A Figure A1). Radiometric and phenological consistency between two temporally close Landsat 8 and Sentinel 2 scenes was checked via simple per pixel correlation analysis. A high correlation coefficient of 0.97 was determined between the mean values of agricultural parcels and no significant mean variation ( $p = 0.47$ ) between the two data was observed (see Appendix A Figure A2).

**Table 1.** Different cropping stages of the considered crops along with their measured Soil Loss Ratio (SLR) value used in the study.

Crop Type	Cropping Stages												Annual C Factor *
	Tillage (S1)		Seedbed (S2)		10% Cover (S3)		50% Cover (S4)		75% Cover (S5)		Harvest (S6)		
	Dates	SLR	Dates	SLR	Dates	SLR	Dates	SLR	Dates	SLR	Dates	SLR	
WW	09/20	0.32	09/22	0.46	10/20	0.38	04/01	0.03	04/15	0.01	08/05	0.02	0.09
WB	08/30	0.32	09/09	0.46	09/23	0.38	10/30	0.03	04/01	0.01	07/16	0.02	0.08
WRy	08/05	0.32	08/16	0.46	09/01	0.38	09/20	0.03	10/20	0.01	07/29	0.02	0.04
WR	08/10	0.32	08/20	0.46	09/01	0.38	09/20	0.03	10/10	0.01	08/05	0.02	0.11
Mz	10/20	0.32	04/15	0.94	05/20	0.45	06/05	0.12	06/20	0.09	09/15	0.44	0.34
SC	10/01	0.32	03/03	0.46	04/10	0.38	05/02	0.03	05/15	0.01	08/03	0.02	0.05
SB	10/01	0.32	04/05	0.85	05/18	0.45	06/05	0.05	06/15	0.03	10/01	0.44	0.22

Dates are expressed as Month/Date; \* regional value obtained from Deumlich et al. [36].

### 2.2.2. Land Use/Land Cover Data

The IACS data provide high spatiotemporal resolution information on arable land use, crop type, field size and shape, and related aspects in a single vector dataset [37,38]. The IACS data from 2014 to 2016 were rasterized and sampled to 30 m resolution. As the focus of this research is on arable land, other land use types were excluded from the analysis. The major crops considered for the study are displayed in Figure 1b,c.

### 2.3. C Factor Value Estimation

In this study, periodic SLR values for each specific crop types, determined by the IACS data, were assigned from long term empirically measured SLR data, depicted in Table 1, as per DIN 19708 [39]. These SLR values were determined according to the corresponding cropping stages of individual crops considered (Table 2). Then, these values were weighted by their corresponding monthly average erosivity proportion values (Table 2, 2nd row) adapted from [40], to result in monthly C factor values ( $C_{litM}$ ). Finally, the annual literature-based C values ( $C_{lit}$ ) of each crop type were assigned from Deumlich et al. [36], a regional average value for northeast Germany.

In order to estimate C values using NDVI, the index was computed for each image as described by Tucker [41]:

$$NDVI = \frac{(NIR - Red)}{(NIR + Red)} \quad (2)$$

The NDVI can take values between -1 and +1 (soil: usually 0.1–0.4, vegetation: 0.2–0.9) and—if observing vegetation—is an expression of the underlying LAI and photosynthetic activity: the higher the NDVI value, the “greener” the vegetation (coverage), indicating that photosynthetically active vegetation is reflecting much of the near-infrared radiation while absorbing the visible range of the spectrum. The NDVI-based C value ( $C_{ndvi}$ ) was calculated for each image [42]:

$$C_{ndvi} = \exp \left[ -\alpha \cdot \frac{NDVI}{(\beta - NDVI)} \right] \quad (3)$$

where  $\alpha$  and  $\beta$  are empirical (dimensionless) fitting parameters. Good correlations were obtained when using a value of 2 for  $\alpha$  and 1 for  $\beta$  [42]. This particular equation has been used in several studies worldwide to calculate C values [4,17,43–46]. Since the equation was developed using daily images by comparing against monthly C factor values, it allows us to calculate monthly ( $C_{ndviM}$ ), and annual C values ( $C_{ndvi}$ ) by aggregating the average values of the scenes accordingly. Finally, the NDVI-derived C factor outputs from Sentinel 2 (at 20 m resolution) were re-sampled to 30 m resolution using the nearest neighborhood method, to maintain the original values, while aligning with the  $C_{ndvi}$  from Landsat 7 and Landsat 8 data for subsequent analysis.

**Table 2.** Satellite images allocation in relation to the expected phenological stages of the various crop types considered in the analysis. The percentage of the ground cover by respective crops' canopy was determined as per Table 1.

Scene dates <sup>a</sup>	2014 IACS data		2015 IACS data		2016 IACS data	
	Monthly R proportion	Landcover data used	Monthly R proportion	Landcover data used	Monthly R proportion	Landcover data used
29 October 2013 <sup>2</sup>	0.03	S3 S3	0.03	S3 S3	0.03	S3 S3
10 February 2014 <sup>1</sup>	0.05	S5 S5	0.03	S3 S3	0.03	S3 S3
30 March 2014 <sup>1</sup>	0.05	S5 S5	0.11	S6 S6	0.05	S3 S3
1 May 2014 <sup>1</sup>	0.1	S2 S4	0.11	S6 S6	0.05	S3 S3
10 June 2014 <sup>2</sup> ; 18 June 2014 <sup>1</sup>	0.17	S5 S5	0.14	S6 S6	0.02	S2 S4
4 July 2014 <sup>1</sup>	0.2	S5 S5	0.14	S6 S6	0.17	0.2
13 August 2014 <sup>2</sup>	0.14	S6 S6	0.11	S6 S6	0.14	0.11
6 September 2014 <sup>1b</sup>	0.11	S1 S3	0.05	S4 S4	0.02	0.17
8 October 2014 <sup>1</sup>	0.03	S2 S2	0.05	S3 S4	0.02	0.17
17 March 2015 <sup>1</sup> ; 25 March 2015 <sup>2</sup>	0.05	S2 S3	0.02	S4 S4	0.02	0.17
10 April 2015 <sup>2</sup>	0.02	S5 S5	0.02	S5 S5	0.02	0.17
5 June 2015 <sup>1</sup> ; 13 June 2015 <sup>2</sup>	0.17	S5 S5	0.17	S5 S5	0.17	0.17
4 July 2015 <sup>3</sup>	0.2	S5 S5	0.2	S5 S5	0.2	0.2
3 August 2015 <sup>3</sup>	0.14	S6 S6	0.14	S6 S6	0.14	0.14
15 September 2015 <sup>3b</sup>	0.11	S1 S1	0.11	S1 S1	0.11	0.11
3 October 2015 <sup>2</sup>	0.03	S2 S3	0.03	S3 S4	0.03	0.03
27 October 2015 <sup>1</sup>	0.03	S3 S4	0.03	S3 S4	0.03	0.03
31 December 2015 <sup>3</sup>	0.05	S3 S3	0.05	S3 S3	0.05	0.05
2 April 2016 <sup>3</sup>	0.02	S4 S5	0.02	S4 S5	0.02	0.02
22 April 2016 <sup>3</sup>	0.02	S5 S5	0.02	S5 S5	0.02	0.02
2 May <sup>3</sup> ; 9 May <sup>3</sup> ; 12 May 2016 <sup>3</sup>	0.1	S5 S5	0.1	S5 S5	0.1	0.1
8 June <sup>2</sup> ; 11 June 2016 <sup>3</sup>	0.17	S5 S5	0.17	S5 S5	0.17	0.17
23 June 2016 <sup>1</sup> ; 21 July 2016 <sup>3</sup>	0.17	S5 S5	0.17	S5 S5	0.17	0.17

<sup>a</sup> Dates are expressed as month.date.year (mm.dd.yy). <sup>b</sup> The intersects of the consecutive IACS data were used to identify the crop types; <sup>1</sup> Landsat 7 data; <sup>2</sup> Landsat 8 data; <sup>3</sup> Sentinel 2 data; S1 to S6, are cropping stages of individual crops (see Table 1).

#### 2.4. Soil Erosion Prediction

Potential soil erosion risk was predicted by employing the USLE (Equation (4)) [6]. In Germany, employing the USLE (or an adapted form of the equation named “ABAG”) to predict soil erosion risk by water is a recommended practice, especially when precise soil loss rates are not required but the demand is rather for trends and patterns of soil erosion for the purpose of agricultural land management [47,48].

$$A = R \cdot K \cdot L \cdot S \cdot C \cdot P \quad (4)$$

where:  $A$  is the predicted average annual soil loss in  $t \text{ ha}^{-1} \text{ y}^{-1}$ .  $R$  ( $N \text{ h}^{-1}$ , Newtons per hour, a commonly used unit in Germany that can readily be converted to  $MJ \text{ mm ha}^{-1} \text{ h}^{-1}$  by multiplying it by a factor of 10) is calculated as the mean annual sum (Figure 1a) of the product of a maximum 30 min rainfall intensity ( $I_{30}$ ) and energy ( $E_i$ ) of a rainfall event (Equation (5)) [6,39]. Eight years of radar rainfall data (RADOLAN from 2006 to 2013), with 5-min temporal and  $1 \times 1 \text{ km}^2$  spatial resolution, obtained from the German Weather Service (DWD), were used to calculate  $EI_{30}$  according to Wischmeier and Smith [6] as:

$$EI_{30} = \sum_{i=1}^n (E_i) * I_{30} \begin{cases} E_i = (11.89 + 8.73 \log I_i) * P_i * 10^{-3}, \text{ for } I_i \geq 0.05 \text{ mm/h} \\ E_i = 0 \text{ for } I_i < 0.05 \text{ mm/h} \\ E_i = 28.33 P_i * 10^{-3} \text{ for } I_i > 76.2 \text{ mm/h} \end{cases} \quad (5)$$

where  $i$  denotes the  $i$ th rainfall event,  $E_i$  is the kinetic energy ( $KJ \text{ m}^{-2}$ ) of the  $i$ th rainfall event,  $P_i$  is the total amount of rainfall (mm) of the  $i$ th rainfall event, and  $I_i$  is the rainfall intensity of the  $i$ th rainfall event ( $\text{mm h}^{-1}$ ). Utilizing radar weather data for rainfall erosivity calculation and erosion prediction has been found to be adequate [49].  $K$  (Equation (6)) is the soil erodibility factor ( $t \text{ h ha}^{-1} N^{-1}$ ) calculated according to Wischmeier and Smith [6] using data available from the German Soil Appraisal “Bodenschätzung” (Figure 2b).

$$\left[ 2.1 * 10^{-4} (12 - a) M^{1.14} + 3.25 (b - 2) + 2.5 (c - 3) \right] / 100 \quad (6)$$

where  $M$  is the particle size parameter,  $a$  is the percentage of organic matter,  $b$  soil structure parameter, and  $c$  is the soil profile permeability class. The topographic factor  $LS$  (Figure 2c) represents the slope length ( $L$ ) calculated according to Hickey [50] and slope steepness ( $S$ ) calculated as per Nearing [51], using a 5-m digital elevation model (DEM). The  $S$  and  $L$  (Equations (7) and (8)) are calculated as:

$$S = -1.5 + 17 / \left[ 1 + e^{(2.3 - 6.1 \sin \theta)} \right] \quad (7)$$

$$L = (l / 22.13)^m \quad (8)$$

where  $\theta$  is the slope angle,  $l$  is the cumulative slope length calculated according to Hickey [50], and  $m$  is slope contingent variable, which takes a value of 0.5 if the slope angle is greater than  $2.86^\circ$ , 0.4 on slopes ranging between  $1.72^\circ$  and  $2.86^\circ$ , 0.3 on slopes between  $0.57^\circ$  and  $1.72^\circ$ , and 0.2 on slopes less than  $0.57^\circ$ . The dimensionless  $C$  factor is the ratio of soil loss under known vegetation cover to that of bare soil. The  $C$  factor is the main manipulation factor in this study and potential soil erosion prediction is done using both  $C_{ndvi}$  (Equation (3)) and  $C_{lit}$  values. For the soil-protecting practice factor,  $P$ , a value of 1 was used because no support practice exists for the study region.

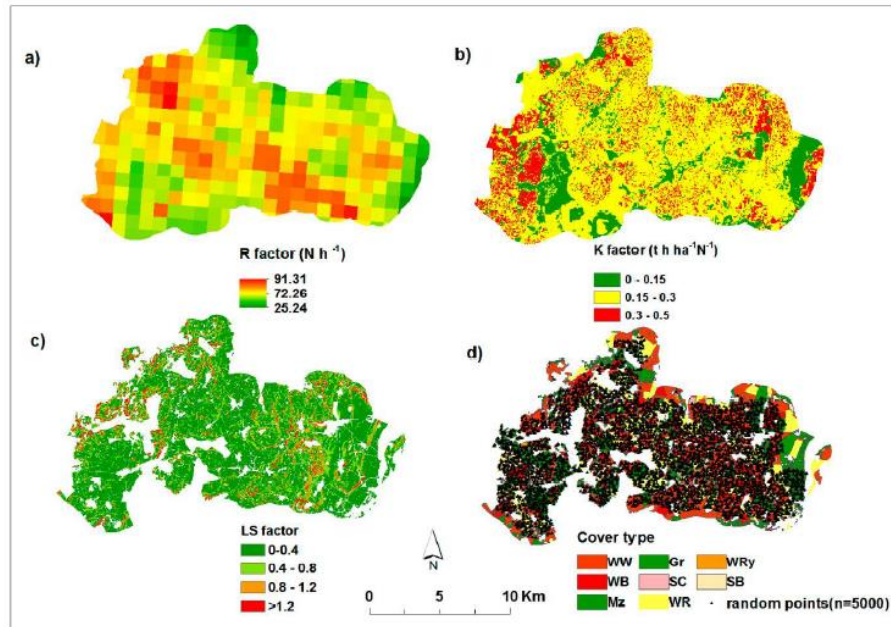


**Figure 2.** (a) Eight-year annual average rainfall erosivity map, (b) Soil erodibility factor map (c) slope length and steepness (LS) factor map, and (d) random points generated for the analysis overlaying the 2015 arable land use.

### 2.5. Statistical Analysis

In order to address the second objective, quantifying the influence of biophysical variables on  $C_{ndvi}$  values, a sample of 5000 spatially balanced random points (Figure 2d), constrained within the arable land of the study area (using ArcMap, v10.2.2) were generated and further used to extract multi-values from the considered biophysical explanatory variables (Table 3). The means and standard deviations of the sample values were compared with the corresponding values from the entire study area, to check the representativeness of samples, using a t-test analysis (see Appendix B Table A1). Multiple linear regression analysis was performed using the extracted values against the corresponding  $C_{ndvi}$  values through R (package “stats”) software version 3.6.0 [52].

The biophysical variables used in the study (Table 3) are topographic features such as slope steepness (degree), slope shape, slope position, slope aspect, edaphic conditions of the area (proxied through K factor values), and seasonal and crop type variation. A digital elevation model (DEM) of a 5-m resolution (Figure 1a), derived by airborne laser scanning, was used for the computation of the topographic features. Slope position and slope shape were calculated through the topographic positioning index [33]. Soil properties of the study area are proxied by soil erodibility condition in the form of the K factor values for the reasons that K is calculated by taking into account the soil texture, soil organic matter content, and particle size distribution of the area [39], in addition to its applicability in quantitative analysis and explanation [53].



**Table 3.** Description of explanatory variables used for regression analysis to investigate the influence of spatiotemporal and crop type variations on  $C_{ndvi}$  values.

Variables	Description	Data Type
<b>Dependent variable</b>		
$C_{ndvi}$	Cover management factor derived from satellite images (Equation (3))	Continuous
<b>Biophysical variables</b>		
Soil	Soil erodibility (K value) (Equation (6))	Continuous
Slope	Slope steepness (degree) calculated from 5 m DEM using ArcMap 10.2.2	Continuous
Aspect	Measure of north - south facing slopes	Continuous
Slope positions	Calculated based on topographic position indexing [31].	Categorical (coded 1 as summit (reference); 2 is upper slope; 4, flat slope; 5, lower slope; 6, depression or valley)
Slope shapes	Measure of land undulation [31].	Categorical (coded 0 as flat (reference); 1 as convex; 2 as concave)
Crop types	Type of Crops grown at a given data point (identified using IACS data)	Categorical (1 is WW (reference); 2 is WB; 3 is Mz; 4 is SC; 5 is WR; 6 is WRy; 7 is SB)

As the data set features some categorical variables such as slope shape, slope position, crop cover type, the multiple regression model is expressed as:

$$y = \beta_0 + \beta_{12}\alpha_2 + \beta_{13}\alpha_3 + X\beta_2 \dots + \varepsilon \quad (9)$$

where  $\beta_{12}$ ,  $\beta_{13}$  represent the coefficient expression of the given categorical variables,  $\alpha_2$  and  $\alpha_3$ , respectively, as compared with a reference variable ( $\alpha_1$  where its coefficient  $\beta_{11}$  is set to 0),  $\alpha_2$  and  $\alpha_3$  represent categorical variables,  $X$  is a non-categorical variable, and  $\beta_2$  is the coefficient for the non-categorical variable [54]. The categorical expression for the different crop types was performed by taking winter wheat as a reference crop, because winter wheat occupied a large proportion of the study area in all the considered years. For slope shape and slope position, flat land and the slope summit categories were taken as reference categorical variables, respectively (Table 3). Changing reference variables does not make any statistical difference in the final output of the regression analysis; rather, it facilitates a simpler comparison between variables.

Finally, the performances of satellite-based C factor estimation and soil loss prediction were assessed by employing root mean square error (RMSE) computation expressed as:

$$RMSE_C = \sqrt{\frac{\sum_1^n (C_{lit} - C_{ndvi})^2}{n}} \text{ and } RMSE_{SL} = \sqrt{\frac{\sum_1^n (SL_{C_{lit}} - SL_{C_{ndvi}})^2}{n}} \quad (10)$$

where  $SL_{C_{lit}}$  is the potential soil loss predicted using  $C_{lit}$ ,  $SL_{C_{ndvi}}$  is the soil loss predicted using  $C_{ndvi}$ , and  $n$  is the number of pixels coinciding in the analysis. Furthermore, the erosion prediction accuracy of using the USLE model in general, or through the two different C values ( $SL_{C_{ndvi}}$  and  $SL_{C_{lit}}$ ) in particular, was discussed by comparing the model output with long term (from 1982 to 1996) average soil erosion values measured from field experiments at the Holzendorf (Latitude 53.386818, Longitude 13.780225) research station [55]. The experimental set up and measured erosion values can be referred from Deumlich et al. [55].

### 3. Results and Discussion

#### 3.1. Comparisons between $C_{ndvi}$ and $C_{lit}$ Estimation

Table 4 indicates the spatial correlation between monthly  $C_{ndviM}$  and  $C_{litM}$  values of the entire landscape. Better correlation between  $C_{ndviM}$  and  $C_{litM}$  values was observed in images taken in the months between spring and mid-summer, with the highest correlation coefficient ( $r = 0.93$ ) computed on the image taken on 09 May 2016. The lowest correlation, however, was observed in the months of

late summer and autumn, while in a few of the images a negative relationship between  $C_{ndviM}$  and  $C_{litM}$  values was observed. In particular, August, September, and October were the months where the highest RMSE was computed. This can be due to variations in the vitality of many winter-sown crops during these periods of the year; NDVI-based C factor values, as opposed to the SLR based values, which mainly reflect the function of the protective ability of the crops in question, are highly influenced by the vitality of the plants rather than the crop-cover percentage [20,42]. In these periods, large areas of the landscape (see Figure 1b,c for proportion of crop cover) are expected to have either maturing and senescing crops (e.g., August) or early-emerging and less-ground covering crops (e.g., October), in which case the NDVI values were lower (Appendix A Figure A3), in turn resulting in elevated monthly  $C_{ndviM}$  values. One possible solution could be to incorporate yellow vegetation indices such as normalized difference tillage index (NDTI), and normalized difference senescent vegetation index (NDSVI), in the process of formulating the C factor equation, for future in order to improve the C value estimation across all seasons [7]. Overall, lower RMSEs were consistently computed on images taken during the month of June in each of the three years considered.

**Table 4.** Comparison between monthly  $C_{ndviM}$  and  $C_{litM}$  values represented by scene dates, for the entire study area.

Scene Dates	Monthly Mean		Correlation Coefficients (r)	RMSE
	$C_{ndviM}$	$C_{litM}$		
10 October 2013	0.205	0.010	0.53	0.185
2 February 2014	0.252	0.010	0.70	0.144
3 March 2014	0.147	0.005	0.89	0.098
1 May 2014	0.158	0.013	0.88	0.119
10 June 2014	0.040	0.004	0.80	0.050
18 June 2014	0.066	0.004	0.67	0.084
4 July 2014	0.100	0.005	−0.05	0.136
8 August 2014	0.240	0.006	0.08	0.241
6 September 2014	0.312	0.011	0.42	0.251
8 October 2014	0.237	0.007	0.36	0.216
17 March 2015	0.284	0.004	0.74	0.144
25 March 2015	0.216	0.004	0.79	0.118
10 April 2015	0.159	0.003	0.80	0.132
5 June 2015	0.112	0.005	0.90	0.095
13 June 2015	0.083	0.005	0.88	0.076
4 July 2015	0.113	0.005	0.40	0.125
3 August 2015	0.381	0.004	−0.58	0.202
15 September 2015	0.350	0.020	−0.32	0.422
3 October 2015	0.295	0.008	0.39	0.229
27 October 2015	0.276	0.006	0.55	0.199
31 December 2015	0.205	0.008	0.56	0.186
2 April 2016	0.277	0.002	0.71	0.175
22 April 2016	0.166	0.004	0.74	0.167
2 May 2016	0.186	0.016	0.89	0.133
9 May 2016	0.177	0.016	0.93	0.107
12 May 2016	0.171	0.016	0.91	0.114
8 June 2016	0.092	0.005	0.84	0.094
11 June 2016	0.059	0.005	0.66	0.096
23 June 2016	0.058	0.007	−0.02	0.110

When comparing  $C_{ndviM}$  values of individual crop-cover types with corresponding  $C_{litM}$  values, a better estimation for winter crops was observed in spring months and, to a lesser extent, in the beginning of summer months (April to the mid of June), while for spring sown crops, better estimation was obtained on images taken exclusively in summer months (June to September) of the year (Appendix A Figure A3),

which closely coincided with the expected growth patterns of the crops in the study region. This can indicate the applicability of the IACS data combining with remote sensing images to capture the temporal variability in C value determination. In general, there was a tendency of high C value estimation using NDVI as a tool compared with  $C_{litM}$  value estimation in all the months considered. Almagro et al. [56] also reported that C values estimated via the NDVI (employing Equation (3)) resulted in over estimation of C factor values compared with plot scale literature values in tropical conditions.

When it comes to annual C value computations, which is the required input factor for the USLE model, average  $C_{ndvi}$  calculations resulted in higher values compared with empirical  $C_{lit}$  values specifically for winter cereals and summer cereal (Figure 3). The highest discrepancies were observed on parcels covered with SC (85%) and WRy (80%) while the lowest discrepancy, around 5% and 5.3%, appeared to be on parcels covered with WR and Mz respectively. Bargiel et al. [57] also noted that C factor determination through remote sensing application gives better accuracy for summer crops than winter grains (without considering WR) in a similar condition in Poland. Annual C values of Mz and WR can be captured with a better accuracy as indicated by the least discrepancy estimated here. Comparatively, the NDVI-derived C value estimation also performed better for SB compared with winter and summer cereals. This could be explained to some extent to the variation in patterns of foliar orientation of these crops. WR, Mz and SB categorized as plagiophile and planophile, respectively, while most cereals categorized as erectophile crops behave differently with respect to canopy spectral reflectance [58]. Erectophile canopy, leaves arranged in vertical manner, could trap reflected radiation within the canopy and reduce the NDVI while the opposite is true for planophile canopy orientation types [29].

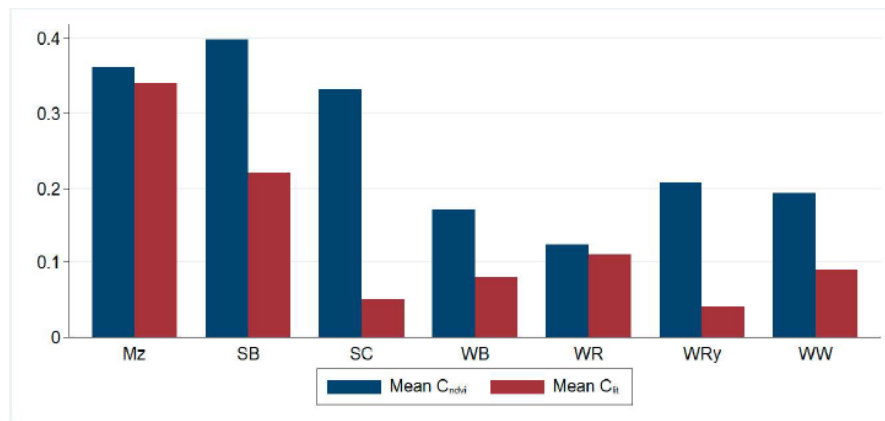


**Figure 3.** Annual average C factor comparisons between  $C_{ndvi}$  and  $C_{lit}$  values among different crops. The  $C_{ndvi}$  values are aggregated average values of the three considered years (from 2013 to 2016).

Figure 4 depicts the spatial distribution of C values computed with the two methods. The classification of the study area indicates discrepancy between the two C value estimations. In case of  $C_{lit}$ , areas classified with C values below 0.1 accounted for 51% of the entire landscape, while  $C_{ndvi}$  values of the same category was computed on just 13% of the study area. However, proportions of the landscape falling in the category between 0.1 and 0.2 were comparatively close to each other: around 33% with  $C_{ndvi}$  and 31% with  $C_{lit}$ . One peculiar thing about the  $C_{ndvi}$  calculation is that it produced continuous and spatially varying C factor values within individual parcel as opposed to a discrete representation by the  $C_{lit}$ . This obviously can indicate the potential of the NDVI-based C factor estimation for capturing spatially explicit variation of different cover types for possible implication of spatially explicit erosion prediction models, provided that the appropriate adjustments are made (see Sections 3.3 and 3.4 for a further discussion of adjustments).

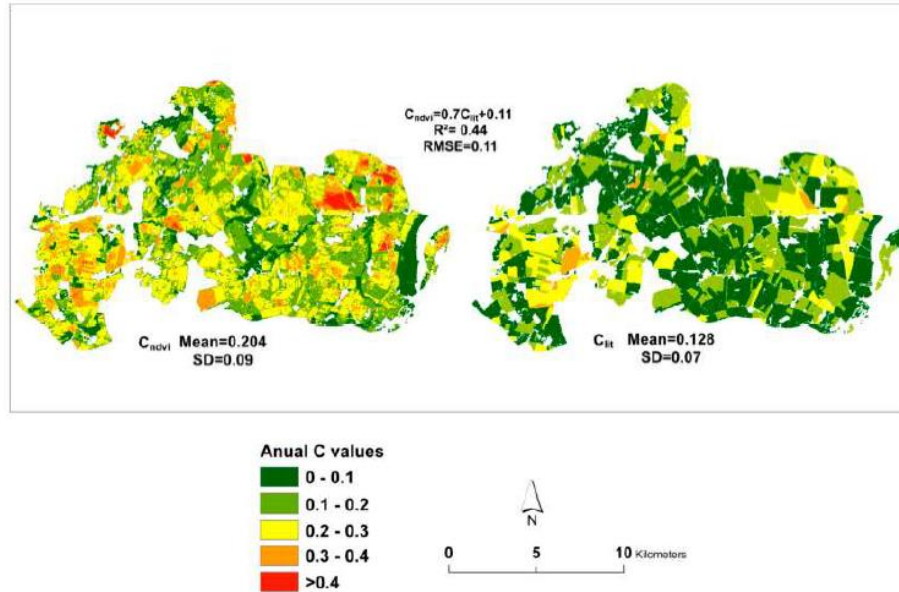


**Figure 4.** Spatial distribution of three years average annual C values calculated from satellite images ( $C_{ndvi}$ ) and literature values ( $C_{lit}$ ) over the entire study area.

### 3.2. Potential Soil Erosion Risk Prediction Using the Two C Estimation Methods

Subsequent modelling of potential soil erosion risk reflected the variation of C factor values. The three-year average annual potential soil loss rates predicted using  $C_{lit}$  ( $SL_{clit}$ ) resulted in values falling below the maximum tolerable soil loss limit (rates  $< 1.4 \text{ t ha}^{-1} \text{ y}^{-1}$ ) [59] set for European conditions, as per Verheijen et al., for all crops, except Mz (Figure 5). On the other hand, in the case of  $SL_{cndvi}$ , only winter-sown crops fall below this limit. All the spring sown crops, however, predicted high potential soil loss rates above the tolerable limit using  $C_{ndvi}$  values inputted in the USLE model. WR- and Mz-covered parcels gave quite close soil loss rates. In recent years, the coverage of bio-energy Mz and WR in the study region has witnessed an incremental trend, which in turn requires to understand the associated environmental impact at wider scale [34,60]. In this regard, we have indicated that remotely sensed data can be reliable input for various environmental monitoring and modelling activities.

Spatially, the potential soil loss rates predicted using the two different C factor inputs revealed an RMSE as high as  $1.17 \text{ t ha}^{-1} \text{ y}^{-1}$ , which was below the maximum tolerable soil erosion limit (Figure 6). However, the spatial distribution of the potential soil erosion risk varied greatly. For example, the proportion of the landscape classified below the maximum tolerable soil loss limit in the case of  $SL_{cndvi}$  was close to 85%, while the same classification in the case of  $SL_{clit}$  accounted for close to 70%. In aggregate, the soil loss rate obtained by employing  $C_{ndvi}$  as a C-factor input for the USLE model resulted in two times higher prediction than when using  $C_{lit}$ .

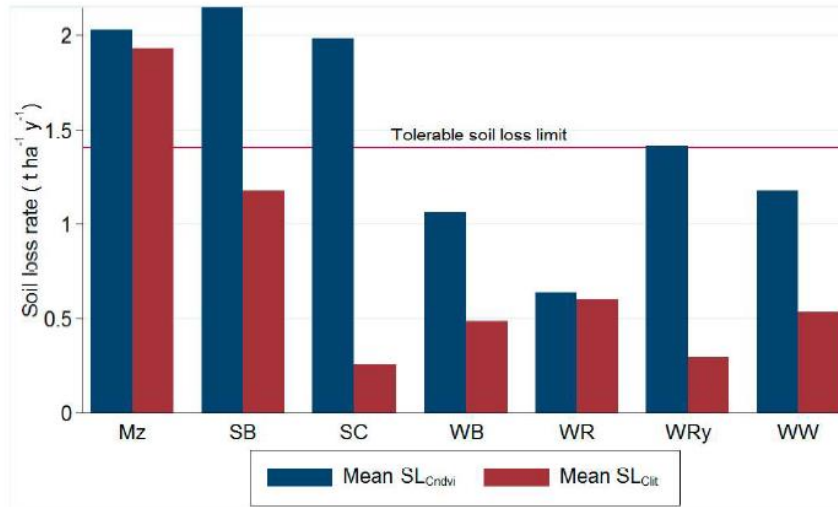


**Figure 5.** The three-year average annual potential soil erosion rates computed using  $C_{ndvi}$  ( $SL_{Cndvi}$ ) and  $C_{lit}$  ( $SL_{Clit}$ ).

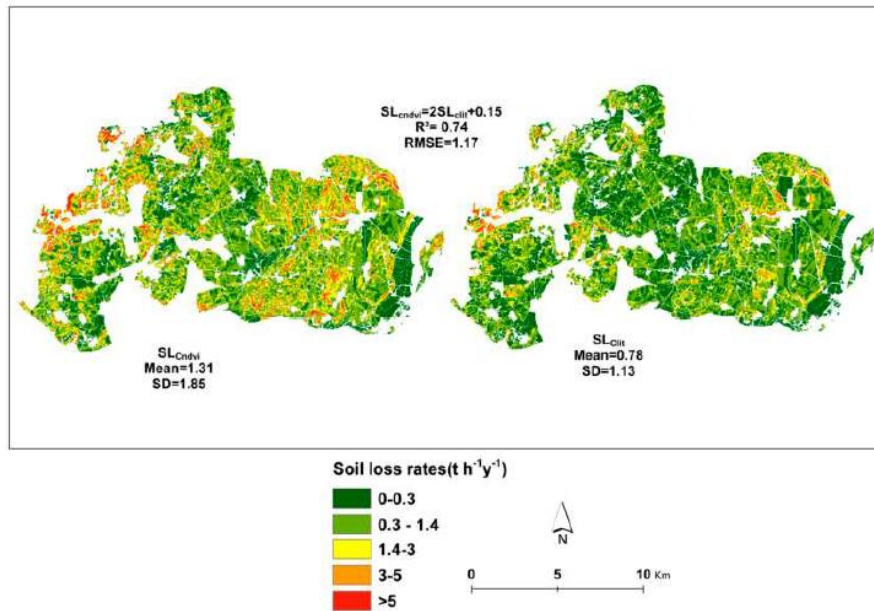


**Figure 6.** Spatial distribution of the predicted average annual potential soil loss rates using  $C_{ndvi}$  ( $SL_{Cndvi}$ ) and  $C_{lit}$  ( $SL_{Clit}$ ) values as inputs in the USLE model.

The accuracy of the USLE model in general was assessed by comparing the potential soil loss rates against the measured long-term average annual soil loss rates. The measured values ranged from 0.5 to 5  $t\ ha^{-1}\ y^{-1}$ ; the lowest value measured from WRy mono cultivation, while the highest was measured from continuous fallow plots. The  $SL_{Clit}$  gave a comparatively closer estimation than the  $SL_{Cndvi}$ , with a

three-year average of  $1.11 \text{ t ha}^{-1} \text{ y}^{-1}$  predicted from the WW and WR sequenced parcels located near the surrounding of the Holzendorf experimental station (see Appendix A Figure A4). The potential soil loss rate predicted using  $C_{\text{ndvi}}$ , however, yielded an average value of  $2.13 \text{ t ha}^{-1} \text{ y}^{-1}$  for the same cropping sequence. The closest comparison here is WRy monoculture. Given the fact that rainfall erosivity increased over the recent years in the study area [61] and the variation in C values of the crop types, WRy had low C factor values compared to WR and WW [36], the model output from  $SL_{\text{clit}}$  can be fairly taken as accurate.  $SL_{\text{cndvi}}$  erosion prediction, on the contrary, overestimated (close to double) the erosion rate as compared to  $SL_{\text{clit}}$ . However,  $SL_{\text{cndvi}}$  can improve spatially explicit identification of soil erosion risks as opposed to  $SL_{\text{clit}}$ . This can be inferred from the relatively higher coefficient of variation (CV) of 91% computed in the case of  $SL_{\text{cndvi}}$  as opposed to 84% in  $SL_{\text{clit}}$  (Appendix A Figure A4). This can indicate the potential of utilizing NDVI-based C factor estimation for physically based erosion models such as SWAT.

### 3.3. Influence of Soil Heterogeneity on $C_{\text{ndvi}}$

Multiple regression analysis revealed that C values estimated from the vegetation index were affected by the biophysical variables considered (Table 5). The sensitivity of  $C_{\text{ndvi}}$  estimations to soil background variation can be explained through the spatial variability of soil erodibility (K) values in the study area. This is in agreement with the findings of Wang et al. [53], who reported that the spatial variability of K factor values can be represented by Landsat TM band 7 variability. In the present study, an increase in the value of soil erodibility resulted in an invariable incremental change in the values of  $C_{\text{ndvi}}$ , although the magnitude varied in different months of a year. Sizeable impact, in terms of magnitude, was observed during spring and the beginning of the summer months. These are the periods when ground cover contrast is expected to be high. Huete et al. [62] indicated that the influence of soil background on plant canopy spectral reflectance is more pronounced on soils with 75% ground cover than on either fully exposed or less ground-covered soils.

The variation in  $C_{\text{ndvi}}$  values resulting from soil background heterogeneity could be well explained through the Red and Near Infrared (NIR) bands reflectance variation, particularly on the highest soil erodibility categories (Figure 7). Soil characteristics such as soil texture, organic matter content and surface roughness are reported to influence the spectrum properties of a landscape [26]. Remarkably consistent variations in the reflectance values of both Red and NIR spectrum were observed on soils with an erodibility class of greater than  $0.3 \text{ t h ha}^{-1} \text{ N}^{-1}$ . The higher the K value, the higher the red reflectance, but the lower the NIR reflectance, which could result in low NDVI values, as NDVI is the normalized ratio of the two bands. This can be attributed to the fact that soils with lower erodibility characteristics have relatively higher organic matter contents, which in turn gives the soils a darker color. Soil with a darker color are reported to have higher greenness value than brighter colors [62]. This could, to a degree, explain how soil erosion risk predicted using  $C_{\text{ndvi}}$  ( $SL_{\text{cndvi}}$ ) yielded higher values, as opposed to  $SL_{\text{clit}}$ , because of the compounding effect of the K and  $C_{\text{ndvi}}$  values in the USLE model (Figure 6).

**Table 5.** Estimates of the multiple regression analysis of  $C_{ndvi}$  values against biophysical variables across the multi temporal images.

Scene Dates	$R^2$	Biophysical Variables																
		Slope Positions					Slope Shapes			Crop Types (with Reference to WW)								
		K Factor	Slope	Aspect	LS Factor	Upper Slope	Flat Slope	Lower Slope	Valley	Convex	Concave	WB	Mz	SC	WR	WRy	SB	Constant
29 October 2013	0.4	0.06	0.00	0.00	0.00	0.01	0.00	0.00	0.01	0.00	-0.12	-0.11*	0.03*	0.14*	-0.24*	-0.02	0.21*	0.25*
10 February 2014	0.6	0.08	0.00	0.00	0.02	0.00	0.01	0.01	0.01	0.01*	0.01	-0.10*	0.23*	0.25*	-0.17*	-0.13*	0.29*	0.22*
30 March 2014	0.8	0.05	0.00	0.00	0.01	0.00	0.00	0.00	0.01*	0.01*	0.01	-0.03*	0.40*	0.35*	-0.05*	-0.03*	0.47*	0.04*
1 May 2014	0.8	0.16*	-0.00	0.00	0.01	-0.00	-0.01	0.01	0.00	0.00	0.00	-0.02*	0.49*	0.02	0.06*	-0.01	0.55*	-0.01
10 June 2014	0.7	0.11*	0.00	0.00	0.00	0.00	0.00	0.00	0.01*	0.00	0.00	0.02*	0.19*	0.01	-0.00	0.02*	0.02*	-0.02*
4 July 2014	0.5	0.09*	-0.00	0.00	0.01	-0.01	-0.02	0.01	0.01	0.01	-0.02*	0.31*	0.01	-0.01	0.08*	0.26*	-0.06*	0.05*
13 August 2014	0.6	0.07	-0.00	0.00	0.04*	-0.00	0.00	0.01	0.02	0.02	-0.01	-0.03*	-0.45*	-0.30*	-0.25*	-0.11*	-0.45*	0.42*
6 September 2014	0.7	0.08	0.00	0.00	0.01	-0.01	0.00	0.01	0.04*	0.00	0.04*	0.04*	-0.43*	-0.21*	0.12*	0.13*	-0.41*	0.40*
08 October 2014	0.4	0.02	-0.00*	0.00	0.01	-0.01	-0.02	-0.02	0.01	0.01	-0.01	0.00	-0.17*	-0.27*	-0.32*	-0.17*	-0.19*	0.38*
25 March 2015	0.7	0.17*	0.00	0.00	0.01	-0.01	-0.00	0.01	0.02*	0.01	0.02*	-0.06*	0.33*	0.36*	-0.06*	0.17*	0.39*	0.10*
10 April 2015	0.8	0.16*	0.00	0.00	0.00	-0.01	-0.00	0.00	0.01*	0.00	0.01*	-0.05*	0.44*	0.47*	-0.05*	0.15*	0.51*	0.03*
13 June 2015	0.8	0.14*	-0.00	0.00	-0.00	-0.00	-0.01	-0.00	0.01	-0.00	0.01	0.03*	0.39*	0.01	-0.00	0.03*	0.20*	-0.02*
4 July 2015	0.5	0.09*	0.00	0.00	0.00	-0.00	-0.01	-0.00	0.01*	-0.01*	-0.01*	0.27*	0.15*	-0.02	-0.04*	0.09*	0.00	0.05*
3 August 2015	0.8	0.09*	-0.00	0.00	0.01*	-0.01	0.00	0.00	-0.01	-0.02*	-0.02*	0.02*	-0.50*	-0.14*	-0.06*	-0.02	-0.52*	0.53*
3 October 2015	0.4	0.13	-0.01*	0.00	0.02	-0.02	-0.02	-0.01	0.01	0.01	0.00	0.02	-0.30*	-0.24*	-0.31*	-0.09*	-0.06*	0.46*
31 December 2015	0.4	0.28*	0.00	0.00	0.00	0.00	0.00	0.01	0.03*	-0.01	0.03*	-0.14*	0.16*	0.41*	-0.16*	0.06*	0.33*	0.14*
2 April 2016	0.6	0.16*	0.00	0.00	0.01	-0.01	-0.01	0.00	0.05*	0.01	0.05*	-0.06*	0.31*	0.42*	-0.14*	-0.14*	0.42*	0.19*
22 April 2016	0.7	0.15*	0.00	0.00	-0.02	0.00	0.00	-0.01	0.03*	0.00	0.03*	0.00	0.49*	0.42*	-0.05*	-0.09*	0.54*	0.06*
12 May 2016	0.9	0.15*	0.00	0.00	0.00	-0.01	-0.01	0.00	0.01*	0.00	0.01*	0.00	0.60*	0.06*	0.04*	-0.03	0.66*	-0.01
8 June 2016	0.8	0.21*	0.00	0.00	0.00	0.01	0.00	0.00	0.02*	-0.01	0.02*	0.01*	0.38*	0.00	0.00	-0.01	0.14*	-0.04*
23 June 2016	0.5	0.02	0.00	0.00	0.00	0.01	0.00	0.01	0.01	0.01	-0.01	0.26*	0.04*	-0.02	0.00	0.04*	-0.02	0.01

\* indicates coefficients statistically significant at  $P < 0.01$ ; Coef. denotes regression coefficient; Adj.  $R^2$  is adjusted coefficient of determination; (-0.00) is due to the rounding off of small values, but the sign is kept indicating directional impact.

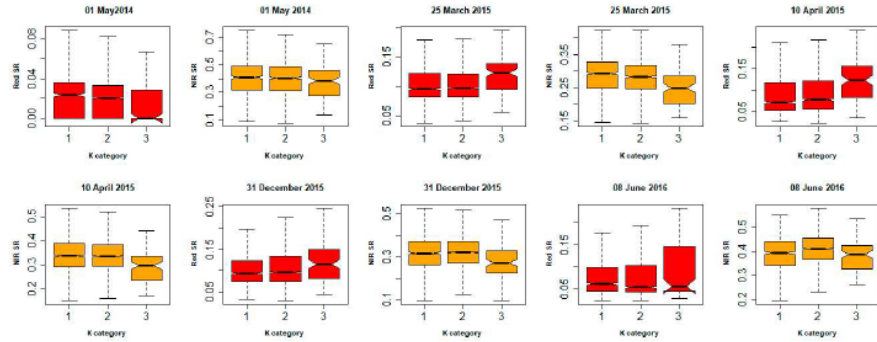


**Figure 7.** Comparison of surface reflectance (SR) values across soil erodibility (K) categories in different images (scene dates chosen based on statistically significant impact on  $C_{ndvi}$  according to Table 4). K categories: 1,  $\leq 0.15$ ; 2,  $= 0.15$  to  $0.3$ ; 3,  $\geq 0.3$ . The notches in the boxes indicate statistical significance in median reflectance of Red and Near Infrared (NIR) along the K categories at a 95% confidence interval.

The  $C_{ndvi}$  values responded differentially to soil background heterogeneity across different crop-cover types and seasons; during winter and spring, the association of  $C_{ndvi}$  with soil condition was pronounced on lands covered with winter sown crops (with the exception of WR) more during summer on the lands covered with spring sown crops (Figure 8). This could be explained in relation to the growth stages of the crops in question, whereby during winter and spring periods, parcels covered with winter-sown crops, or with spring sown crops during the summer period, would exhibit mixed spectral characteristics of both the exposed soil and vegetation of not fully-closed canopies. However, as time proceeded, the canopies of the respective crops in the respective seasons would fully cover the parcels; hence, the radiometric signal is less dominated by the soil background reflectance [26].

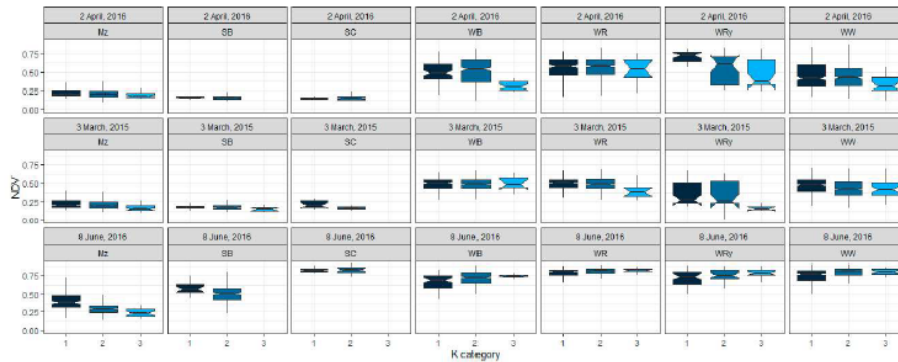


**Figure 8.** Impact of soil heterogeneity (categorized as 1,  $K \leq 0.15$ ; 2,  $K = 0.15$  to  $0.3$ ; 3,  $K \geq 0.3$ ) on NDVI values across different crop cover types and seasons in the study area (notches indicate a significant variation in median NDVI along the K category at a 95% confidence interval).

The least pronounced impact of heterogeneous soil background reflectance on parcels covered with WR can be explained by the nature of the architectural orientation of the crop canopy. WR, plagiophile canopy, is reported to have a higher plant area index compared with WW (belonging to erectophile), even at the same phenological stage [58]. This can also be inferred from Figure 8 in our study, where, despite both WR and WRy being expected to cover around 75% of the ground in the images dated 02 April 2016 (Table 2), their NDVI values and response to K value categories varied significantly.



Land surfaces covered with WR showed no significant response to soil heterogeneity and had comparatively higher NDVI values consistently (Figure 8). However, a further investigation with ground measurements needs to be done to further understand the relationship of crop canopy structure and C factor value estimation for future.

Other spectral indices such as the enhanced vegetation index (EVI) and soil adjusted vegetation index (SAVI) have been developed to increase sensitivity to changes in biomass while reducing the impact of soil background noise on vegetation spectral property [63]. However, these indices may introduce a higher sensitivity to topographic variability, which might take effect in rugged/mountainous areas [19]. Therefore, consideration of all biophysical variables in calibrating spectral indices for the purpose of environmental monitoring such as erosion prediction remains imperative.

#### 3.4. Influence of Topographic Features on $C_{ndvi}$

The regression analysis also revealed that  $C_{ndvi}$  values showed consistently significant response to varying slope shapes of the landscape (Table 5). Slope aspect, however, did not show any significant relationship with  $C_{ndvi}$  estimation. Matsushita et al. [19] also reported that topographical features such as aspect do not exhibit significant influence on band ratio indices such as NDVI. Although slope steepness showed a significant impact on  $C_{ndvi}$  values in just two images, the regression coefficient was a very small number close to zero; hence, it is not discussed here.

Convex shaped slope, as compared to flat slope, demonstrated significant incremental implications on  $C_{ndvi}$  values, with the highest coefficient of 0.05 ( $P < 0.01$ ;  $R^2 = 0.57$ ) predicted on the image taken on 02 April 2016 (Table 5). Concave shaped slope, on the other hand, revealed to have a negative relationship with the estimated  $C_{ndvi}$  values compared with the flat slope. The impact of concave slope on  $C_{ndvi}$  values was predominantly observed on images taken from the end of June to August. This can be due to the indirect influence of topographic attributes on vegetation status, as concave slopes, located towards the depression parts of the study area [31], are most likely assumed to be cooler in summer as compared to flat land; hence, the crops could senesce late and could remain vital for a longer time. In addition, this could also be due to the fact that drainage patterns vary with slope shape, bearing implications on soil moisture conditions of a landscape, in such a way that concave slopes produce less runoff compared with flat and convex slopes [64,65]. In the study area the different slope shapes also have a complex interaction with prevailing soil types, due to erosion and deposition processes [55]. Concave part of slope act as depositional sites while the convex parts of the slope are dominated by eroded soils. These attributes of the landscape could also play a role in the status of crop growth and subsequently in  $C_{ndvi}$  estimates.

Convex slopes seemed to increase  $C_{ndvi}$  value estimations, with considerable magnitude recorded on images taken in winter and early springtime. The impact of varying slope shape varied with crop growth stages (Figure 9). During springtime (e.g., image 02 April 2016), the impact of slope shape on the NDVI values was more evident for winter crops, parcels covered with summer crops exhibiting a typical NDVI value for bare soil. In the middle of the summer season (04 July 2014), when most winter crops were approaching maturity stage, the impact of slope shape, specifically concave slope, exerted an influence on the NDVI values of winter crops. Towards August (03 August 2015), the influence of slope shape variation was entirely limited to summer crops because winter crops had most likely been harvested. In general, while using NDVI for C factor estimation, considerations must be taken into account to accommodate for land formation influence on the status of the vegetation.

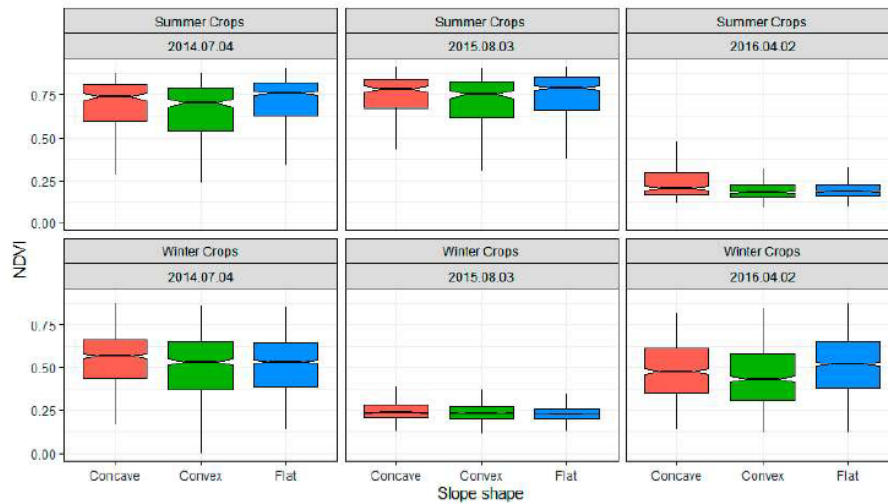


**Figure 9.** Box plots indicating influences of slope shapes on NDVI values across crop categories and seasons. Winter Crops are composed of WW, WB, WR, and Wry, while Summer Crops are Mz, SB, and SC. Notches indicate significant impact between slope shape categories on median NDVI values (the scene dates are chosen based on statistically significant impact on  $C_{ndvi}$  estimates according to Table 5).

#### 4. Conclusions

In the present study, we used annually updated high resolution land use data, high resolution multi-temporal remote sensing data, and topographic and soil attribute data to quantify deviations between NDVI based C value estimations ( $C_{ndvi}$ ) and traditional literature-based C values ( $C_{lit}$ ) in addition to quantifying the sensitivity of  $C_{ndvi}$  estimation in large agricultural landscape. Combining these datasets enhanced the quantification of the discrepancies between  $C_{ndvi}$  and  $C_{lit}$ . A higher discrepancy was observed among winter cereals than summer crops. The discrepancy in C values between  $C_{ndvi}$  and  $C_{lit}$  was also found to be season dependent with a closer relation observed in early spring to midsummer, with consistently lowest RMSE values for data from June. Subsequently modelling soil erosion using  $C_{ndvi}$  as input factor could yield higher annual mean soil loss rate values, while it could potentially improve the spatially explicit erosion risk identification.

In quantifying the sensitivity of  $C_{ndvi}$ , the K factor was reliable and consistent to explain the response of  $C_{ndvi}$  values to soil background heterogeneity. Higher erodibility condition, particularly K values above  $0.3 \text{ t h ha}^{-1} \text{ N}^{-1}$ , was associated with significantly higher  $C_{ndvi}$  value estimation: up to 0.28 times higher. It was also indicated that the relationship between  $C_{ndvi}$  estimates and heterogeneous soil conditions can be further dissected according to the canopy structure of different crops; namely, Plagiophile crops, found to be less response to background soil conditions than erectophile types. Identifying land cover type to specific species level, by coupling remote sensing data with the IACS data, allowed quantifying the sensitivity of  $C_{ndvi}$  to soil background heterogeneity in relation to crops' growth stage.

The research also indicated that variable slope shape can be reliably used in quantifying the sensitivity of  $C_{ndvi}$  estimates to topographical variations. Convex and concave slopes were found to have opposite implications on  $C_{ndvi}$  values, in that the concave slope was associated with lower  $C_{ndvi}$  values (up to 0.01 times smaller values compared with flat slope), while the convex slope had an incremental implication (up to 0.05 times higher values compared with flat slope). The impact of different slope shapes also showed variability according to season; a more evident implication of the concave slope was in late summer, while the association of convex slope with higher  $C_{ndvi}$  values spread from spring to the beginning of autumn. The results can be useful inputs in improving the

capacity of  $C_{ndvi}$  estimation for landscapes as complex as the present study region. In addition, utilizing remote sensing data for the purpose of capturing spatiotemporal variation in C factor determination and subsequently serving as input factor for process-based soil erosion modelling can be enhanced by considering the quantified sensitivity of  $C_{ndvi}$  estimations. The information obtained from such modelling practice could also benefit the evaluation of several agricultural land management options in large and complex agricultural landscapes efficiently and more accurately.

For future research, we suggest to explicitly study C factor determination, including spatially distributed climatic data along with yellow vegetation indices in order to improve the applicability and transferability of the  $C_{ndvi}$  method to regions with similar conditions.

**Author Contributions:** Conceptualization, D.A.A., D.D. (Detlef Deumlich), and B.Š.; Data curation, D.A.A. and D.D. (Daniel Doktor); Formal analysis, D.A.A.; Investigation, D.A.A. and D.D. (Detlef Deumlich); Methodology, D.A.A., D.D. (Detlef Deumlich) and D.D. (Daniel Doktor); Resources, D.D. (Detlef Deumlich) and B.Š.; Supervision, D.D. (Detlef Deumlich) and B.Š.; Writing—original draft, D.A.A.; Writing—review and editing, D.A.A., D.D. (Detlef Deumlich), B.Š., and D.D. (Daniel Doktor). All authors have read and agreed to the published version of the manuscript.

**Funding:** This research received no external funding.

**Acknowledgments:** The first author is a recipient of the Czech Republic government scholarship for their PhD study. This study is part of their PhD work. The first author also benefited from financial assist from Palacký University Olomouc through the grant (IGA\_PrF\_2020\_020) and from the project of the National Agency for Agricultural Research of the Czech Republic No. QK1810233. We would also acknowledge ZALF in Müncheberg for the first author's research stay. Finally, we acknowledge Horst H. Gerke, from ZALF, for his helpful comments and editing works on the manuscript.

**Conflicts of Interest:** The authors declare no conflict of interest.

## Appendix A

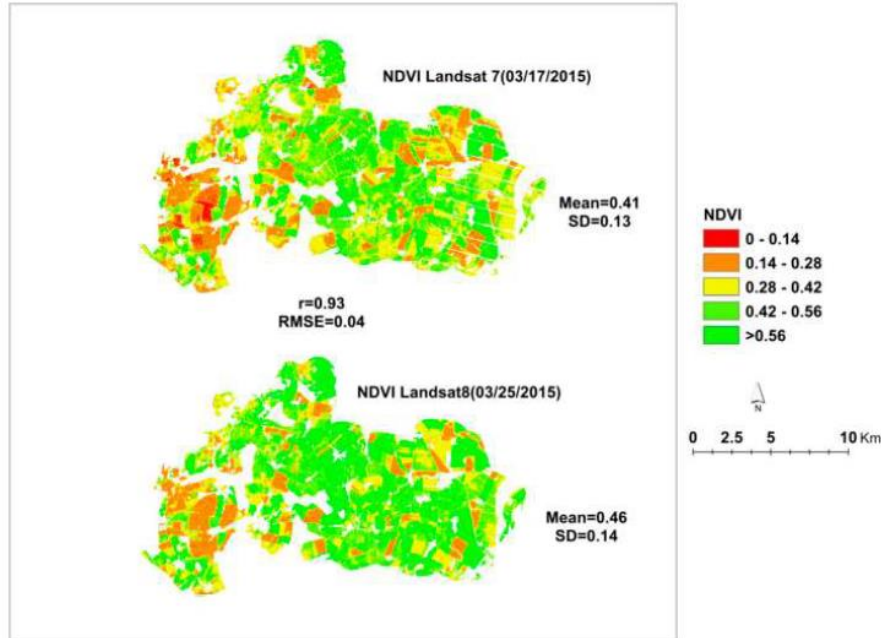


**Figure A1.** Comparison of NDVI values between two closely taken images from Landsat 7 and Landsat 8 satellites, indicating comparably similar distribution and statistics.

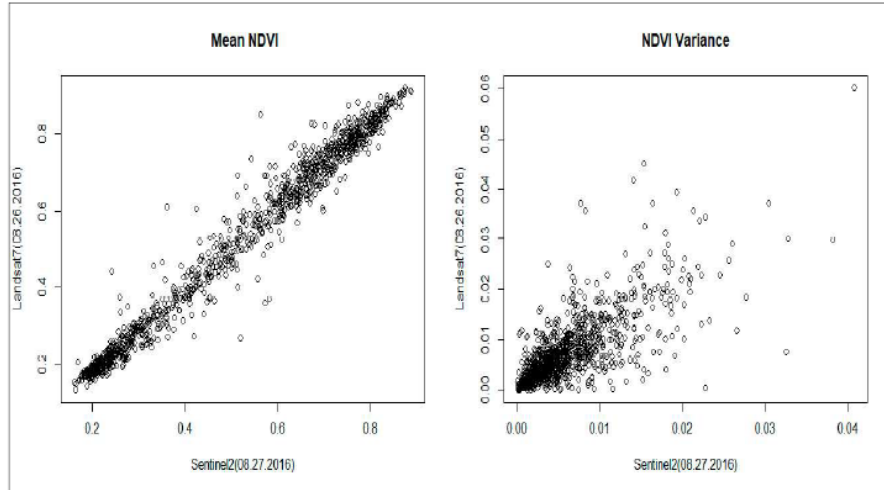


**Figure A2.** Mean and variance NDVI comparisons between Sentinel 2 and Landsat 7 images; there was no significant difference between the means ( $p = 0.47$ ) in these two closely sensed data. Correlation coefficient was  $r = 0.97$ . Values are the averages of each parcel ( $n = 1130$  parcels) from 2016 IACS data extracted using the R package “raster.”

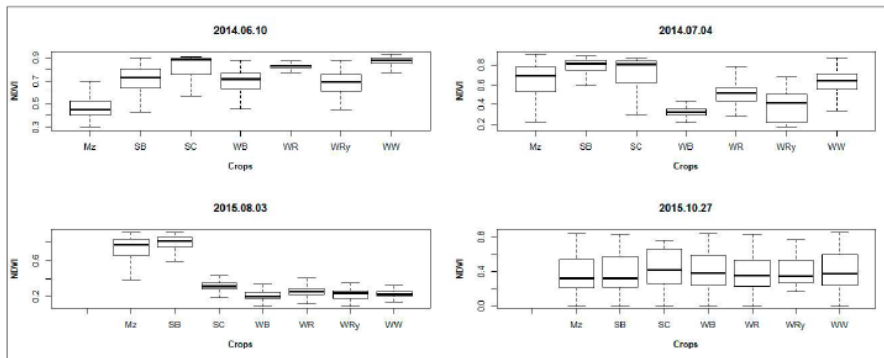


**Figure A3.** NDVI variation across different crop cover types in the study area. In June, almost all crop covers had a median NDVI > 0.5. As the summer progressed, winter-sown crops such as WRy, WB, and WW showed a decline in median NDVI values, which could elevate the  $C_{ndvi}$  values of the study area.

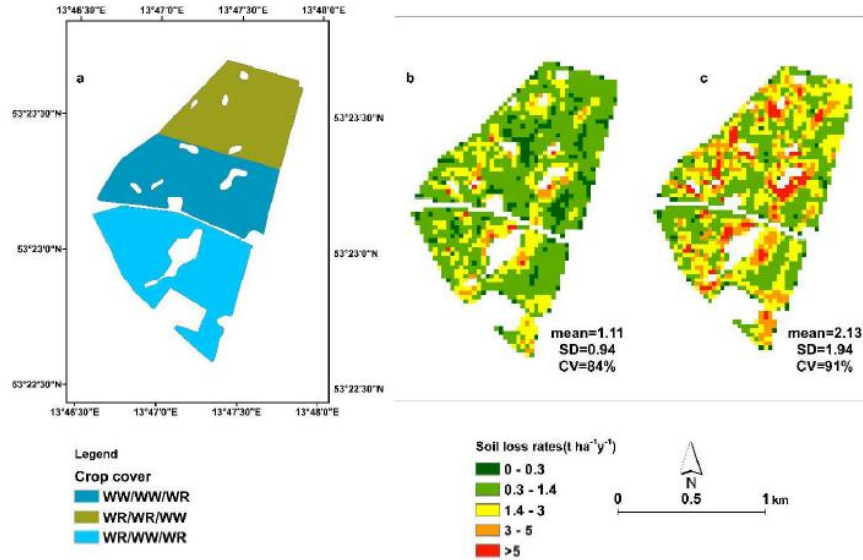


**Figure A4.** Three years average potential soil erosion rate in a catchment around Holzendorf experimental station: (a) land cover type from 2014 to 2016 cropping year identified through the IACS data; (b) and (c) erosion predicted using  $C_{lit}$  ( $SL_{lit}$ ) and using  $C_{ndvi}$  ( $SL_{ndvi}$ ), respectively. Compared to the long-term experimental results, which ranged from 0.5 to 5  $t\ ha^{-1}\ y^{-1}$ , the values predicted using the USLE can fairly be taken as representative.

## Appendix B

**Table A1.** Data comparison between randomly extracted data points (samples) and the whole scene statistics (population). The t-test indicated no statistical difference between the two groups ( $p = 0.92$ ,  $t$  value = 2.0 for the means; and  $p = 0.99$ ,  $t$  value = 2.0 for standard deviations).

Variables	Mean		Standard Deviation	
	Sample ( $n = 5000$ )	Population	Sample ( $n = 5000$ )	Population
Slope	2.52	2.58	1.95	2.14
K value	0.2	0.19	0.07	0.07
LS factor	0.36	0.37	0.38	0.40
<b><math>C_{ndvi}</math> by scene dates</b>				
29 October 2013	0.21	0.19	0.21	0.21
10 February 2014	0.26	0.25	0.20	0.19
30 March 2014	0.14	0.13	0.21	0.20
1 May 2014	0.17	0.14	0.25	0.23
18 June 2014	0.07	0.07	0.12	0.11
4 July 2014	0.12	0.11	0.15	0.15
13 August 2014	0.25	0.24	0.24	0.24
6 September 2014	0.32	0.31	0.27	0.27
8 October 2014	0.24	0.23	0.23	0.23
17 March 2015	0.29	0.29	0.21	0.20
25 March 2015	0.22	0.21	0.19	0.18
10 April 2015	0.16	0.15	0.22	0.21
5 June 2015	0.12	0.10	0.23	0.21
13 June 2015	0.09	0.08	0.17	0.16
4 July 2015	0.11	0.11	0.14	0.14

Table A1. Cont.

Variables	Mean		Standard Deviation	
	Sample ( <i>n</i> = 5000)	Population	Sample ( <i>n</i> = 5000)	Population
7 July 2015	0.12	0.11	0.14	0.14
3 August 2015	0.38	0.37	0.25	0.25
3 October 2015	0.30	0.29	0.25	0.25
27 October 2015	0.28	0.27	0.24	0.24
31 December 2015	0.21	0.2	0.22	0.22
2 April 2015	0.28	0.26	0.25	0.24
22 April 2015	0.21	0.18	0.26	0.25
2 May 2015	0.22	0.17	0.30	0.28
9 May 2015	0.21	0.16	0.30	0.28
12 May 2015	0.20	0.16	0.28	0.26
8 June 2015	0.09	0.08	0.17	0.17
23 June 2015	0.06	0.06	0.11	0.11

## References

- Pimentel, D.; Burgess, M. Soil erosion threatens food production. *Agriculture* **2013**, *3*, 443–463. [CrossRef]
- Šarapatka, B.; Bednář, M. Assessment of potential soil degradation on agricultural land in the Czech Republic. *J. Environ. Qual.* **2015**, *44*, 154–161. [CrossRef] [PubMed]
- Borrelli, P.; Robinson, D.A.; Fleischer, L.R.; Lugato, E.; Ballabio, C.; Alewell, C.; Meusburger, K.; Modugno, S.; Schütt, B.; Ferro, V.; et al. An assessment of the global impact of 21st century land use change on soil erosion. *Nat. Commun.* **2017**, *8*, 2013. [CrossRef] [PubMed]
- Alexandridis, T.K.; Sotiropoulou, A.M.; Bilas, G.; Karapetsas, N.; Silleos, N.G. The effects of seasonality in estimating the C-Factor of soil erosion studies. *Land. Degrad. Dev.* **2015**, *26*, 596–603. [CrossRef]
- Schönbrodt, S.; Saumer, P.; Behrens, T.; Seeber, C.; Scholten, T. Assessing the USLE crop and management factor C for soil erosion modeling in a large mountainous watershed in Central China. *J. Earth Sci.* **2010**, *21*, 835–845. [CrossRef]
- Wischmeier, W.H.; Smith, D.D. *Predicting Rainfall Erosion Losses—A Guide to Conservation Planning*; U.S. Department of Agriculture: Washington, WA, USA, 1978.
- Feng, Q.; Zhao, W.; Ding, J.; Fang, X.; Zhang, X. Estimation of the cover and management factor based on stratified coverage and remote sensing indices: A case study in the Loess Plateau of China. *J. Soils Sediments* **2018**, *18*, 775–790. [CrossRef]
- Gyssels, G.; Poesen, J.; Bochet, E.; Li, Y. Impact of plant roots on the resistance of soils to erosion by water: A review. *Prog. Phys. Geogr.* **2005**, *29*, 189–217. [CrossRef]
- Arnold, J.G.; Srinivasan, R.; Muttiyah, R.S.; Williams, J.R. Large area hydrologic modeling and assessment Part I: Model development. *J. Am. Water. Resour. Assoc.* **1998**, *34*, 73–89. [CrossRef]
- Neitsch, S.L.; Arnold, J.G.; Kiniry, J.R.; Williams, J.R. *Soil and Water Assessment Tool Theoretical Documentation*; Version 2005; 2005. Available online: <https://swat.tamu.edu/media/1292/SWAT2005theory.pdf> (accessed on 27 November 2019).
- Young, R.A.; Onstad, C.A.; Bosch, D.D.; Anderson, W.P. AGNPS—A nonpoint-source pollution model for evaluating agricultural watersheds. *J. Soil Water Conserv.* **1989**, *44*, 168–173.
- Zhao, W.; Fu, B.; Qiu, Y. An upscaling method for cover-management factor and its application in the loess Plateau of China. *Int. J. Environ. Res. Public Health* **2013**, *10*, 4752–4766. [CrossRef]
- Morgan, R.P.C. *Soil Erosion and Conservation*, 3rd ed.; Blackwell Publishing: Oxford, UK, 2005; ISBN 1-4051-1781-8.
- Panagos, P.; Borrelli, P.; Meusburger, K.; Alewell, C.; Lugato, E.; Montanarella, L. Estimating the soil erosion cover-management factor at the European scale. *Land Use Policy* **2015**, *48*, 38–50. [CrossRef]
- Ali, S.A.; Hagos, H. Estimation of soil erosion using USLE and GIS in Awassa Catchment, Rift valley, Central Ethiopia. *Geoderma Reg.* **2016**, *7*, 159–166. [CrossRef]
- Ganasri, B.P.; Ramesh, H. Assessment of soil erosion by RUSLE model using remote sensing and GIS—A case study of Nethravathi Basin. *Geosci. Front.* **2016**, *7*, 953–961. [CrossRef]

17. Pechanec, V.; Mráz, A.; Benc, A.; Cudlín, P. Analysis of spatiotemporal variability of C-factor derived from remote sensing data. *J. Appl. Remote Sens.* **2018**, *12*, 1. [CrossRef]
18. Schmidt, S.; Alewell, C.; Meusburger, K. Mapping spatio-temporal dynamics of the cover and management factor (C-factor) for grasslands in Switzerland. *Remote Sens. Environ.* **2018**, *211*, 89–104. [CrossRef]
19. Matsushita, B.; Yang, W.; Chen, J.; Onda, Y.; Qiu, G. Sensitivity of the Enhanced Vegetation Index (EVI) and Normalized Difference Vegetation Index (NDVI) to topographic effects: A case study in high-density cypress forest. *Sensors* **2007**, *7*, 2636–2651. [CrossRef]
20. De Jong, S.M. Derivation of vegetative variables from a Landsat TM image for modelling soil erosion. *Earth Surf. Process. Landf.* **1994**, *19*, 165–178. [CrossRef]
21. Montandon, L.M.; Small, E.E. The impact of soil reflectance on the quantification of the green vegetation fraction from NDVI. *Remote Sens. Environ.* **2008**, *112*, 1835–1845. [CrossRef]
22. Vrieling, A. Satellite remote sensing for water erosion assessment: A review. *CATENA* **2006**, *65*, 2–18. [CrossRef]
23. De Asis, A.M.; Omasa, K. Estimation of vegetation parameter for modeling soil erosion using linear Spectral Mixture Analysis of Landsat ETM data. *ISPRS J. Photogramm. Remote Sens.* **2007**, *62*, 309–324. [CrossRef]
24. Wang, G.; Wentle, S.; Gertner, G.Z.; Anderson, A. Improvement in mapping vegetation cover factor for the universal soil loss equation by geostatistical methods with Landsat Thematic Mapper images. *Int. J. Remote Sens.* **2002**, *23*, 3649–3667. [CrossRef]
25. Deng, Y.; Chen, X.; Chuvieco, E.; Warner, T.; Wilson, J.P. Multi-scale linkages between topographic attributes and vegetation indices in a mountainous landscape. *Remote Sens. Environ.* **2007**, *111*, 122–134. [CrossRef]
26. Ding, Y.; Zhao, K.; Zheng, X.; Jiang, T. Temporal dynamics of spatial heterogeneity over cropland quantified by time-series NDVI, near infrared and red reflectance of Landsat 8 OLI imagery. *Int. J. Appl. Earth Obs.* **2014**, *30*, 139–145. [CrossRef]
27. Borrelli, P.; Meusburger, K.; Ballabio, C.; Panagos, P.; Alewell, C. Object-oriented soil erosion modelling: A possible paradigm shift from potential to actual risk assessments in agricultural environments. *Land Degrad. Dev.* **2018**, *29*, 1270–1281. [CrossRef]
28. Gitelson, A.A.; Kaufman, Y.J.; Stark, R.; Rundquist, D. Novel algorithms for remote estimation of vegetation fraction. *Remote Sens. Environ.* **2002**, *80*, 76–87. [CrossRef]
29. Jackson, R.D.; Pinter, P.J. Spectral response of architecturally different wheat canopies. *Remote Sens. Environ.* **1986**, *20*, 43–56. [CrossRef]
30. Lischeid, G.; Kalettka, T.; Merz, C.; Steidl, J. Monitoring the phase space of ecosystems: Concept and examples from the Quillow catchment, Uckermark. *Ecol. Indic.* **2016**, *65*, 55–65. [CrossRef]
31. Deumlich, D.; Schmidt, R.; Sommer, M. A multiscale soil-landform relationship in the glacial-drift area based on digital terrain analysis and soil attributes. *J. Plant Nutr. Soil Sci.* **2010**, *173*, 843–851. [CrossRef]
32. Wulf, M.; Jahn, U.; Meier, K. Land cover composition determinants in the Uckermark (NE Germany) over a 220-year period. *Reg. Environ. Chang.* **2016**, *16*, 1793–1805. [CrossRef]
33. WRB-IUSS. *World Reference Base for Soil Resources 2014, Update 2015. International Soil Classification System for Naming Soils and Creating Legends for Soil Maps*; World Soil Resources Report 106; WRB-IUSS; FAO: Rome, Italy, 2014.
34. Vogel, E.; Deumlich, D.; Kaupenjohann, M. Bioenergy maize and soil erosion—Risk assessment and erosion control concepts. *Geoderma* **2016**, *261*, 80–92. [CrossRef]
35. Wetter Online. Climate in the Uckermark Region. Available online: [https://www.wetteronline.de/?pcid=pc\\_rueckblick\\_climate&gid=10291&iid=10289&pid=p\\_rueckblick\\_climatecalculator&sid=Default&var=NS&analysis=annual&startyear=1992&endyear=2016&iid=10289](https://www.wetteronline.de/?pcid=pc_rueckblick_climate&gid=10291&iid=10289&pid=p_rueckblick_climatecalculator&sid=Default&var=NS&analysis=annual&startyear=1992&endyear=2016&iid=10289) (accessed on 30 November 2019).
36. Deumlich, D.; Mioduszewski, W.; Kocmit, A. Analysis of sediment and nutrient loads due to soil erosion in rivers in the Odra catchment. In *Agricultural Effects on Ground and Surface Waters: Research at the Edge of Science and Society, Proceedings of the Symposium Held at Wageningen, Wageningen, The Netherlands, October 2000*; Joop, S., Frans, C., Jaap, W., Eds.; IAHS Press, Center for Ecology and Hydrology: Wallingford, UK, 2002; pp. 279–286. ISBN 0144-7815.
37. Nicola, L.-J.; Dietmar, S.; Annette, O. Analysing data of the Integrated Administration and Control System (IACS) to detect patterns of agricultural land-use change at municipality level. *Landsc. Online* **2016**, *48*, 1–24. [CrossRef]

38. Steinmann, H.-H.; Dobers, E.S. Spatio-temporal analysis of crop rotations and crop sequence patterns in Northern Germany: Potential implications on plant health and crop protection. *J. Plant Dis. Protect.* **2013**, *120*, 85–94. [CrossRef]
39. Bodenbeschaffenheit—Ermittlung der Erosionsgefährdung von Böden durch Wasser mit Hilfe der ABAG. Soil Quality—Determination of Soil Erosion Risk of Soils by Water Using ABAG; DIN 19708; Deutsches Institut für Normung e.V.: Berlin, Germany, 2005. (In German)
40. Deumlich, D. Erosive niederschläge und ihre eintrittswahrscheinlichkeit im nordosten deutschlands. *Meteorol. Z.* **1999**, *8*, 155–161. [CrossRef]
41. Tucker, C.J. Red and photographic infrared linear combinations for monitoring vegetation. *Remote Sens. Environ.* **1979**, *8*, 127–150. [CrossRef]
42. Van der Knijff, J.M.; Jones, R.J.A.; Montanarella, L. *Soil Erosion Risk Assessment in Italy*; EUR 19022 EN.; European Soil Bureau, Joint Research Center of the European Commission: Ispra, Italy, 1999.
43. Durigon, V.L.; Carvalho, D.F.; Antunes, M.A.H.; Oliveira, P.T.S.; Fernandes, M.M. NDVI time series for monitoring RUSLE cover management factor in a tropical watershed. *Int. J. Remote Sens.* **2014**, *35*, 441–453. [CrossRef]
44. Gupta, S.; Kumar, S. Simulating climate change impact on soil erosion using RUSLE model—A case study in a watershed of mid-Himalayan landscape. *J. Earth Syst. Sci.* **2017**, *126*, 255. [CrossRef]
45. Vatandaşlar, C.; Yavuz, M. Modeling cover management factor of RUSLE using very high-resolution satellite imagery in a semiarid watershed. *Environ. Earth Sci.* **2017**, *76*, 267. [CrossRef]
46. Vijith, H.; Seling, L.W.; Dodge-Wan, D. Effect of cover management factor in quantification of soil loss: Case study of Sungai Akah subwatershed, Baram River basin Sarawak, Malaysia. *Geocarto Int.* **2018**, *33*, 505–521. [CrossRef]
47. Gutzler, C.; Helming, K.; Balla, D.; Dannowski, R.; Deumlich, D.; Glemnitz, M.; Knierim, A.; Mirschel, W.; Nendel, C.; Paul, C.; et al. Agricultural land use changes—A scenario-based sustainability impact assessment for Brandenburg, Germany. *Ecol. Indic.* **2015**, *48*, 505–517. [CrossRef]
48. Deumlich, D.; Mioduszewski, W.; Kajewski, I.; Tippl, M.; Dannowski, R. GIS-based risk assessment for identifying source areas of non-point nutrient emissions by water erosion (Odra Basin and sub catchment Uecker). *Arch. Agron. Soil Sci.* **2005**, *51*, 447–458. [CrossRef]
49. Fischer, F.; Hauck, J.; Brandhuber, R.; Weigl, E.; Maier, H.; Auerswald, K. Spatio-temporal variability of erosivity estimated from highly resolved and adjusted radar rain data (RADOLAN). *Agric. For. Meteorol.* **2016**, *223*, 72–80. [CrossRef]
50. Hickey, R. Slope angle and slope length solutions for GIS. *Cartography* **2000**, *29*, 1–8. [CrossRef]
51. Nearing, M.A. A Single, continuous function for slope steepness influence on soil loss. *Soil Sci. Soc. Am. J.* **1997**, *61*, 917–919. [CrossRef]
52. R Core Team. *R: A language and Environment for Statistical Computing*; R Foundation for Statistical Computing: Vienna, Austria, 2019.
53. Wang, G.; Gertner, G.; Fang, S.; Anderson, A.B. Mapping multiple variables for predicting soil loss by geostatistical methods with TM images and a slope map. *Photogramm. Eng. Remote Sens.* **2003**, *69*, 889–898. [CrossRef]
54. Stata User's Guide. Available online: <https://www.stata.com/manuals13/u.pdf> (accessed on 7 June 2018).
55. Deumlich, D.; Ellerbrock, R.H.; Frielinghaus, M. Estimating carbon stocks in young moraine soils affected by erosion. *CATENA* **2018**, *162*, 51–60. [CrossRef]
56. Almagro, A.; Thomé, T.C.; Colman, C.B.; Pereira, R.B.; Marcato Junior, J.; Rodrigues, D.B.B.; Oliveira, P.T.S. Improving cover and management factor (C-factor) estimation using remote sensing approaches for tropical regions. *Int. Soil Water Conserv. Res.* **2019**, *7*, 325–334. [CrossRef]
57. Bargiel, D.; Herrmann, S.; Jadczyzyn, J. Using high-resolution radar images to determine vegetation cover for soil erosion assessments. *J. Environ. Manag.* **2013**, *124*, 82–90. [CrossRef]
58. Truckenbrodt, S.C.; Schmullius, C.C. Seasonal evolution of soil and plant parameters on the agricultural Gebesee test site: A database for the set-up and validation of EO-LDAS and satellite-aided retrieval models. *Earth Syst. Sci. Data* **2018**, *10*, 525–548. [CrossRef]
59. Verheijen, F.G.A.; Jones, R.J.A.; Rickson, R.J.; Smith, C.J. Tolerable versus actual soil erosion rates in Europe. *Earth Sci. Rev.* **2009**, *94*, 23–38. [CrossRef]



60. Glemnitz, M.; Wurbs, A.; Roth, R. Derivation of regional crop sequences as an indicator for potential GMO dispersal on large spatial scales. *Ecol. Indic.* **2011**, *11*, 964–973. [[CrossRef](#)]
61. Gericke, A.; Kiesel, J.; Deumlich, D.; Venohr, M. Recent and future changes in rainfall erosivity and implications for the soil erosion risk in Brandenburg, NE Germany. *Water* **2019**, *11*, 904. [[CrossRef](#)]
62. Huete, A.R.; Jackson, R.D.; Post, D.F. Spectral response of a plant canopy with different soil backgrounds. *Remote Sens. Environ.* **1985**, *17*, 37–53. [[CrossRef](#)]
63. Huete, A.R.; Didan, K.; Miura, T.; Rodriguez, E.; Gao, X.; Ferreira, L. Overview of the radiometric and biophysical performance of the MODIS vegetation indices. *Remote Sens. Environ.* **2002**, *83*, 195–213. [[CrossRef](#)]
64. Rieke-Zapp, D.H.; Nearing, M.A. Slope shape effects on erosion. *Soil Sci. Soc. Am. J.* **2005**, *69*, 1463. [[CrossRef](#)]
65. Sensoy, H.; Kara, O. Slope shape effect on runoff and soil erosion under natural rainfall conditions. *iForest* **2014**, *7*, 110–114. [[CrossRef](#)]



© 2020 by the authors. Licensee MDPI, Basel, Switzerland. This article is an open access article distributed under the terms and conditions of the Creative Commons Attribution (CC BY) license (<http://creativecommons.org/licenses/by/4.0/>).

## 7.2. Publication II

**Ayalew, Dawit Ashenafi**; Deumlich, Detlef; Šarapatka, Bořivoj (2021): Agricultural landscape-scale C factor determination and erosion prediction for various crop rotations through a remote sensing and GIS approach. In *European Journal of Agronomy*. 123, p. 126203. DOI: 10.1016/j.eja.2020.126203

[IF<sub>2019</sub>, 3.726]



Contents lists available at ScienceDirect

European Journal of Agronomy

journal homepage: [www.elsevier.com/locate/eja](http://www.elsevier.com/locate/eja)

## Agricultural landscape-scale C factor determination and erosion prediction for various crop rotations through a remote sensing and GIS approach

Dawit Ashenafi Ayalew<sup>a,\*</sup>, Detlef Deumlich<sup>b</sup>, Bořivoj Šarapatka<sup>a</sup><sup>a</sup> Palacký University Olomouc, Department of Ecology and Environmental Sciences, Šlechtitelů 27, 783 71, Olomouc, Czech Republic<sup>b</sup> Leibniz-Centre for Agricultural Landscape Research (ZALF), RAI, Working Group "Hydropedology", Eberswalder Straße 84, 15374, Müncheberg, Germany

## ARTICLE INFO

## Keywords:

Crop rotation  
Remote sensing  
C factor  
Soil erosion  
IACS

## ABSTRACT

In arable land management, different crop rotation patterns and sequences, such as changing agricultural land use to erosion prone crops, or crops providing less ground cover, can greatly influence soil loss rate through their impact on soil cover status (C factor value). The influence of crop rotation on C value and on erosion rate is often determined on an experimental plot scale, so the results are often erroneous when extrapolated to large heterogeneous landscapes, where they fail to capture the spatiotemporal variability beyond the experimental sites. In the present study we have endeavored to investigate the impact of various crop rotation patterns on C value and on subsequent soil erosion rate, at a landscape level, by combining 28 time-series satellite images (from 2013 to 2016) along with annually updated land-use data, via the integrated administration and control system (IACS), from the Uckermark district of north eastern Germany. In total, 21 different crop sequences were investigated. Winter wheat (WW), winter rape (WR), and maize (Mz) were found to be the predominant arable crops grown in the study area. The highest average annual C values were estimated from crop sequences involving Mz and sugar beet (SB), both as pre-crops and succeeding crops. The highest value of 0.39 was computed from SB/Mz rotation. On the other hand, crop rotation involving WR gave significantly lower annual C values in all the years considered, with the lowest average annual C value of 0.07 calculated on WR parcels preceded by winter cereals. It was also apparent that crop rotation patterns influenced C value in a temporally variable manner. Among the self-sequencing patterns, WR/WR reduced the C value significantly compared with Mz/Mz and to a lesser extent compared with WW/WW. Continuous cultivation of Mz increased the potential soil loss rate by as much as 72 % compared to WR/WR and by 51 % compared to WW/WW. It was also possible to determine the spatial distribution of the impact of crop rotation on soil erosion risk within the study area. The results obtained agreed with the results of other international and regional studies. Overall, the output from this research could contribute towards further efficient investigation of the impact of agronomic practices on the environment in a large agricultural landscape, without the need to set up multi-location experimental plots.

### 1. Introduction

In arable lands, decisions of land-use management can have a direct impact on the rate of soil loss (Preiti et al., 2017). Changing agricultural land use to incorporate erosion-prone crops and crops providing less ground cover could significantly accelerate the rate of soil erosion (Morgan, 2005; Simonneaux et al., 2015). Crop rotation, a decision to be made by farmers for various intrinsic and extrinsic reasons, is the sequencing of different crops grown on a given area of land (Castellazzi et al., 2008; Glemnitz et al., 2011). Rotating different crops has been reported to have a positive effect on sustainable agricultural practices in

several ways, such as improving long-term soil fertility, soil aggregate stability and enhancing diversity at landscape level, provided that compatible crop types are sequenced (Leteinturier et al., 2006; Morgan, 2005; Peltonen-Sainio et al., 2019; Steinmann and Dobers, 2013). For instance Jankauskas and Jankauskiene (2003), report that the composition of crops involved in a rotation system significantly affects the capacity of the rotation system to prevent soil erosion. Bullock (1992) also indicates that short-term rotation of maize and soybeans results in degradation of physical and chemical properties of the soil compared with rotations comprising of various compatible crops.

There have, however, been worldwide reports of an increasing trend

\* Corresponding author.

E-mail address: [dawitashenafi.ayalew01@upol.cz](mailto:dawitashenafi.ayalew01@upol.cz) (D.A. Ayalew).

<https://doi.org/10.1016/j.eja.2020.126203>

Received 16 March 2020; Received in revised form 11 November 2020; Accepted 12 November 2020

Available online 30 November 2020

1161-0301/© 2020 Elsevier B.V. All rights reserved.

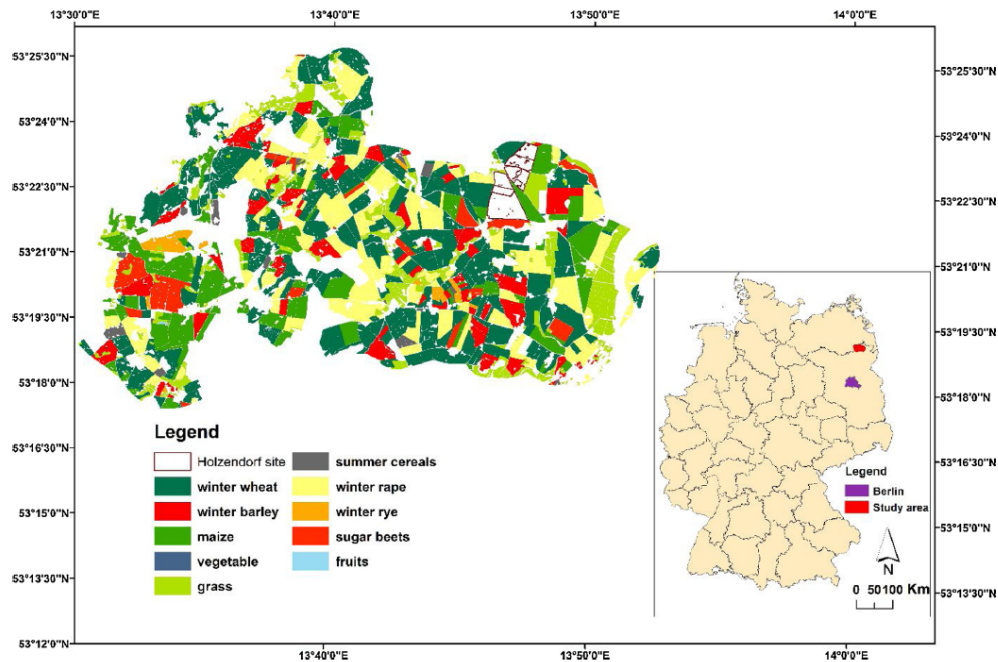


Fig. 1. Overview of study area and arable land use according to IACS 2015. (Geographical location source: <http://www.diva-gis.org/gdata>)

of growing crops in monoculture, if not in short rotations of less compatible crops, for economic, technological, and policy-related reasons (Bennett et al., 2012). The decision to rotate different crops, which is not of a random probability according to Glennitz et al. (2011) and Stein and Steinmann (2018), entails a spatiotemporal variation in the context of the impact it may have on soil erosion rate on a larger landscape scale. Therefore, understanding the spatiotemporal dynamics of various crop rotations, in relation to their impact on soil erosion on a large agricultural landscape scale, is a subject that demands due attention. There is still a lack of reliable assessment of the impact of various crop rotation patterns on land degradation in general, or soil erosion in particular, at a regional level (Lorenz et al., 2013), while this is fundamental in understanding other related phenomena, such as climate change mitigation and hydrological processes on a global scale (Alewell et al., 2019).

The influence of crop rotation on soil erosion can be assessed by the crop cover and management (C-factor) values from the Universal Soil Loss Equation (USLE) model. More often than not, plot experiments are laid out to determine C values for specific crop rotations (Deuschle et al., 2019; Preiti et al., 2017). However, determining crop rotation patterns at plot level is not only a time consuming and costly practice (Gabriels et al., 2003; Preiti et al., 2017), but it also fails to accommodate spatiotemporal variations beyond the area of the experimental location (Peltonen-Sainio et al., 2019). Even the availability of such information is limited in many cases (Gabriels et al., 2003; GUO et al., 2015). One of the key inputs lacking in the assessment of crop rotation systems, and subsequent use in erosion prediction models on a large heterogeneous agricultural landscape scale, is spatiotemporally refined agricultural land-use data, namely information on specific crop sequences (Glennitz et al., 2011; Lorenz et al., 2013; Waldhoff et al., 2017). In Germany, where the present study site is based, a number of studies have used district level statistical cropping data to assign empirical C values in relation to crop rotation on a large agricultural landscape scale

(Auerswald, 2002; Deumlich et al., 2005; Koschke et al., 2013) although the values obtained are static. Yet, assigning empirical C values to land-use maps is problematic, due to inaccuracy resulting from gaps in transition periods between two main crops (Auerswald et al., 2003). The use of remote sensing data for such a purpose is, therefore, topical and has been suggested by a number of researchers (Leteinturier et al., 2006; Peltonen-Sainio et al., 2019; Waldhoff et al., 2017) as it incorporates the spatiotemporal dynamics of rotation systems and their implications on C values and erosion rates.

Yet, studying cropping practices in general, or crop rotation in particular, using remote sensing data is not a well-established practice (Bégué et al., 2018). In their literature review work, Bégué et al. (2018) indicate that not more than 10 % of remote sensing studies focused on cropping practices. When it comes to crop rotation, the majority of studies focused on identifying rotation patterns and classifying the pre-crops and succeeding crops in general (Conrad et al., 2016; Kipka et al., 2016; Martínez-Casasnovas et al., 2005; Mueller-Warrant et al., 2016; Panigrahy and Sharma, 1997; Sahajpal et al., 2014).

In the present research, therefore, we used multi-temporal satellite images in combination with parcel level land-use data, the Integrated Administration and Control System (IACS), to investigate the influence of actually practiced crop rotation patterns on C factor values and the subsequent impact on potential soil erosion risks across a large heterogeneous agricultural landscape. The overarching aim of the research is to indicate ways of alleviating the problem of determining C values, and subsequent soil erosion rates, for various crop rotation patterns, with respect to addressing temporal variability in a large heterogeneous landscape.

The three specific objectives of the study are to: i) investigate the impact of various crop rotation patterns on C factor values and on subsequent potential soil erosion rate; ii) temporally evaluate the influences of crop rotations on C factor values in order to capture inter-annual variability in various cropping sequences; iii) assess the spatial

**Table 1**  
Cropping calendar and representative satellite image allocation in each season.

Cropping calendar	2013/2014				2014/2015				2015/2016			
	Autumn	Winter	Spring	Summer	Autumn	Winter	Spring	summer	Autumn	Winter	Spring	summer
	Image dates*	10.29.13 <sup>2</sup>	02.10.14 <sup>1</sup>	03.30.14 <sup>1</sup> 05.01.14 <sup>1</sup>	06.10.14 <sup>1</sup> 07.04.14 <sup>1</sup> 08.13.1 <sup>2</sup>	09.06.14 <sup>1</sup> 10.08.14 <sup>1</sup>	03.17.15 <sup>1</sup>	03.25.15 <sup>2</sup> 04.10.15 <sup>2</sup>	06.05.15 <sup>1</sup> 06.13.15 <sup>2</sup> 07.04.15 <sup>2</sup> 08.03.15 <sup>2</sup>	09.15.15 <sup>2</sup> 10.03.15 <sup>2</sup> 10.27.15 <sup>1</sup>	12.31.15 <sup>2</sup>	04.02.16 <sup>1</sup> 04.22.16 <sup>1</sup> ; 05.09.16 <sup>1</sup> ; 05.12.16 <sup>3</sup>

\* Dates are expressed as month.day.year.

<sup>1</sup> Landsat 7 data.

<sup>2</sup> Landsat 8.

<sup>3</sup> Sentinel 2 data.

distribution of the impact of crop rotation on potential soil erosion risks in the study area. In the end, the outcome of the study could have implications for large-scale agroecosystem modelling studies in the study area and beyond.

## 2. Material and methods

### 2.1. Study area

The study area is in the Uckermark district of the north eastern part of the Brandenburg state of Germany (Fig. 1). The area is characterized as having heterogeneous soil type across varying topographical form; slightly eroded Luvisols to Calcic Regosols dominate the hill tops and upper slopes, while Luvisol or Haplic Luvisol occur mid-slope. In depression areas Stagnosols prevail (Deumlich et al., 2010; Wulf et al., 2016). The area has temperate and continental climatic conditions with annual average air temperature ranging between 7.8 °C and 9.5 °C (Vogel et al., 2016). An average annual precipitation of 460.3 mm was recorded at Grünow weather station between the years 1992–2016 (Wetteronline.de, 2018). Land use in the area is predominantly agricultural (Glemnitz et al., 2011), mostly covered by winter cereals, winter rape, maize, and sugar beet (Lischeid et al., 2016).

### 2.2. Data and processing

#### 2.2.1. Satellite imagery

Twenty-eight images from Landsat 7 and Landsat 8 (using path 193, row 23), and Sentinel 2A (using tile ID 33UVV), covering a period from 2013 to 2016, were downloaded from the USGS (<https://earthexplorer.usgs.gov/>) and the Copernicus Hub (<https://scihub.copernicus.eu/dhus/#/home>) respectively. All images have been atmospherically corrected. In order to represent the four growing seasons, at least one image from each season was included (See Table 1 for allocation of images according to cropping calendar). Images showing cloud cover of less than 30 % were used for the purpose. Most of the images covering the study area were cloud free, and cloud mask data was used to exclude cloud covered pixels from further analysis. Finally, the study area was defined in each image using the IACS shape.

#### 2.2.2. Crop rotation (sequence) identification

The Integrated Administration and Control System (IACS), which was implemented by the EU for direct payments, provides parcel level land-use data (Stein and Steinmann, 2018; Steinmann and Dobers, 2013). IACS data from 2013 to 2016 were used for the present study to determine crop rotation. The IACS dataset consisted of up to 1127 single entries (number of parcels) per year for the considered study area. Each entry provides information on agricultural land use, such as crop type,

**Table 2**  
Proportion (%) of arable land use during the considered years.

Land use	Abbreviation	percentage of entire arable landscape used for given crop				Average
		2013	2014	2015	2016	
Winter wheat	WW	23.3	23.2	22.0	20.7	22.3
Winter Barley	WB	6.6	6.6	7.9	5.9	6.8
Winter Rye	WRy	4.5	2.4	1.2	1.1	2.3
Winter Rapeseed	WR	12.7	14.0	12.2	11.0	12.5
Maize	Mz	10.3	10.7	9.3	10.0	10.1
Sugar Beets	SB	0	2.3	1.8	1.3	1.4
Summer Cereals	SC	3.2	2.5	2.5	1.5	2.4
Grass*	Gr	35.0	34.0	32.5	35.2	34.2
Fruits and vegetables	FG	0.3	0.8	0.2	0.9	0.5
Others**		4.2	3.4	10.5	12.8	7.7

\* Grass includes all forms of, annual or permanent, cultivation of grass and fodder species in the entire agricultural landscape.

\*\* Includes potatoes, peas, beans, fallow fields, buffer strips.

**Table 3**

Crop sequences (CS) considered for analysis based on the parcel proportion of the specified pre-crop and the landscape coverage (parcel proportion >5% and coverage >0.5 % considered for analysis).

Succeeding crops	Pre-crops	Coverage of the CS as proportion of entire landscape (%)			Specified pre-crop as a proportion of the CS (%)		
		2013/14	2014/15	2015/16	2013/14	2014/15	2015/16
WW	WW	6.6	6.7	7.6	22.8	26.9	27.1
	WR	10.1	11.7	11.8	54.7	65.6	72.1
	Mz	4.4	3.7	3.1	41.2	36.0	33.7
	WB	1.3	1.7	1.6	17.9	14.6	16.4
	SB	-	1.1	0.6	-	34.1	40.0
	WRy	1.2	-	-	31.4	-	-
	SC	-	-	0.6	-	-	26.2
WR	WR	1.7	1.5	1.2	8.9	8.6	7.6
	WW	8.9	5.9	6.6	31.3	23.9	23.6
	Mz	0.6	0.5	0.8	5.6	5.0	8.3
	WB	4.7	5.3	4.9	64.2	45.2	51.4
	WRy	0.9	-	-	26.7	-	-
	SC	0.9	-	-	33.3	-	-
	Mz	2.7	2.9	3.3	25.2	28.6	35.9
Mz	WW	3.9	2.5	5.0	13.8	10.0	17.9
	WR	1.9	0.8	1.1	10.6	5.0	6.7
	SB	-	0.8	-	-	25.0	-
	WB	-	-	1.2	-	-	12.9
	WRy	0.6	0.7	0.3	15.1	39.2	11.3
	WW	6.3	6.3	3.9	21.8	25.4	14.0
	WB	-	0.9	0.7	-	7.7	7.1
WB	WR	3.7	1.9	-	19.8	10.7	-
	WW	1.3	1.2	0.8	5.0	5.1	5.0
	Mz	0.9	-	-	8.4	-	-

(-) CSs did not fulfill the threshold, hence not considered for analysis.

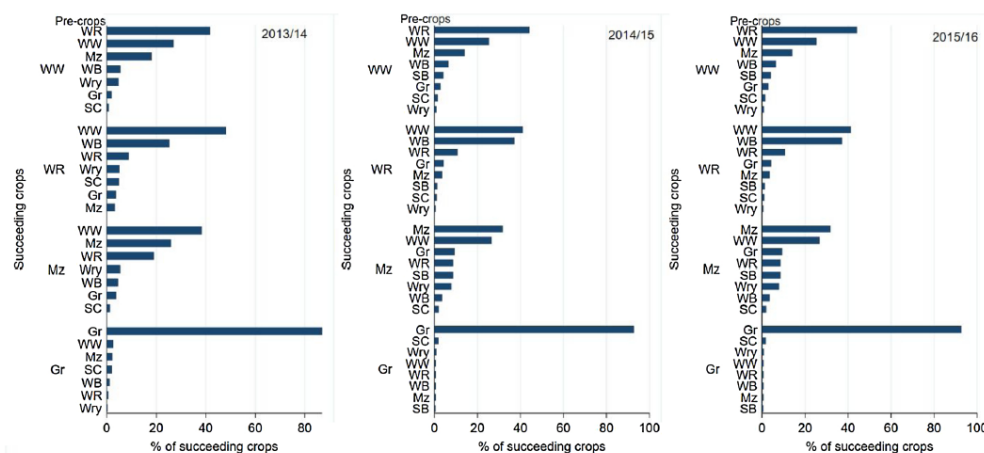


**Fig. 2.** Proportion of pre-crops, of the principal land use types, in the study area.

parcel area, etc. for a single parcel of land specified by an official numerical code (ID). A number of researchers have pointed out that there is a potential change of parcel identification number from year to year, which could result in a mismatch for rotation study (Leteinturier et al., 2006; Stein and Steinmann, 2018). However, to avoid any mismatch, we used the crop ID, through query builder of the ArcGIS10.2.2, to identify crop sequence patterns.

Crop sequences in the study area were determined by intersecting consecutive IACS shape files through the *Geoprocessing* tool, which then provided an intersected polygon map for each cropping calendar (See Table 1 for cropping calendar). The final intersected polygon then has its own consecutive years' crop history, from which the predominant/major crops in the study area were taken as succeeding crops to determine their pre-crops by means of the query building tool in the ArcGIS

environment. A similar approach was applied by Leteinturier et al. (2006), using IACS datasets to formulate crop sequence indicators. The percentage of the land-use pattern in the study area is depicted in Table 2. Winter wheat (WW), Grass (Gr), Winter Rape (WR), and Maize (Mz) are considered as predominant/major crops as they covered more than 10 % of the landscape in the study periods; while the others (WB, WRy, SB, and SC) were taken as minor crops. All possible single year crop sequences of the indicated land cover types, except fruits and vegetables, were determined, and hence a total of 64 sequences (i.e. 8 crop types in sequence with 8 different crop types, including self-sequencing) could be obtained (Appendix Table A1).

Year on year proportions of each crop sequence, and its share of the entire landscape, were calculated (see Appendix Table A1). As analysis of all 64 crop sequences would not be feasible, a threshold was set. Crop

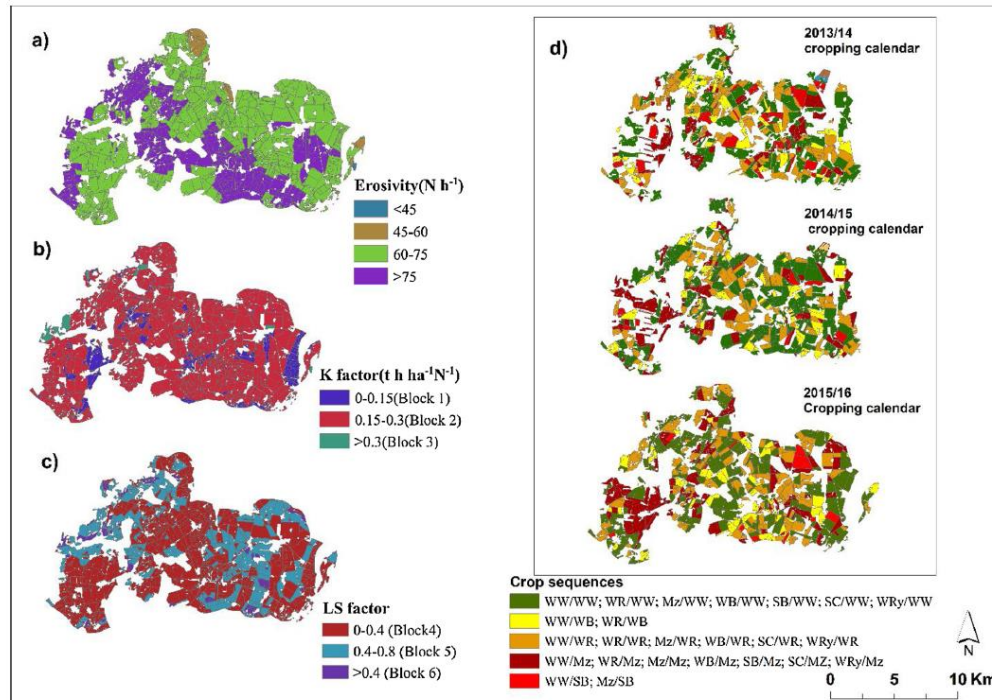


Fig. 3. Map of a) Rainfall erosivity, b) soil erodibility, c) slope length and steepness (LS) blocking, and d) crop sequences considered in the analysis from 2013 to 2016 cropping calendars (the shape of the map in each year varies due to the spatial variation of the cropping patterns in each year’s ICAS shape).

sequences with a proportion of more than 5% of the specified pre-crop in that particular year, and coverage of at least 0.5 % of the entire agricultural landscape (a sum of more than 75 ha of parcels [3 standard deviation] in each cropping calendar year) were selected for the final analysis. As a result of variations in the year on year proportion of minor crops, a slightly different set of crop sequences was considered in each cropping calendar (Table 3).

When it comes to the pre-crops of the predominant/major crops, there appeared to be year on year variation (Fig. 2), apart from grass (Gr). Most of the grass-covered parcels (close to 90 %) retained the same land-use throughout the entire study period; as a result, Gr was not included in the analysis of crop rotation.

2.3. Potential soil erosion modelling and C factor determination

The USLE predicts annual soil erosion rate through six compartmentalized factors, e.q.1, (Wischemeier and Smith, 1978):

$$A=R.K.L.S.C. P \tag{1}$$

where, A is predicted annual soil erosion rate ( $t\ ha^{-1}\ y^{-1}$ ).

- R is rainfall erosivity factor ( $N\ h^{-1}$ , unit commonly used in Germany and can easily be converted to Metric units by increasing it by one order of magnitude). We used average erosivity over eight years (2006–2013), calculated using  $1\ km^2$  spatial and 5-minute temporal resolution radar data (RADOLAN) obtained from the German Weather Service (Fig. 3a). The use of radar weather data for rainfall erosivity estimation and soil erosion modelling has been found to be satisfactory (Fischer et al., 2016).
- K stands for the soil erodibility factor ( $t\ h\ ha^{-1}\ N^{-1}$ ) (Fig. 3b), which was determined using data obtained from the German soil appraisal

“Bodenschätzung” (DIN 19708, 2005DIN 19708, 2005; Vogel et al., 2016) by employing the equation developed by Wischemeier and Smith (1978).

- L and S are the topographic factors which indicate the slope length (L) (calculated according to Hickey (2000) and steepness of the slope (S) (determined according to Nearing (1997) using a 5 m resolution digital elevation model (Fig. 3c).
- C stands for the cover and management factor, which is the concern of this study. The USLE C factor values for crop rotations are calculated using the Soil Loss Ratio (SLR), representing the ratio of soil loss under a specific crop cover to that of bare soil of similar topographic and edaphic conditions (Morgan, 2005; Wischemeier and Smith, 1978). The measurement is repeated several times (periods) in a growing year, corresponding to different phenological stages of the given crop, from ploughing to harvesting. Finally, these SLR values are weighted by the corresponding percentage mean annual rainfall erosivity (R) values and the final summation provides the annual C-value (eq.2).

$$C = \sum_i^n SLR_i \frac{R_i}{R} \tag{2}$$

where, C is the annual C-factor,  $SLR_i$  the soil loss ratio for the period i,  $R_i$  is the rainfall erosivity of the month i, R is the annual rainfall erosivity, and n is the number of periods used in the summation. As pointed out earlier, while dealing with large scale investigations, measurement of SLR for each and every crop type and rotation is inefficient and costly (Gabriels et al., 2003; Panagos et al., 2015). van der Knijff et al. (1999) suggested employing an NDVI-(normalized difference vegetation index) based equation (Eq.3) for regional scale C-factor determination

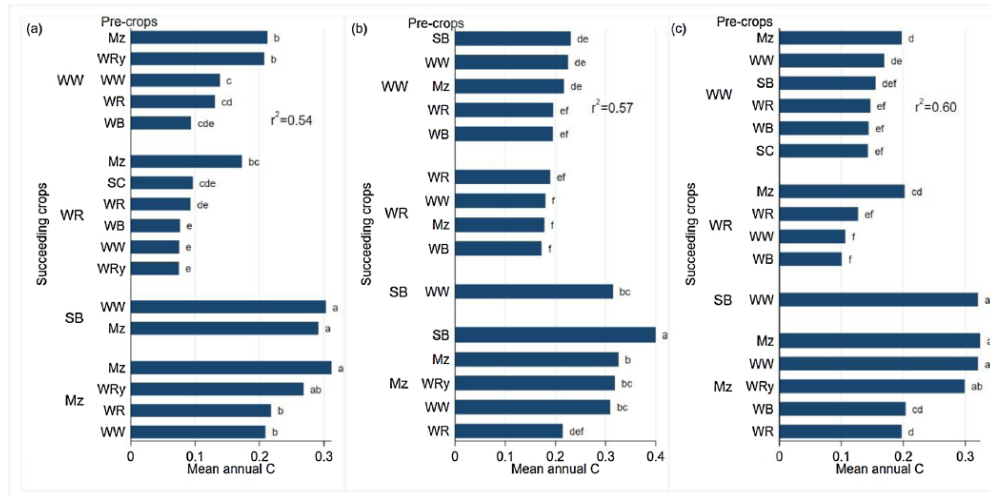


Fig. 4. The impact of different crop rotations on mean annual C factor values (a) 2013/14, b) 2014/15, c) 2015/16 cropping calendar; columns followed by the same letter(s) are not significantly different from each other according to LSD ( $P < 0.05$ ).

$$C = \exp \left[ -\alpha \frac{NDVI}{(\beta - NDVI)} \right] \quad (3)$$

where,  $\alpha$  and  $\beta$  are parameters of the NDVI-C correlation by which values 2 and 1 are found to yield reasonable results. This method has been employed by several studies worldwide (Durigon et al., 2014; Pechanec et al., 2018; Vatandaşlar and Yavuz, 2017; Vijith et al., 2018). The C factor values are, then, determined using eq.3 from each crop sequence pattern (Fig. 3d) for the USLE model.

- P is soil support practice factor, such as contour farming or terracing, for this region a value of 1 is applied as support practices are not implemented.

The USLE model was executed in GIS environment. Finally, the performance of the erosion model was validated by comparing the model output with a long-term (1984–1996) plot-scale experiment output of different crop rotation schemes conducted at Holzendorf research site (Fig. 1). Crop rotations involving Mz/Mz and WRy/WRy were considered for validation. Details of the composition of the experimental rotation scheme can be found in the results of Deumlich et al. (2018) and the long-term measured erosion rates are also depicted in the Appendix Fig. B1.

#### 2.4. Statistical analysis

In order to look into the impact of various crop rotations on C-factor values, and on the subsequent soil erosion rates, Analysis of Variance (ANOVA) through the Generalized Linear Model (GLM) was employed, using the R statistical software (R Core Team, 2019). The average C factor value and soil loss rate of each parcel were extracted using the R spatial analysis package (“extract”). The extracted values are the average values of each agricultural parcel. This method enhanced the capacity to trace back values through the parcel ID. However, in order to control variations which could arise from differences in soil type and topographical features rather than mere crop rotation, we used three blocks of soil erodibility values, considered to represent the heterogeneous soil condition of the study area, (block 1,  $K < 0.15$ ; block 2,  $0.15 < K < 0.3$ ; and block 3,  $K > 0.30$ ) and three blocks of LS factor (block4,  $LS < 0.4$ ; block 5,  $0.4 < LS < 0.8$ ; block 6,  $LS > 0.8$ ) (Fig. 3b and c). These

blocking categories were determined after running regression analysis of C values against several topographic and soil variables in the study area (Ayalew et al., 2020). These two variables were found to correlate well with NDVI-derived C values in the study area. Additionally, in analyzing the impact of crop rotations on potential soil erosion risk, to avoid discrepancies which could result from spatial variation of R factor values, a uniform eight-year average R value of  $73 \text{ N h}^{-1}$  was used to normalize the soil erosion output. Finally, statistical significance differences between the various crop rotations were determined through the Least Significance Difference (LSD) mean separation test at  $P < 0.05$ .

### 3. Results and discussion

#### 3.1. Crop rotations and C values

The most prevalent year on year crop rotations (sequences), in terms of their share in the agricultural landscape, were found to be those involving WW, WR, and Mz crops in all the three years considered (Table 3). Similar findings have been reported by Steinmann and Dobers (2013) in a crop rotation study conducted in northern Germany. However, incorporation of Mz in the rotation (crop sequencing) scheme can be considered as a recent trend. A decade ago Mz was not commonly included in the crop rotation system in the study area, as per Prager et al. (2011). The importance of Mz is also expected to increase in the future, due to the demand for energy production (Lorenz et al., 2013). For WW, the main pre-crops were WR (42 %) followed by self-sequencing of WW (27 %) and Mz (14 %). For WR the main pre-crops were WW (44 %) and WB (31 %), while for Mz the main pre-crops were found to be WW (34.5 %), self-sequencing of Mz (28 %), and WR (12 %). So, among arable crops, WW and Mz were the most self-sequenced crops, with respect to area coverage, the three-year average amounting to 7% and 3%, respectively, of the entire landscape (Appendix Table A1). More or less similar findings on the proportion of pre-crops of WW has been reported by Lorenz et al. (2013) for the Saxony region of Germany.

The ANOVA result revealed that different crop sequence patterns had significant implications for both average annual C values (Fig. 4) and predicted average annual potential soil erosion rates in all the years considered. The highest average annual C values were estimated for crop sequences involving Mz and SB, as both pre-crops and succeeding crops. The maximum average annual C value of 0.39 (Fig. 4b) was computed



**Table 4**  
Intra-annual variation of crop rotation impact on monthly mean C values.

Succeeding crop	Pre-crop	Months*									
		February	March	April	May	June	July	August	September	October	December
WW	WW	0.223 <sup>ab</sup> <sub>cd</sub>	0.168 <sup>f</sup> <sub>g</sub>	0.079 <sup>d</sup> <sub>e</sub>	0.060 <sub>d</sub>	0.013 <sub>f</sub>	0.098 <sup>d</sup> <sub>e</sub>	0.498 <sup>a</sup>	0.471 <sup>a</sup>	0.363 <sup>a</sup>	0.170 <sup>bc</sup>
	WR	0.199 <sup>ab</sup> <sub>cd</sub>	0.118 <sub>g</sub>	0.054 <sup>d</sup> <sub>e</sub>	0.018 <sub>d</sub>	0.007 <sub>f</sub>	0.068 <sup>e</sup>	0.490 <sup>a</sup>	0.473 <sup>a</sup>	0.420 <sup>a</sup>	0.132 <sup>bc</sup>
	Mz	0.314 <sup>a</sup>	0.228 <sub>ef</sub>	0.128 <sup>c</sup> <sub>d</sub>	0.052 <sub>d</sub>	0.034 <sub>ef</sub>	0.094 <sup>d</sup> <sub>e</sub>	0.430 <sup>a</sup> <sub>b</sub>	0.233 <sup>bc</sup>	0.321 <sup>a</sup> <sub>b</sub>	0.296 <sup>ab</sup>
	WB	0.138 <sup>cd</sup>	0.132 <sub>g</sub>	0.054 <sup>d</sup> <sub>e</sub>	0.038 <sub>d</sub>	0.008 <sub>f</sub>	0.068 <sup>e</sup>	0.489 <sup>a</sup>	0.485 <sup>ab</sup>	0.351 <sup>a</sup> <sub>b</sub>	0.121 <sup>bc</sup>
	SB	-	0.290 <sub>de</sub>	0.162 <sup>c</sup> <sub>d</sub>	0.009 <sub>d</sub>	0.034 <sub>ef</sub>	0.099 <sup>c</sup> <sub>de</sub>	0.469 <sup>a</sup>	0.021 <sup>c</sup>	0.125 <sup>b</sup>	0.361 <sup>a</sup>
	SC	0.233 <sup>ab</sup> <sub>cd</sub>	0.141 <sub>efg</sub>	0.054 <sup>d</sup> <sub>e</sub>	0.026 <sub>d</sub>	0.001 <sub>if</sub>	0.078 <sup>d</sup> <sub>e</sub>	0.354 <sup>a</sup> <sub>b</sub>	0.385 <sup>a</sup>	0.334 <sup>a</sup> <sub>b</sub>	0.174 <sup>bc</sup>
	WRy	0.298 <sup>a</sup>	0.147 <sup>f</sup> <sub>g</sub>	0.084 <sup>c</sup> <sub>de</sub>	0.031 <sub>d</sub>	0.024 <sub>f</sub>	0.222 <sup>a</sup> <sub>b</sub>	0.470 <sup>a</sup>	0.564 <sup>a</sup>	0.515 <sup>a</sup>	-
WR	WW	0.121 <sup>d</sup>	0.116 <sub>g</sub>	0.037 <sup>e</sup>	0.084 <sub>d</sub>	0.005 <sub>f</sub>	0.043 <sup>e</sup>	0.486 <sup>a</sup>	0.411 <sup>a</sup>	0.179 <sup>b</sup>	0.077 <sup>c</sup>
	WR	0.147 <sup>cd</sup>	0.130 <sub>g</sub>	0.060 <sup>d</sup> <sub>e</sub>	0.035 <sub>d</sub>	0.013 <sub>f</sub>	0.041 <sup>e</sup>	0.462 <sup>a</sup>	0.444 <sup>a</sup>	0.296 <sup>a</sup> <sub>b</sub>	0.116 <sup>bc</sup>
	Mz	0.282 <sup>ab</sup>	0.200 <sup>f</sup> <sub>g</sub>	0.078 <sup>d</sup> <sub>e</sub>	0.196 <sub>c</sub>	0.019 <sub>f</sub>	0.042 <sup>e</sup>	0.305 <sup>a</sup> <sub>b</sub>	0.337 <sup>ab</sup>	0.293 <sup>a</sup> <sub>b</sub>	0.188 <sup>bc</sup>
	WB	0.124 <sup>d</sup>	0.133 <sub>g</sub>	0.043 <sup>e</sup>	0.057 <sub>d</sub>	0.008 <sub>f</sub>	0.033 <sup>e</sup>	0.407 <sup>a</sup> <sub>b</sub>	0.435 <sup>a</sup>	0.190 <sup>b</sup>	0.075 <sup>c</sup>
	WRy	0.120 <sup>d</sup> <sub>c</sub>	0.095 <sub>g</sub>	0.009 <sup>e</sup>	0.097 <sub>d</sub>	0.001 <sub>f</sub>	0.077 <sub>de</sub>	0.442 <sup>a</sup> <sub>b</sub>	0.499 <sup>a</sup>	0.391 <sup>a</sup>	0.172 <sup>bc</sup>
Mz	WW	0.275 <sup>ab</sup> <sub>cd</sub>	0.342 <sub>cd</sub>	0.341 <sup>b</sup>	0.422 <sub>a</sub>	0.383 <sub>bc</sub>	0.204 <sup>b</sup>	0.102 <sup>c</sup> <sub>d</sub>	0.303 <sup>abc</sup>	0.171 <sup>b</sup>	0.158 <sup>bc</sup>
	WR	0.295 <sup>a</sup>	0.260 <sub>def</sub>	0.201 <sup>c</sup>	0.249 <sub>bc</sub>	0.169 <sub>d</sub>	0.171 <sup>b</sup> <sub>c</sub>	0.162 <sup>b</sup> <sub>cd</sub>	0.445 <sup>a</sup>	0.228 <sup>a</sup> <sub>b</sub>	0.130 <sup>bc</sup>
	Mz	0.437 <sup>a</sup>	0.435 <sub>b</sub>	0.426 <sub>c</sub>	0.441 <sub>a</sub>	0.354 <sub>c</sub>	0.171 <sup>b</sup>	0.125 <sup>b</sup> <sub>cd</sub>	0.106 <sup>c</sup>	0.219 <sup>a</sup> <sub>b</sub>	0.443 <sup>a</sup>
	WB	0.272 <sup>ab</sup> <sub>c</sub>	0.229 <sub>efg</sub>	0.168 <sup>c</sup> <sub>d</sub>	0.369 <sub>ab</sub>	0.153 <sub>de</sub>	0.140 <sup>b</sup> <sub>cde</sub>	0.233 <sup>b</sup> <sub>c</sub>	0.181 <sup>bc</sup>	0.094 <sup>b</sup>	0.153 <sup>bc</sup>
	SB	-	0.544 <sub>a</sub>	0.537 <sup>a</sup>	0.481 <sub>a</sub>	0.491 <sub>a</sub>	0.265 <sup>a</sup>	0.066 <sup>c</sup> <sub>d</sub>	0.028 <sup>c</sup>	0.082 <sup>b</sup>	0.429 <sup>a</sup>
	SC	0.544 <sup>a</sup>	0.570 <sub>ab</sub>	0.565 <sup>a</sup> <sub>b</sub>	0.369 <sub>a</sub>	0.371 <sub>cd</sub>	0.148 <sup>b</sup> <sub>cde</sub>	0.009 <sup>c</sup> <sub>d</sub>	0.325 <sup>abc</sup>	0.031 <sup>b</sup>	0.232 <sup>abc</sup>
R <sup>2</sup>		0.44	0.62	0.70	0.62	0.73	0.44	0.61	0.60	0.55	0.35

Mean values followed by the same letter(s) in a column are not significantly different from each other as per LSD ( $P < 0.05$ ). (-) indicates not considered in the analysis.

\*The months are represented by individual satellite images which were selected according to best coefficient of determination values ( $r^2$ ); and the missing months are due to unavailability of representative cloud free images.

for SB/Mz sequencing, in the 2014/15 cropping calendar. Among the major crops, Mz was found to exhibit higher C values. Specifically, when Mz was sequenced after SB or Mz, higher C factor values were observed. However, if WR was used as a pre-crop for Mz, the values declined significantly and consistently compared with pre-crops of either SB or Mz itself. The importance of incorporating rapeseed in a rotation scheme has been discussed widely for major crops such as wheat (Peltonen-Sainio et al., 2019; Weiser et al., 2017). Weiser et al. (2017) indicate that wheat preceded by an oil seed crop yields higher than wheat preceded by other cereals. Peltonen-Sainio et al. (2019), employing NDVI based pre-crop value determination, also found that rapeseed enhanced the pre-crop value for many succeeding crops in Finland. In the present study, it is also demonstrated that WR, used as a pre-crop for Mz, can significantly enhance the cover status of Mz covered parcels,

particularly compared with self-sequencing of Mz or succeeding a pre-crop of SB (Fig. 4b).

Crop sequences involving WR showed a tendency to consistently reduce the average annual C value. The lowest average annual C value, amounting to 0.07, was determined on parcels covered with WR, with pre-crops of winter cereals (Fig. 4a). On the other hand, Mz was found to result in higher C values when it preceded WR. In the study region SB rarely preceded WR during the years considered (Fig. 2) so it was not possible to determine pre-crop influence of SB on WR. Glennitz et al. (2011) also indicated that SB and WR are taken as alternative pre-crop options in crop sequencing schemes in the study region.

When it comes to WW, by far the major cash crop grown in the region, it consistently resulted in higher annual average C values when preceded by Mz or SB. However, crop sequencing of WR/WW could have

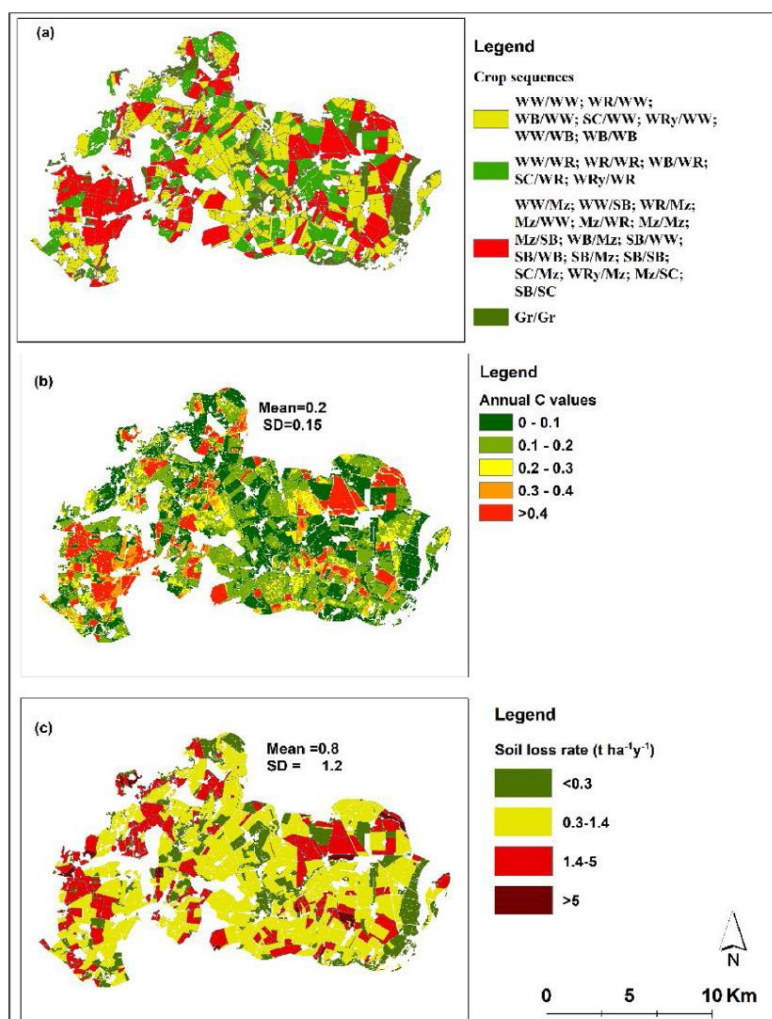


Fig. 5. a) spatial distribution of crop sequence patterns in 2015/16 cropping calendar; b) the corresponding distribution of average annual C values; c) the corresponding distribution of potential soil loss rates.

the potential to reduce the annual average C value compared with the alternative pre-crop of SB or self-sequencing of WW (Fig. 4a, b, and c). Therefore, with respect to C factor management and soil erosion considerations, sequencing WW after WR could do better in the study area compared with succeeding Mz or SB. Winter rape, however, as a blank seed in a fine seed bed is highly susceptible to erosion during thunderstorms in August (discussed below).

Among the self-sequencing patterns, WR/WR gave the lowest average annual C values in all the three considered cropping calendars, resulting in a value of 0.11, which was significantly lower than Mz/Mz (0.35) and WW/WW (0.19). Gabriels et al. (2003) report that continuous cropping of Mz in a rotation scheme, conducted at watershed scale in Belgium, resulted in highest annual C factor values. This could be due to the longest period of uncovered soil conditions resulting from Mz cultivation, in contrast with WR's almost year-round soil coverage.

The influence of crop rotation patterns on C values, however, was

found to vary intra-annually, as can be inferred from Table 4. WW parcels which were pre-cropped with SB had significantly lower monthly C values (Table 4, light-grey shaded columns) than WW parcels preceded by any other considered pre-crops during early autumn (September or October). This could be due mainly to the fact that parcels occupied by SB had not yet been harvested in these months, and hence the vegetation cover of SB remained vital lowering the values. However, during early spring (March and April), WW succeeding SB showed significantly higher monthly C values (0.29 and 0.162 respectively) compared with, for example, WR/WW (0.118 and 0.054 respectively). This could be explained as a result of the late sowing date for WW as a consequence of later harvesting of the SB pre-crop (<opt\_COMMENT id="optOqhWoi3z5WVxb7deD4fpTmKGTwsy2vSV">The name of the journal is Agricultural Systems.Castellazzi et al., 2008; Frielinghaus and Bork, 2000). Regarding WR, despite consistently giving the lowest annual C values when succeeding winter cereals (Fig. 4), during late

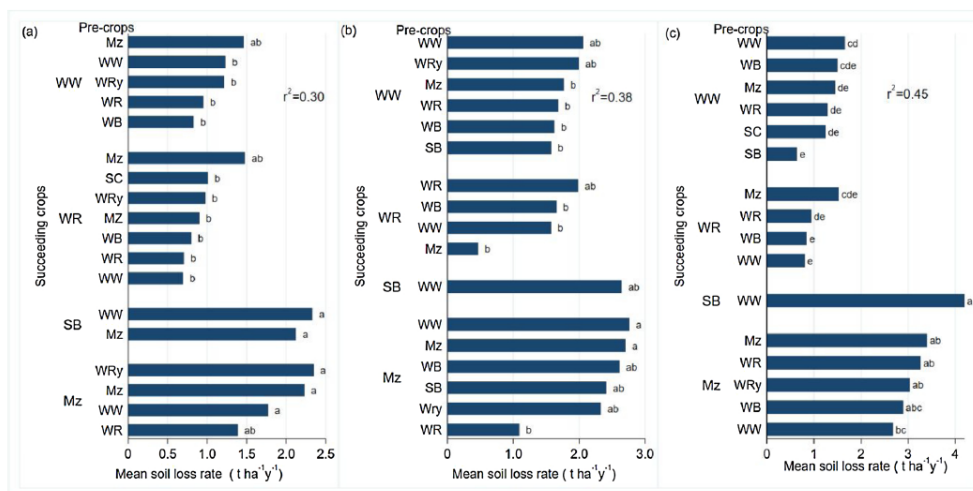


Fig. 6. Potential impact of crop rotation patterns on predicted mean annual soil loss rate: a) 2013/14, b) 2014/15, c) 2015/16 cropping calendar. Bars followed by the same letter(s) are not significantly different from each other according to LSD ( $P < 0.05$ ). The predicted erosion rate represents only parcels with soil erodibility class between 0.15 - 0.3 (block2; Fig. 3b) and LS values between 0.4 - 0.8 (block5; Fig. 3c) in order to uniformly compare crop rotation impact.

summer (August) and early autumn (September) the values calculated were found to be higher (Table 4). This could be due to the early phenological stages of WR in which the crop cover status is not expected to be more than 10 % (DIN 19708, 2005DIN 19708, 2005). Parcels covered with Mz, however, showed the exact opposite of crop sequencing involving WR. Parcels changing from Mz or SB to a succeeding crop of Mz showed the lowest monthly C values in August and September (Table 4, dark-gray columns); this could be attributed to the vegetation vitality status of the respective pre-crops which still effectively increased NDVI values, which in turn reduced the calculated C values. The results of the present study could indicate the importance of explicit consideration of temporal variability of crop rotation, with respect to protecting agricultural land against the impact of soil erosion by water (Preiti et al., 2017); and particularly essential for the study region, as Gericke et al. (2019), modelling rainfall erosivity in relation to climate change, report a likely incremental trend in rainfall erosivity in the future. The results could also show the possibility of employing multi-temporal satellite to capture temporal variability of C factor determination, with the implication for large scale ecosystem modelling studies. Process-based environmental impact assessment models, such as the Soil and Water Assessment Tool (SWAT), which require temporally explicit crop rotation input data, can benefit from such a practice.

When we consider the spatial distribution of C values in relation to different crop sequences, crop rotation components incorporating Mz and SB within the entire agricultural landscape corresponded with higher mean annual C values (Fig. 5a and b). In the 2015/16 cropping calendar, around 17 % (2931 ha) of the entire agricultural landscape involved these crops, as both preceding and succeeding crop sequencing components, which in turn corresponded well with the 21 % classification of the landscape with annual C values greater than 0.3. The spatial distribution of the lowest annual C values ( $< 0.1$ ), on the other hand, corresponded with crop sequences involving WR and Gr.

### 3.2. Crop rotation and potential soil erosion risk

With respect to the prediction of potential soil erosion, crop rotation patterns involving SB and Mz as succeeding crops consistently and significantly resulted in higher average annual soil loss rates (Fig. 6). Specifically, SB has slow early growth and establishment rate, which can

contribute to the calculated high soil loss rate. Additionally, Koch et al. (2018), reported that SB succeeding Mz and WW produced a smaller leaf area index compared with SB succeeding peas in a field trial conducted in Germany. This may influence the canopy cover status of SB following such pre-crops as Mz. The second highest soil erosion rate was calculated in a Mz/Mz pattern. Self-sequencing maize (Mz/Mz) resulted in 72 % higher soil erosion rates compared with self-sequencing of WR and 51 % higher compared with self-sequencing of WW (Fig. 6c). This is in agreement with the findings by Koschke et al. (2013), in a scenario-based model conducted in Germany, that silage corn performed worst in soil erosion prevention with regard to crop rotation management; and by Lorenz et al. (2013), whose findings indicate that crop rotation patterns incorporating Mz and SC are associated with higher erosion risk. This can be attributed to the fact that Mz is not able to provide year-round soil cover protection, unlike the self-sequencing pattern of WR, or winter cereals which, more or less, provide better soil coverage. Similarly, Preiti et al. (2017) report that rotations involving potatoes, a wide spaced and row planted crop like maize, generated the highest amounts of runoff in a plot experiment conducted in the Mediterranean climate.

Yet, the influence of various pre-crops on major succeeding crops varied from year to year (Figs. 4 and Fig. 6). The variation could be associated with inter-annual weather variability, crop management variability (such as tillage methods, soil fertility management) and variation in the physical condition of the parcels (Peltonen-Sainio et al., 2019). For instance, the majority (close to 75 %) of the WW/SB crop rotation in 2013/14 covered parcels with an average LS factor  $< 0.4$  (block 4; see section 2.4 for block descriptions) while in 2014/15 only 60 % of the rotation took place on parcels under block 4 category. Rotations of root crops (SB) and row cultivated plants (Mz), therefore need to be considered for rotation on less sloping or flat areas in accordance with the good agricultural practice (Auerwald, 2002; Gutzler et al., 2015). The results indicate the possibility of deriving cultivation recommendations for sloping areas, by taking into account the risk of erosion and thus helping to reduce the risk of nutrient and pesticide input to other ecosystems (such as water) or damage to infrastructures.

However, interpreting the predicted soil erosion results requires caution as the coefficients of determination ( $r^2$ ) were relatively small in all the three considered cropping calendars (Fig. 6a, b, and c). This could

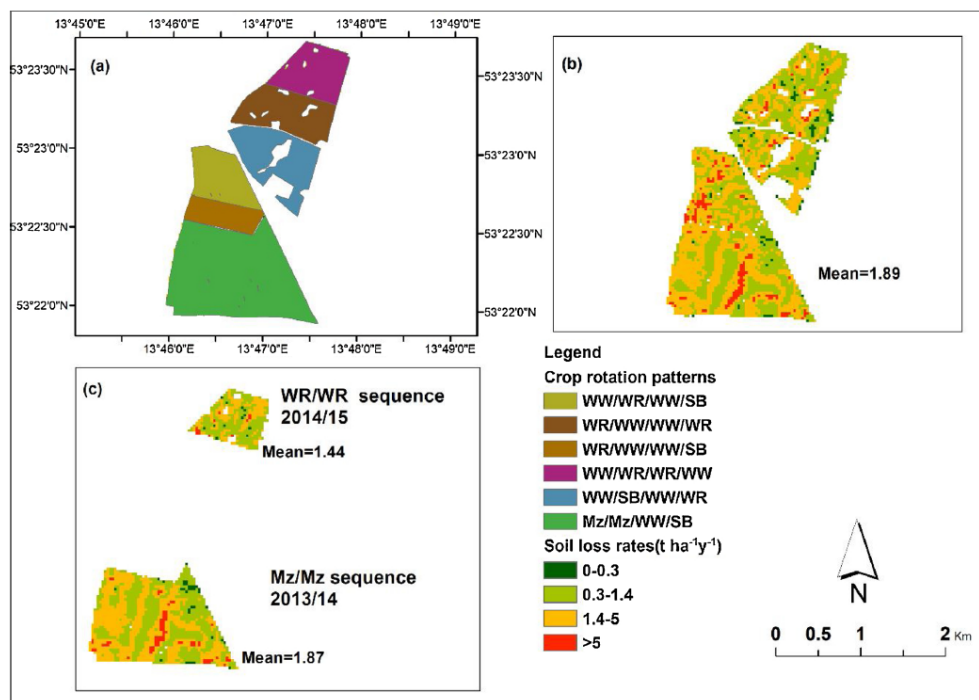


Fig. 7. Predicted potential soil loss rate in relation to crop rotation pattern at and near Holzendorf research site: a) crop rotation pattern (from 2013 to 2016); b) three-year average soil loss rate; c) soil loss rate predicted on MZ and WR self-sequencing parcels.

be due to the smothering effect of the extraction method on spatial variability of the USLE input factors used, as the output of the soil erosion was the average of a given parcel. The results from the present study, however, could help in identifying trends of potential soil erosion risk in relation to crop management patterns, as depicted in Fig. 5c.

When it comes to the model validation, the USLE model predicted a three-year average potential soil loss rate of  $1.89 \text{ t ha}^{-1} \text{ y}^{-1}$  for several crop rotation patterns (Fig. 7a and b) in and around the Holzendorf experimental site. The potential soil loss rates predicted in the present study showed reasonably acceptable outputs compared with the measured soil erosion rates (Appendix Fig. B1) for the two considered crop rotation patterns. The long-term crop rotation plots consisted of, among others, monocultures of winter rye and maize and continuous fallow plots (Deumlich et al., 2018). The continuously fallowed experimental plot produced the highest average soil loss rate of  $5 \text{ t ha}^{-1}$  (Fig. B1). The lowest long-term average soil loss rate of  $0.5 \text{ t ha}^{-1}$  was recorded on the WRy monoculture plot while the Mz monoculture plot experienced an average soil loss rate of  $1.0 \text{ t ha}^{-1}$ . The measured soil loss rate on Mz monocropping plot varied annually from almost nil up to  $4 \text{ t ha}^{-1}$  coinciding with the rainfall depth pattern of the study area (Deumlich et al., 2018). In this regard, our potential soil erosion modelling of the Mz/Mz sequence in the 2013/14 cropping calendar resulted in an average soil loss rate of  $1.87 \text{ t ha}^{-1} \text{ y}^{-1}$  (Fig. 7c), a comparatively close prediction and within the range of the actual measured soil loss rate for Mz monoculture (Fig. B1).

On the other hand, the WR/WR sequence in the 2014/15 cropping calendar, considered to be representative of the WRy monoculture of the experimental set-up, since both crops have a comparable canopy cover pattern in the study area (DIN 19708, 2005DIN 19708, 2005), resulted in a slightly higher average soil loss rate,  $1.4 \text{ t ha}^{-1} \text{ y}^{-1}$  (Fig. 7c), than the long-term recorded average soil loss rate (Fig. B1). Though the predicted

average value showed a slight over-estimation compared with the long-term measured average, which could be attributed to the increasing trend of rainfall erosivity over the years (Gericke et al., 2019), the spatial distribution of the potential soil loss rate indicated that 60 % of the parcel was classified below the maximum tolerable soil loss rate of  $1.4 \text{ t ha}^{-1} \text{ y}^{-1}$  (Verheijen et al., 2009) rendering the model output to be fairly acceptable.

Overall, using remote sensing data for C value calculation of various rotation patterns and subsequently modelling erosion rates can be taken as a valid practice to predict erosion risk trends in relation to land management practice in a spatiotemporally distributed manner. More often, the C factor assessment is carried out using empirical values representing a cross-sectional period of certain degrees of soil cover in conjunction with the proportion of the rainfall erosivity derived from long-term studies. The NDVI derived method, on the other hand, can variably capture the actual soil cover status. In the future, however, validation using erosion data representing the current erosivity conditions of the study area will be essential.

Finally, the applicability of results from crop rotation research has a far-reaching significance in sustainable management of resources and sustainable agricultural practices (Schönhart et al., 2011). Crop rotation has been found to enhance the capacity of ecosystems to provide basic services to human beings, such as in water supply (Lei et al., 2019) as well as providing regulating services (Koschke et al., 2013). The employment of satellite images for the study of crop rotation is also pertinent in understanding the influence of pre-crops on several aspects of the agronomic performance of subsequent crops, as discussed by Peltonen-Sainio et al. (2019) in addition to quantifying the effect of rotation on yield benefit (Beal Cohen et al., 2019). The results of the present research, therefore, may also be useful in determining the impact of different agricultural management systems on the

Table A1

All crop sequences (CS) identified using the IACS data and their proportion (%) from the entire landscape and the parcel proportion (%) of the specified pre-crop.

CS	Pre-crops	Coverage of the CS as proportion of entire landscape (%)			Specified pre-crop as a proportion of the CS (%)		
		2013/14	2014/15	2015/16	2013/14	2014/15	2015/16
WW	WW	6.5	6.7	7.6	22.8	27.0	27.1
	WR	10.4	11.7	11.8	54.7	65.6	72.1
	Mz	4.4	3.7	3.1	41.2	36.0	33.7
	WB	1.3	1.7	1.6	17.9	14.6	16.4
	SB	0.0	1.1	0.6	0.0	34.1	40.0
	SC	0.2	0.4	0.6	7.6	20.0	26.2
	WRy	1.2	0.2	0.1	31.4	11.8	5.0
	Gr	0.5	0.8	0.8	1.8	2.9	3.5
	WW	9.0	5.9	6.6	31.3	23.9	23.6
	WR	1.7	1.5	1.2	9.0	8.6	7.6
WR	Mz	0.6	0.5	0.8	5.6	5.0	8.3
	WB	4.7	5.3	5.0	64.2	45.2	51.4
	SB	0.0	0.2	0.0	0.0	5.7	0.0
	SC	0.9	0.2	0.3	33.3	7.3	12.3
	WRy	1.0	0.1	0.3	26.7	3.9	10.0
	Gr	0.7	0.6	0.2	2.6	2.3	0.8
	WW	4.0	2.5	5.0	13.8	10.0	18.0
	WR	2.0	0.8	1.1	10.6	4.5	6.7
	Mz	2.7	3.0	3.3	25.2	28.6	36.0
	WB	0.5	0.3	1.2	6.4	2.8	13.0
Mz	SB	0.0	0.8	0.4	0.0	25.0	30.0
	SC	0.1	0.2	0.1	4.6	9.1	3.1
	WRy	0.6	0.7	0.8	15.1	39.2	27.5
	Gr	0.4	0.9	0.3	1.5	3.3	1.5
	WW	6.3	6.3	3.9	21.8	25.4	14.0
	WR	3.7	1.9	0.6	19.8	10.7	3.4
	Mz	0.3	0.7	0.9	3.2	6.7	9.5
	WB	0.4	0.9	0.7	5.2	7.7	7.1
	SB	0.0	0.0	0.0	0.0	1.1	2.5
	SC	0.3	0.3	0.8	12.1	16.4	34.0
WB	WRy	0.4	0.0	0.9	10.5	0.0	32.5
	Gr	0.4	0.1	0.2	1.5	0.4	0.8
	WW	0.4	0.1	0.3	1.3	0.4	1.1
	WR	0.6	0.4	0.0	3.5	2.1	0.2
	Mz	0.7	0.6	0.2	6.8	6.0	2.7
	WB	0.0	1.6	0.0	0.0	13.6	0.0
	SB	0.0	0.0	0.0	0.0	0.0	0.0
	SC	0.3	0.0	0.0	9.1	0.0	0.0
	WRy	0.3	0.0	0.3	7.0	2.0	11.3
	Gr	0.2	0.0	0.1	0.7	0.1	0.5
WRy	WW	1.3	0.8	1.2	4.4	3.4	4.2
	WR	0.1	0.1	0.1	0.7	0.4	0.4
	Mz	0.9	0.2	0.1	8.4	1.4	0.8
	WB	0.1	0.5	0.4	1.7	4.3	4.3
	SB	0.0	0.1	0.0	0.0	3.4	2.5
	SC	0.1	0.2	0.0	3.0	7.3	1.5
	WRy	0.2	0.2	0.0	5.8	11.8	0.0
	Gr	0.1	0.4	0.0	0.3	1.4	0.2
	WW	0.3	0.3	0.2	1.0	1.0	0.6
	WR	0.0	0.2	0.0	0.0	1.0	0.0
SB	Mz	0.3	0.7	0.1	2.4	6.7	1.5
	WB	0.0	0.4	0.0	0.6	3.4	0.4
	SB	0.0	0.1	0.1	0.0	3.4	7.5
	SC	0.3	0.0	0.1	9.1	0.0	3.1
	WRy	0.0	0.0	0.1	1.2	2.0	2.5
	Gr	0.3	0.1	0.2	1.3	0.4	1.1
	Gr	23.4	21.8	20.6	90.2	81.2	90.4
	WW	0.7	0.2	0.5	2.5	0.6	1.9
	WB	0.3	0.2	0.3	4.1	1.2	2.9
	WR	0.2	0.2	0.7	0.9	0.8	4.4
Gr	Mz	0.6	0.2	0.3	5.6	1.4	3.8
	WRy	0.0	0.2	0.0	0.0	9.8	0.0
	SB	0.0	0.1	0.2	0.0	3.4	17.5
	SC	0.6	0.4	0.3	19.7	21.8	12.3

environment in general, and on the capacity of the environment to provide ecosystem services. In addition, for large and complex agricultural landscapes, it may serve as an efficient and cost-effective means of determining crop rotation patterns without the need to conduct vast numbers of plot-scale experiments across multiple locations, particularly for areas with limited availability of relevant crop rotation data.

#### 4. Conclusions

The study utilized time-series remotely-sensed data, along with fine-resolution land-use data to investigate the influence of short-term crop rotation or sequencing patterns on cover and management factor (C) values, and on subsequent soil erosion rate in a large agricultural landscape. The results obtained agreed with established experimental

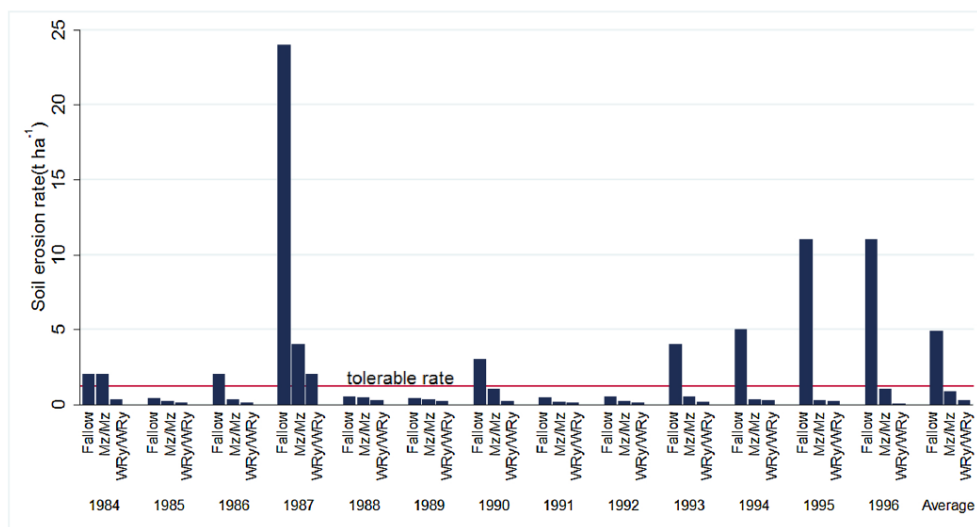


Fig. B1. Long-term measured soil erosion rate at Holzendorf experimental station. Adapted from Deumlich et al. (2018).

rotation output worldwide. Therefore, such an approach can be useful for areas with limited availability of established rotation data. Among the considered rotations, self-sequencing Mz was found to increase the soil loss rate compared with self-sequencing WR and WW. WR, on the other hand, as a preceding crop to both Mz and WW, can improve annual C values and subsequently reduce annual soil loss rate. The influence of rotation patterns was also found to vary intra-annually. In this regard, using SB as a pre-crop to winter cereals resulted in significantly higher C values during winter and early spring months, while reducing C values in late summer and early autumn. On the other hand, when used as either a pre-crop or succeeding crop, WR consistently resulted in lower annual C values, but higher values were computed during the early establishment period of the crop. This can provide the basis for erosion modelling studies in temporally explicit and spatially resolved models.

Overall, the results of this research could be an input for further efficient investigation of agronomic practices and their impact on the environment on a large heterogeneous agricultural landscape scale. The results could also be helpful as an input for agricultural land management planning. However, the variations considered in the present study could not include management practice variations resulting from individual farm decisions. For the future, therefore, the use of disaggregated data, including agricultural management decisions, such as tillage, residue management practice and fertilization schemes, could further improve the output.

#### CRedit authorship contribution statement

**Dawit Ashenafi Ayalew:** Conceptualization, Data curation, Formal analysis, Investigation, Methodology, Writing - original draft, Writing - review & editing. **Detlef Deumlich:** Conceptualization, Data curation, Investigation, Resources, Writing - review & editing. **Borivoj Sarapatka:** Conceptualization, Resources, Supervision, Writing - review & editing.

#### Declaration of Competing Interest

The authors report no declarations of interest.

#### Acknowledgment

The main author is a recipient of the Czech government scholarship for PhD study. This study is part of the PhD work. This research benefited from financial assistance from Palacký University Olomouc through a grant (IGA\_PrF\_2019\_020) and from the National agency for agricultural research of the Czech Republic (QK1810233). We would also like to thank ZALF for facilitating the research. Finally, we would like to thank Dr. Daniel Doktor, from Helmholtz Centre for Environmental Research-UFZ, for his helpful advice on the remote sensing element of the paper and for providing some of the Sentinel 2 data.

#### Appendix A

.

#### Appendix B

.

#### References

- Alewel, C., Borrelli, P., Meusburger, K., Panagos, P., 2019. Using the USLE: chances, challenges and limitations of soil erosion modelling. *Int. Soil Water Conserv. Res.* 7 (3), 203–225. <https://doi.org/10.1016/j.iswcr.2019.05.004>.
- Auerswald, K., 2002. Estimating the C factor of the universal soil loss equation from cropping statistics for sites with sub-continental to sub-atlantic climate north of the alps (in german). *Landnutzung und Landentwicklung* 43, 1–5.
- Auerswald, K., Kainz, M., Fiener, P., 2003. Soil erosion potential of organic versus conventional farming evaluated by USLE modelling of cropping statistics for agricultural districts in Bavaria. *Soil Use Manage.* 19 (4), 305–311. <https://doi.org/10.1079/SUM2003212>.
- Ayalew, D.A., Deumlich, D., Sarapatka, B., Doktor, D., 2020. Quantifying the sensitivity of NDVI-Based C factor estimation and potential soil Erosion prediction using spaceborne earth observation data. *Remote Sens. (Basel)* 12 (7), 1136. <https://doi.org/10.3390/rs12071136>.
- Beal Cohen, A.A., Seifert, C.A., Azzari, G., Lobell, D.B., 2019. Rotation effects on corn and soybean yield inferred from satellite and field-level data. *Agron. J.* 111 (6), 2940–2948. <https://doi.org/10.2134/agronj2019.03.0157>.
- Bégué, A., Arvor, D., Bellon, B., Betbeder, J., Abelleira, D.de P.D., Ferraz, R., Lebourgeois, V., Lelong, C., Simões, M., R. Verón, S., 2018. Remote sensing and cropping practices: a review. *Remote Sens. (Basel)* 10 (2), 99. <https://doi.org/10.3390/rs10010099>.
- Bennett, A.J., Bending, G.D., Chandler, D., Hilton, S., Mills, P., 2012. Meeting the demand for crop production: the challenge of yield decline in crops grown in short



## Curriculum Vitae

<b>Name:</b>	Dawit Ashenafi Ayalew
<b>Born:</b>	May 01, 1981
<b>Education:</b>	
2016 to present	PhD study – Ecology, Palacký University Olomouc, Czech Republic
2009 to 2011	MSc Sustainability Science, University of Tokyo, Japan
2006 to 2007	Postgraduate Diploma Int. Horticulture, University of Essex, UK
<b>Work Experience</b>	
1999 to 2003	BSc Horticulture, Jumma University, Ethiopia
2013 to 2016	Lecturer, Ambo University, Ambo, Ethiopia
2012 to 2014	Agronomist, Yara International, Addis Ababa, Ethiopia
2003 to 2009	Researcher, at Jimma Agricultural Research Center, Jimma, Ethiopia
<b>Abroad research stays</b>	
01/10/2017– 31/01/2018	Leibniz-Centre for Agricultural Landscape Research (ZALF), Müncheberg, Germany
01/07/2019 – 30/09/2019	Internship Helmholtz Centre for Environmental Research-UFZ, Leipzig, Germany



## **Publications in peer-reviewed journals with IF**

**Ayalew, Dawit A.**; Deumlich, Detlef; Šarapatka, Bořivoj; Doktor, Daniel (2020): Quantifying the Sensitivity of NDVI-Based C Factor Estimation and Potential Soil Erosion Prediction using Spaceborne Earth Observation Data. In *Remote Sensing* 12 (7), p. 1136. DOI: 10.3390/rs12071136.

**Ayalew, Dawit Ashenafi**; Deumlich, Detlef; Šarapatka, Bořivoj (2021): Agricultural landscape -scale C factor determination and erosion prediction for various crop rotations through a remote sensing and GIS approach. In *European Journal of Agronomy*. 123, p. 126203. DOI: 10.1016/j.eja.2020.126203.

Netopil, P., Šarapatka, B., **Ayalew, D. A.**, & Drncová, K. (2021). Multi-temporal analysis of erosional plots using aerial images and deep soil probes. *Physical Geography*, (Under Review).

## **Presentations on international conferences**

**Ayalew D. A.**, Deumlich D., Šarapatka B. (2019): Quantifying the sensitivities of NDVI based C factor estimations and potential soil erosion predictions using remote sensing and GIS. (Oral presentation). Presented at Pedologické dny 2019, 11 – 13 September 2019, SRNÍ, Czech Republic

**Ayalew D. A.**, Deumlich D., Šarapatka B. (2019): Large agricultural landscape scale investigation of the impact of crop rotation on cover factor(C) and potential soil erosion rates using remote sensing and GIS. (Oral presentation). Presented at the 5th BIOHYDROLOGY 2019 conference, 24 - 27 July 2019, Valencia, Spain

**Ayalew D. A.**, Deumlich D., Šarapatka B. (2018): Spatiotemporal cover factor analysis of a large geographic region: coupling remotely sensed data with the integrated administration and control system (INVEKOS) data. (Poster). TERENO international conference. 08-12 October 2018, Berlin, Germany.